

1 Review of Jet Measurements in Heavy Ion Collisions

2 Megan Connors,^{1,2} Christine Nattrass,³ Rosi Reed,⁴ and Sevil Salur⁵
3

4 ¹*Georgia State University, Atlanta, GA,
USA-30302.*

5 ²*RIKEN BNL Research Center, Upton,
NY 11973-5000*

6 ³*University of Tennessee, Knoxville, TN,
USA-37996.*

7 ⁴*Lehigh University, Bethlehem, PA,
USA-18015.*

8 ⁵*Rutgers University, Piscataway,
NJ USA-08854.*

9 *All authors contributed equally to this manuscript. Authors are listed alphabetically.*

10 (Dated: December 19, 2017)

11 A hot, dense medium called a Quark Gluon Plasma (QGP) is created in ultrarelativistic
12 heavy ion collisions. Early in the collision, hard parton scatterings generate high mo-
13 mentum partons that traverse the medium, which then fragment into sprays of particle
14 called jets. Understanding how these partons interact with the QGP and fragment into
15 final state particles provides critical insight into quantum chromodynamics. Experi-
16 mental measurements from high momentum hadrons, two particle correlations, and full
17 jet reconstruction at the Relativistic Heavy Ion Collider (RHIC) and the Large Hadron
18 Collider (LHC) continue to improve our understanding of energy loss in the QGP. Run
19 2 at the LHC recently began and there is a jet detector at RHIC under development.
20 Now is the perfect time to reflect on what the experimental measurements have taught
21 us so far, the limitations of the techniques used for studying jets, how the techniques
22 can be improved, and how to move forward with the wealth of experimental data such
23 that a complete description of energy loss in the QGP can be achieved.

24 Measurements of jets to date clearly indicate that hard partons lose energy. Detailed
25 comparisons of the nuclear modification factor between data and model calculations led
26 to quantitative constraints on the opacity of the medium to hard probes. However, while
27 there is substantial evidence for softening and broadening jets through medium interac-
28 tions, the difficulties comparing measurements to theoretical calculations limit further
29 quantitative constraints on energy loss mechanisms. Since jets are algorithmic descrip-
30 tions of the initial parton, the same jet definitions must be used, including the treatment
31 of the underlying heavy ion background, when making data and theory comparisons. We
32 call for an agreement between theorists and experimentalists on the appropriate treat-
33 ment of the background, Monte Carlo generators that enable experimental algorithms
34 to be applied to theoretical calculations, and a clear understanding of which observables
35 are most sensitive to the properties of the medium, even in the presence of background.
36 This will enable us to determine the best strategy for the field to improve quantitative
37 constraints on properties of the medium in the face of these challenges.

38 PACS numbers: 25.75.Dw

16 CONTENTS

17 I. Introduction	33	H. Comparing different types of measurements	20
18 A. Formation and evolution of the Quark Gluon Plasma	2	III. Overview of experimental results	20
19 B. Jet definition	2	A. Cold nuclear matter effects	21
20 C. Interactions with the medium	4	2. Reconstructed jets	21
21 D. Separating the signal from the background	6	1. Inclusive charged hadrons	21
22 II. Experimental methods	7	3. Dihadron correlations	22
23 A. Detectors	8	4. Summary of cold nuclear matter effects for jets	22
24 B. Centrality determination	8	B. Partonic energy loss in the medium	22
25 C. Inclusive hadron measurements	9	1. Jet R_{AA}	24
26 D. Dihadron correlations	10	2. Dihadron correlations	25
27 1. Background subtraction methods	11	3. Dijet imbalance	26
28 E. Reconstructed jets	11	4. γ -hadron, γ -jet and Z -jet correlations	27
29 1. Jet-finding algorithms	13	5. Hadron-jet correlations	29
30 2. Dealing with the background	13	6. Path length dependence of inclusive R_{AA} and jet	30
31 F. Particle Flow	14	v_n	30
32 G. Unfolding	16	7. Heavy quark energy loss	30
	17	8. Summary of experimental evidence for partonic	32
	50	energy loss in the medium	

51 C. Influence of the medium on the jet
 52 1. Fragmentation functions with jets
 53 2. Boson tagged fragmentation functions
 54 3. Dihadron correlations
 55 4. Jet-hadron correlations
 56 5. Dijets
 57 6. Jet Shapes
 58 7. Particle composition
 59 8. LeSub
 60 9. Jet Mass
 61 10. Dispersion
 62 11. Girth
 63 12. Grooming
 64 13. Subjettiness
 65 14. Summary of experimental evidence for medium
 66 modification of jets
 67 D. Influence of the jet on the medium
 68 1. Evidence for out-of-cone radiation
 69 2. Searches for Molière scattering
 70 3. The rise and fall of the Mach cone and the ridge
 71 4. Summary of experimental evidence for
 72 modification of the medium by jets
 73 E. Summary of experimental results

74 IV. Discussion and the path forward
 75 A. Understand bias
 76 B. Make quantitative comparisons to theory
 77 C. More differential measurements
 78 D. An agreement on the treatment of background in
 79 heavy ion collisions

80 V. Acknowledgements

81 References

82 1

83 I. INTRODUCTION

84 In ultrarelativistic heavy ion collisions, the temper-
 85 ature is so high that the nuclei melt, forming a hot,
 86 dense liquid of quarks and gluons called the Quark Gluon
 87 Plasma (QGP). Hard quark and gluon scatterings occur
 88 early in the collision, prior to the formation of the QGP.
 89 These quarks and gluons, known as partons, traverse
 90 the medium and then fragment into collimated sprays
 91 of particles called jets. These partons lose energy to the
 92 medium and the jets they produce are thus modified.
 93 This process, called jet quenching, is studied with exper-
 94 imental measurements of high momentum hadrons, two
 95 particle correlations, and jet reconstruction at the Rela-
 96 tivistic Heavy Ion Collider (RHIC) and the Large Hadron
 97 Collider (LHC). After nearly two decades of experimen-
 98 tal measurements have taught us so far, we reflect on the
 99 limitations of the techniques used for studying jets, how
 100 the techniques can be improved, and how to move for-
 101 ward with the wealth of experimental data such that a
 102 complete description of energy loss in the QGP can be
 103 achieved.

104 Our goal in the following sections is to provide an
 105 overview of what we have learned from jet measure-
 106 ments and what the field needs to do in order to im-
 107 prove our quantitative understanding of jet quenching

108 and the properties of the medium from RHIC energies
 109 ($\sqrt{s_{NN}} = 7.7-200$ GeV) to LHC energies ($\sqrt{s_{NN}} = 2.76-$
 110 5.02 TeV). We will discuss measurements using the AL-
 111 ICE, ATLAS, and CMS detectors at the LHC, and the
 112 BRAHMS, PHENIX, Phobos, and STAR detectors at
 113 RHIC. The main goal of this paper is to review experi-
 114 mental techniques and measurements. While we discuss
 115 some models and their interpretation, a full review of the
 116 theory of partonic interactions with the medium is out-
 117 side the scope of this paper. In this section, we provide
 118 an overview of the formation of the QGP and other pro-
 119 cesses which impact the measurement of jets and their
 120 interaction with the medium. One key factor in measur-
 121 ing jets in heavy ion collisions is accounting for the effect
 122 of the fluctuating background on different observables.
 123 Section II discusses the various measurement techniques
 124 and approaches to background subtraction and suppres-
 125 sion and how these techniques may impact the results
 126 and their interpretation. We include measurements of
 127 nuclear modification factors, dihadron and multi-hadron
 128 correlations, and reconstructed jets. We follow this with
 129 a discussion of results in Section III organized by what
 130 they tell us about the medium. Do jets lose energy in
 131 the medium? Is fragmentation modified in the medium?
 132 Do jets modify the medium? Are there cold nuclear mat-
 133 ter effects? We show that there is substantial evidence
 134 for both partonic energy loss and modified fragmenta-
 135 tion. The evidence for modification of the medium by
 136 jets is considerably more scant. Our understanding of
 137 cold nuclear matter effects is rapidly evolving, but cur-
 138 rently there do not appear to be substantial cold nuclear
 139 matter effects for jets.

140 We conclude with a discussion of what we have learned
 141 and the way forward for the field in Section IV. There
 142 are extensive detailed measurements of jets, benefited by
 143 improved detector technologies, high cross sections, and
 144 higher luminosities, and there have been dramatic im-
 145 provements in our theoretical understanding and capa-
 146 bilities. However, experimental techniques and the bias
 147 they may impose are frequently neglected, and it is not
 148 currently possible to apply experimental algorithms to
 149 most models. The current status of comparisons between
 150 models and data motivates our call for an agreement be-
 151 tween theorists and experimentalists on the appropriate
 152 treatment of the background, Monte Carlo generators
 153 that enable experimental algorithms to be applied to the-
 154 oretical calculations, and a clear understanding of which
 155 observables are most sensitive to the properties of the
 156 medium, even in the presence of background. This will
 157 enable us to quantitatively constrain properties of the
 158 medium.

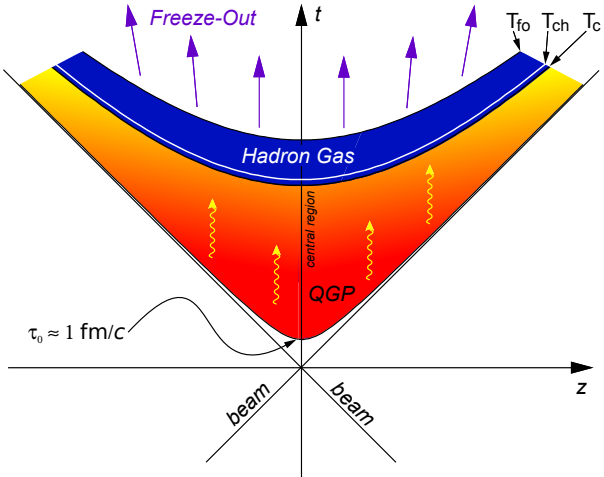


FIG. 1 A light cone diagram showing the stages of a heavy ion collision. The abbreviation T_{fo} is for the thermal freeze-out temperature, T_{ch} is for the chemical freeze-out temperature, and T_c is for the critical temperature where the phase transition between a hadron gas and a QGP occurs. τ_0 is the formation time of the QGP. Figure courtesy of Thomas Ullrich.

159 **A. Formation and evolution of the Quark Gluon Plasma**

160 Quarks and gluons become deconfined under extremely
 161 high energy and density conditions. This deconfined state
 162 became known as the QGP (Shuryak, 1980). With
 163 the advancements in accelerator physics, it can be created
 164 and studied in high energy heavy ion collisions.

165 The formation of the QGP requires energy densities
 166 above $0.2\text{-}1 \text{ GeV/fm}^3$ (Bazavov *et al.*, 2014; Karsch,
 167 2002). These energy densities can currently be reached
 168 in high energy heavy ion collisions at RHIC located at
 169 Brookhaven National Laboratory in Upton, NY and the
 170 LHC located at CERN in Geneva, Switzerland. Estimates
 171 of the energy density indicate that central heavy
 172 ion collisions with an incoming energy per nucleon pair as
 173 low as $\sqrt{s_{NN}} = 7.7 \text{ GeV}$, the lower boundary of collision
 174 energies accessible at RHIC, can reach energy densities
 175 above 1 GeV/fm^3 (Adare *et al.*, 2016e) and that collisions
 176 at 2.76 TeV , accessible at the LHC, reach energy
 177 densities as high as 12 GeV/fm^3 (Adam *et al.*, 2016i;
 178 Chatrchyan *et al.*, 2012d). Contrary to initial naïve expectations
 179 of a gas-like QGP, the QGP formed in these
 180 collisions was shown to behave like a liquid of quarks
 181 and gluons (Adams *et al.*, 2005b; Adcox *et al.*, 2005; Ar-
 182 sene *et al.*, 2005b; Back *et al.*, 2005; Heinz and Snellings,
 183 2013).

184 The heavy ion collision and the evolution of the fireball,
 185 as depicted in Figure 1, has several stages, and the mea-
 186 surement of the final state particles can be affected by one
 187 or all of these stages depending on the production mecha-
 188 nism and interaction time within the medium. The initial

189 state of the incoming nuclei is not precisely known, but
 190 its properties impact the production of final state parti-
 191 cles. The incoming nuclei are often modeled as either an
 192 independent collection of nucleons called a Glauber ini-
 193 tial state (Miller *et al.*, 2007), or a wall of coherent gluons
 194 called a Color Glass Condensate (Iancu *et al.*, 2001). In
 195 either initial state model, both the impact parameter of
 196 the nuclei and fluctuations in the positions of the incom-
 197 ing quarks or gluons, called partons, lead to an asym-
 198 metric nuclear overlap region. This asymmetric overlap
 199 is shown schematically in Figure 2. The description of
 200 the initial state most consistent with the data is between
 201 these extremes (Moreland *et al.*, 2015). The proposed
 202 electron ion collider is expected to resolve ambiguities
 203 in the initial state of heavy ion collisions (Aprahamian
 204 *et al.*, 2015).

205 In all but the most central collisions, some fraction of
 206 the incoming nucleons do not participate in the collision
 207 and escape unscathed. These nucleons, called spectators,
 208 can be observed directly and used to measure the impact
 209 parameter of the collision. Before the formation of the
 210 QGP, partons in the nuclei may scatter off of each other
 211 just as occurs in $p+p$ collisions. An interaction with a
 212 large momentum transfer (Q) is called a hard scattering,
 213 a process which is, in principle, calculable with perturba-
 214 tive quantum chromodynamics (pQCD). The majority of
 215 these hard scatterings are $2\rightarrow 2$, which result in high mo-
 216 mentum partons traveling 180° apart in the plane trans-
 217 verse to the beam as they travel through the evolving
 218 medium. These hard parton scatterings are the focus of
 219 this paper.

220 As the medium evolves, it forms a liquid of quarks and
 221 gluons. The liquid reaches local equilibrium, with tem-
 222 perature fluctuations in different regions of the medium.
 223 The liquid QGP phase is expected to live for $1\text{-}10 \text{ fm}/c$,
 224 depending on the collision energy (Harris and Muller,
 225 1996). As the medium expands and cools, it reaches
 226 a density and temperature where partonic interactions
 227 cease, a hadron gas is formed, and the hadron fractions
 228 are fixed. This point in the collision evolution is called
 229 chemical freeze-out (Adam *et al.*, 2016j; Adams *et al.*,
 230 2005b; Fodor and Katz, 2004). As the medium expands
 231 and cools further, collisions between hadrons cease and
 232 hadrons reach their final energies and momenta. This
 233 stage of the collision, thermal freeze-out, occurs at a
 234 somewhat lower temperature than the chemical freeze-
 235 out.

236 Thermal photons, in a manner analogous to black
 237 body radiation, reveal that the QGP may reach temper-
 238 atures of $300\text{-}600 \text{ MeV}$ in central collisions at both
 239 200 GeV (Adare *et al.*, 2010a) and 2.76 TeV (Adam *et al.*,
 240 2016g). The temperature can also be inferred from the
 241 sequential melting of bound states of a bottom quark and
 242 antiquark (Chatrchyan *et al.*, 2012g). The ratios of final
 243 state hadrons are used to determine that the chemical
 244 freeze-out temperature is around 160 MeV (Adam *et al.*,

245 2016j; Adams *et al.*, 2005b; Fodor and Katz, 2004) and 301 sions, in principle they form a well calibrated probe. The 246 that the thermal freeze out occurs at about 100–150 MeV, 302 initial production must scale by the number of nucleon 247 depending on the collision energy and centrality (Abelev 303 collisions, which means that their interactions with the 248 *et al.*, 2013b; Adcox *et al.*, 2004; Arsene *et al.*, 2005a; 304 medium would cause deviations from this scaling. Since 249 Back *et al.*, 2007).

250 The properties of the medium are determined from 306 the final state particles that are measured. The initial 307 gluon density can be related to the final state hadron 308 multiplicity through the concept of hadron-parton dual- 309

254 ity (Van Hove and Giovannini, 1988), leading to estimates 310 of gluon densities of around 700 per unit pseudorapidity 311 at the top RHIC energy of $\sqrt{s_{NN}} = 200$ GeV (Adler *et al.*, 312 2005) and 2000 per unit pseudorapidity at the top LHC 313 energy of $\sqrt{s_{NN}} = 5.02$ TeV (Aad *et al.*, 2012, 2016c; 314 Aamodt *et al.*, 2010; Adam *et al.*, 2016d; Chatrchyan 315 *et al.*, 2011a).

261 The azimuthal anisotropy in the momentum distribu- 317 tion of final state hadrons is the result of the initial state 318 anisotropy. The survival of these anisotropies provides 319 evidence that the medium flows in response to pres- 320 sure gradients (Aad *et al.*, 2014b; Adam *et al.*, 2016a; 321 Adler *et al.*, 2001, 2003c; Alver *et al.*, 2007; Chatrchyan 322 *et al.*, 2014b). This asymmetry is illustrated schemat- 323 ically in Figure 2. The shape and magnitude of these 324 anisotropies can be used to constrain the viscosity to 325 entropy ratio, revealing that the QGP has the lowest 326 viscosity to entropy ratio ever observed (Adams *et al.*, 327 2005b; Adcox *et al.*, 2005; Arsene *et al.*, 2005b; Back 328 *et al.*, 2005). Hadrons containing strange quarks are en- 329 hanced in heavy ion collisions above expectations from 330 $p+p$ collisions (Abelev *et al.*, 2013f, 2014b; Khachatryan 331 *et al.*, 2017d). This is due to a combination of the sup- 332 pression of strangeness in $p+p$ collisions due to the lim- 333

278 ited phase space for the production of strange quarks, 334 and the higher energy density available for the produc- 335 tion of strange quarks in heavy ion collisions. Corre- 336 lations between particles may provide evidence for in- 337 creased production of strangeness due to the decreased 338 strange quark mass in the medium (Abelev *et al.*, 2009c; 339 Adam *et al.*, 2016f). Baryon production is enhanced for 340 both light (Abelev *et al.*, 2006; Adler *et al.*, 2004; Arsene 341 *et al.*, 2010) and strange quarks (Abelev *et al.*, 2013f, 342 2014b, 2008; Khachatryan *et al.*, 2017d), an observation 343 generally interpreted as evidence for the direct produc- 344 tion of baryons through the recombination of quarks in 345 the medium (Dover *et al.*, 1991; Fries *et al.*, 2003; Greco 346 *et al.*, 2003; Hwa and Yang, 2003).

292 Hard parton scattering occurs early in the collision evo- 347 lution, prior to the formation of the QGP, so that their 293 interactions with the QGP probe the entire medium evo- 348 lution. Therefore, they can be used to reveal the prop- 294 erties of the medium, such as its stopping power and 349 transport coefficients. Since the differential production 295 cross section of these hard parton scatterings is calcula- 350 ble in pQCD, and these calculations have been validated 296 over many orders of magnitude in proton-proton colli- 351 352 353

305 sions, in principle they form a well calibrated probe. The 306 initial production must scale by the number of nucleon 307 collisions, which means that their interactions with the 308 medium would cause deviations from this scaling. Since 309 the majority of these hard partons are produced in pairs, 310 they can be used both as a probe and a control. Particle 311 jets of this nature are formed in e^+e^- and proton-proton 312 ($p+p$) collisions as well and are observed to fragment sim- 313 ilarly in e^+e^- and $p+p$ collisions.

314 In a heavy ion collision, where a QGP is formed, the 315 hard scattered quarks and gluons are expected to interact 316 strongly with the hot QCD medium due to their color 317 charges, and lose energy, either through collisions with 318 medium partons, or through gluon bremsstrahlung. The 319 energy loss of high momentum partons due to strong 320 interactions is a process called jet quenching, and re- 321 sults in modification of the properties of the result- 322 ing jets in heavy ion collisions compared to expecta- 323 tions from proton-proton collisions (Baier *et al.*, 1995; 324 Bjorken, 1982; Gyulassy and Plumer, 1990). This en- 325 ergy loss was first observed in the suppression of high 326 momentum hadrons produced in heavy ion collisions at 327 RHIC (Adams *et al.*, 2003b; Adler *et al.*, 2003b; Back 328 *et al.*, 2004) and later also observed at the LHC (Aamodt 329 *et al.*, 2011b; Chatrchyan *et al.*, 2012e). The modification 330 can be observed through measurements of jet shapes, 331 particle composition, fragmentation, splitting functions and 332 many other observables. Detailed studies of jets to char- 333 acterize how and why partons lose energy in the QGP 334 require an understanding of how evidence for energy loss 335 may be manifested in the different observables, and the 336 effect of the large and complicated background from other 337 processes in the collision.

338 Early studies of the QGP focused on particles produced 339 through soft processes, measuring the bulk properties of 340 the medium. With the higher cross sections for hard pro- 341 cesses with increasing collision energy, higher luminosity 342 delivered by colliders, and detectors better suited for jet 343 measurements, studies of jets are enabling higher preci- 344 sion measurements of the properties of the QGP (Akiba 345 *et al.*, 2015). The 2015 nuclear physics Long Range Plan 346 (LRP) (Aprahamian *et al.*, 2015) highlighted the partic- 347 ular need to improve our quantitative understanding of 348 jets in heavy ion collisions. Here we assess our current 349 understanding of jet production in heavy ion collisions in 350 order to inform what shape future studies should take in 351 order to optimize the use of our precision detectors.

352 B. Jet definition

353 In principle, using a jet finding algorithm to cluster all 354 of the daughter particles of a given parton will give access 355 to the full energy and momentum of the parent parton. 356 However, even in e^+e^- collisions, the definition of a jet 357 is ambiguous, even on the partonic level. For instance,

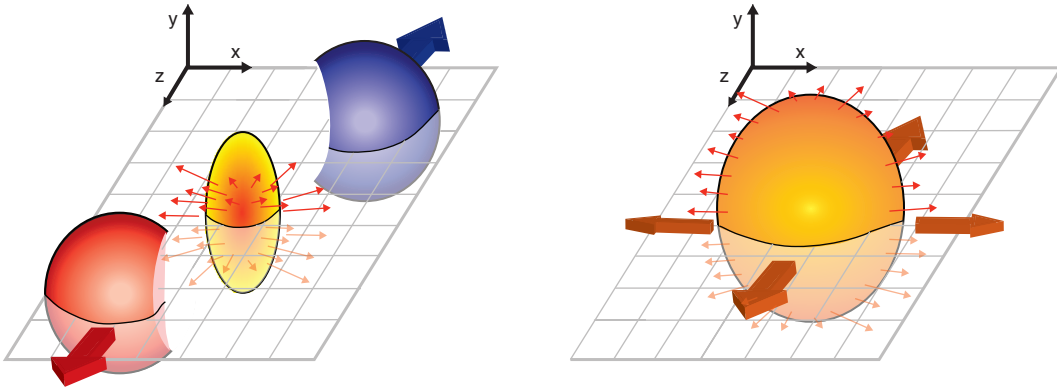


FIG. 2 Schematic diagrams showing the initial overlap region (left) and the spatial anisotropy generated by this anisotropic overlap region. This anisotropy can be quantified using the Fourier coefficients of the momentum anisotropy. Figure courtesy of Boris Hippolyte.

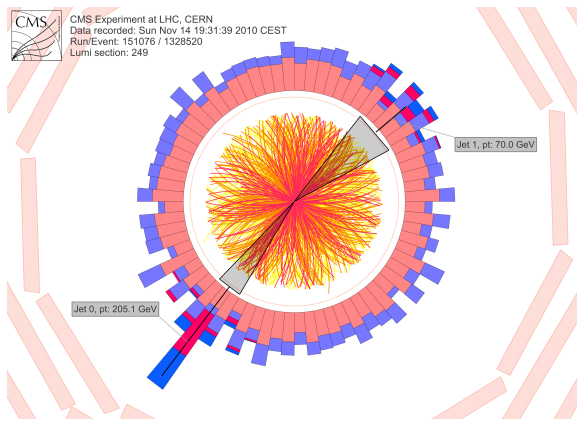


FIG. 3 Event display showing a dijet event in a Pb+Pb collision at $\sqrt{s_{\text{NN}}} = 2.76$ TeV (CMS, 2010). This shows the large background for jet measurements in heavy ion collisions.

in $e^+e^- \rightarrow q\bar{q}$, the quark may emit a gluon. If this gluon is emitted at small angles relative to the quark, it is usually considered part of the jet, whereas if it is emitted at large angles relative to the parent parton, it may be considered a third jet. This ambiguity led to the Snowmass Accord, which stated that in order to be comparable, experimental and theoretical measurements had to use the same definition of a jet and that the definition should be theoretically robust (Huth *et al.*, 1990).

The choice of which final state particles should be included in the jet is also somewhat arbitrary and more difficult in $A+A$ collisions than in $p+p$ collisions. Figure 3 shows an event display from a Pb+Pb collision at $\sqrt{s_{\text{NN}}} = 2.76$ TeV, showing the large background in the event. If a hard parton emits a soft gluon and that gluon thermalizes with the medium, are the particles from the hadronization of that soft gluon part of the jet or part

of the medium? Any interaction between daughters of the parton and medium particles complicates the definition of what should belong to the jet and what should not. This ambiguity in the definition of the observable itself makes studies of jets qualitatively different from, e.g., measurements of particle yields. These aspects of jet physics need to be taken into account in the choice of a jet finding algorithm and background subtraction methods in order to be able to interpret the resulting measurements.

One of the main motivations for studies of jets in heavy ion collisions was to provide measurements of observables with a production cross-section that can be calculated using pQCD, which yields a well calibrated probe. In certain limits, this is feasible, although it is worth noting that many observables are sensitive to non-perturbative effects. One such non-perturbative effect is hadronization, which can affect even the measurements of relatively simple observables such as the jet momentum spectra.

In addition to the ambiguities inherent in the definition of what is and is not a jet, there is the question of how to deal with the large background in heavy ion collisions. For example, measurements of reconstructed jets usually have a minimum momentum threshold for constituents in order to suppress the background contribution. If the corrections for these analysis techniques are insensitive to assumptions about the background and hadronization, the results may still be perturbatively calculable. However, these techniques for dealing with the background may also bias the measured jet sample, for instance by selecting gluon jets at a higher rate than quark jets. In the context of jets in a heavy ion collision, these analysis cuts are part of the definition of the jet and can not be ignored.

The interpretation of the measurement of any observable cannot be fully separated from the techniques used to measure it because both measurements and theoreti-

408 cal calculations of jet observables must use the same definition of a jet. As we review the literature, we discuss 409 how the jet definitions and techniques used in experiment 410 may influence the interpretation of the results. Even 411 though our goal is an understanding of partonic interactions 412 within the medium, a detailed understanding of 413 soft particle production is necessary to understand the 414 methods for suppressing and subtracting the contribution 415 of these particles to jet observables.

417 C. Interactions with the medium

418 There are several models used to describe interactions 419 between hard partons and the medium, however, a full review of theoretical calculations is beyond the 420 scope of this paper. We briefly summarize theoretical 421 frameworks for interactions of hard partons with the 422 medium here and refer readers to (Burke *et al.*, 2014; 423 Qin and Wang, 2015) and the references therein for 424 details. The production of final state particles in nuclear 425 collisions is described by assuming that these processes 426 can be factorized (Majumder, 2007a; Majumder and Van 427 Leeuwen, 2011). The nuclear parton distribution 428 functions $x_a f_a^A(x_a)$ and $x_b f_b^B(x_b)$ describe the probability 429 of finding partons with momentum fraction x_a and x_b , 430 respectively. The differential cross sections for partons a and b interacting with each other to produce a parton c with a momentum p can be described using pQCD. 431 The production of a final state hadron h is then given by 432 fragmentation function $D_c^h(z)$ where $z = p^h/p$ is the 433 fraction of the parton's momentum carried by the final state 434 hadron. The differential cross section for the production 435 of hadrons as a function of their transverse momenta p_T 436 and rapidity y at leading order is then given by

$$437 \frac{d^3\sigma^h}{dyd^2p_T} = \frac{1}{\pi} \int dx_a \int dx_b f_a^A(x_a) f_b^B(x_b) \frac{d\sigma_{ab \rightarrow cX}}{d\hat{t}} \frac{D_c^h(z)}{z}. \quad (1)$$

438 where $\hat{t} = (\hat{p} - x_a P)^2$, \hat{p} is the four-momentum of parton c , and P is the average momentum of a nucleon in nucleus A. The nuclear parton distribution functions and the fragmentation functions cannot be calculated perturbatively. The parton distribution functions describe the initial state of the incoming nuclei. Any differences between the nuclear and proton parton distribution functions, which describe the distribution of partons in a nucleon, are considered cold nuclear matter effects. Cold nuclear matter effects may include coherent multiple scattering within the nucleus (Qiu and Vitev, 2006), gluon shadowing and saturation (Gelis *et al.*, 2010), or partonic energy loss within the nucleus (Bertocchi and Treleani, 1977; Vitev, 2007; Wang and Guo, 2001). Most models for interactions of partons with a QGP factorize this process and only modify the fragmentation functions (Majumder, 2007a). One goal of studies of high momentum particles in heavy ion collisions is to study the modification of these fragmentation functions, which will allow us to understand how and why partons lose energy within the QGP and to determine the microscopic

439 structure of the medium. We note that the theoretical 440 definition in Equation 1 associates the production of a 441 final state hadron with a particular parton. This is not 442 possible experimentally, so the experimentally measured 443 quantity also referred to as a fragmentation function is 444 not the same as $D_c^h(z)$ in Equation 1.

445 Medium-induced gluon radiation (bremsstrahlung) 446 and collisions with partons in the medium cause the partons 447 to lose energy to the medium, often described as 448 a modification of the fragmentation functions in Equation 449 1. There are four major approaches to describing 450 these interactions. The GLV model (Djordjevic and Gyulassy, 451 2004; Djordjevic *et al.*, 2005; Djordjevic and Heinz, 452 2008; Vitev and Gyulassy, 2002; Wicks *et al.*, 2007) 453 and its CUJET implementation (Buzzatti and Gyulassy, 454 2012) assumes that the scattering centers in the medium 455 are nearly static and that the mean free path of a parton 456 is much larger than the color screening length in the 457 medium. This assumption is valid for a thinner medium.

458 The Higher Twist (Majumder, 2012) framework assumes 459 medium modified splitting functions during fragmentation 460 calculated by including higher twist corrections 461 to the differential cross sections for deep inelastic 462 scattering off of nuclei. These corrections are enhanced 463 by the length of the medium. The higher twist model 464 has also been adapted to include multiple gluon emissions 465 (Collins *et al.*, 1985; Majumder, 2012; Majumder and Van 466 Leeuwen, 2011).

467 In the BDMPS (Baier *et al.*, 1997, 1998, 2000) approach 468 and its equivalents (Albacete *et al.*, 2005; Armesto *et al.*, 469 2012; Eskola *et al.*, 2005; Wiedemann, 2000b, 2001; 470 Zakharov, 1996) the effect of multiple parton scatterings 471 is evaluated using a path integral over a path ordered 472 Wilson line (Wiedemann, 2000a,b). This assumes infinite 473 coherence of the radiated gluons and a thick medium. Ya- 474 JEM (Renk, 2008, 2013a) and JEWEL (Zapp, 2014a,b) 475 are Monte Carlo implementations of the BDMPS framework.

476 The energy loss mechanism in the AMY model is similar 477 to BDMPS but the rate equations for partonic energy 478 loss are solved numerically and convoluted with differential 479 pQCD cross sections and fragmentation functions 480 to determine the final state differential hadronic 481 cross sections (Arnold *et al.*, 2002; Jeon and Moore, 482 2005; Qin *et al.*, 2009, 2008). This is applied in a realistic 483 hydrodynamical environment (Qiu and Heinz, 2012; 484 Qiu *et al.*, 2012; Song and Heinz, 2008a,b). The MAR- 485 TINI model (Qin *et al.*, 2008; Schenke *et al.*, 2011) is 486 a Monte Carlo model implementation of the AMY formalism 487 which uses PYTHIA (Sjostrand *et al.*, 2006) to describe 488 the hard scattering and a Glauber initial state (Miller *et al.*, 489 2007). Partonic energy loss occurs in the medium, taking 490 temperature and hydrodynamical flow into account (Nonaka and Bass, 2007; Schenke *et al.*, 491 2010, 2011).

492 There are additional approaches, including embedding

495 jets into a hydrodynamical fluid (Tachibana *et al.*, 2017) 501 and using the correspondence between Anti-deSitter 502 and conformal field theories (Gubser, 2007). There 503 is a new description of jet quenching in which coherent 504 parton branching plays a central role to the jet-medium 505 interactions (Casalderrey-Solana *et al.*, 2013; Mehtar- 506 Tani and Tywoniuk, 2015). In this work it is assumed 507 that the hierarchy of scales governing jet evolution allow 508 the jet to be separated into a hard core, which interacts 509 with the medium as a single coherent antenna, and softer 510 structures that will interact in a color decoherent fash- 511 ion. In order for this to be valid, there must be a large 512 separation of the intrinsic jet scale and the characteristic 513 momentum scale of the medium. While this certainly is 514 valid for the highest momentum jets at the LHC, it is 515 not clear at which scales in collision energy and jet en- 516 ergy this assumption breaks down. We refer readers to 517 a recent theoretical review for a more complete picture 518 of theoretical descriptions of partonic energy loss in the 519 QGP (Qin and Wang, 2015).

520 Medium-induced bremsstrahlung occurs when the 521 medium exchanges energy, color, and longitudinal mo- 522 mentum with the jet. Since both the energy and longi- 523 tudinal momentum of the hard partons exceeds that of 524 the medium partons, these exchanges cause the parton 525 as a whole to lose energy. Additionally, since the hard 526 partons have much higher transverse momentum than the 527 medium partons, any collision will reduce the momentum 528 of the jet as a whole. Both of these effects will broaden 529 the resulting jet and soften the average final state parti- 530 cles produced from the jet. Collisional energy loss simi- 531 larly broadens and softens the jet. Partonic energy loss 532 in the medium is quantified by the jet transport coeffi- 533 cients $\hat{q} = Q^2/L$, where Q is the transverse momentum 534 lost to the medium and L is the path-length traversed; \hat{e} , 535 the longitudinal momentum lost per unit length; and \hat{e}_2 , 536 the fluctuation in the longitudinal momentum per unit 537 length (Majumder, 2013; Muller, 2013).

538 The JET collaboration systematically compared each 539 of these models to data to determine how well the trans- 540 port properties of partons in the medium can be con- 541 strained (Burke *et al.*, 2014). This substantially im- 542 proved our quantitative understanding of partonic en- 543 ergy loss in the medium, but only used a small fraction 544 of the available data. The Jetscape collaboration (Col- 545 laboration”, 2017) has formed to develop a Monte Carlo 546 framework which enables combinations of different mod- 547 els of the initial state, the hydrodynamical evolution of 548 medium, and partonic energy loss to be used within the 549 same framework. The goal is a Bayesian analysis compar- 550 ing models to data to quantitatively determine properties 551 of the medium, similar to (Bernhard *et al.*, 2016; Novak 552 *et al.*, 2014). Jetscape will incorporate many of the avail- 553 able jet observables into this Bayesian analysis. Part of 554 the motivation for this paper is to evaluate which exper- 555 imental observables might provide effective input for this 556

557 effort and what factors need to be considered for these 558 comparisons.

559 In light of the ambiguities in the jet definition dis- 560 cussed above, we note that whether or not the energy 561 is lost depends on this definition. The functional exper- 562 imental definition of lost energy is any energy which no 563 longer retains short-range correlations with the parent 564 parton, meaning that it is further than about half a unit 565 in pseudorapidity and azimuth. Energy which retains 566 short-range correlations with the parent parton is still 567 considered part of the jet and any short-range modifica- 568 tions are considered modifications of the fragmentation 569 function.

570 564 D. Separating the signal from the background

571 Hard partons traverse a medium which is flowing and 572 expanding, with fluctuations in the density and temper- 573 ature. Since the mean transverse momentum of uniden- 574 tified hadrons in Pb+Pb collisions at $\sqrt{s_{\text{NN}}} = 2.76$ TeV 575 is 680 MeV/c (Abelev *et al.*, 2013g), sufficiently high 576 p_T hadrons are expected to be produced dominantly in 577 jets and production from soft processes is expected to be 578 negligible. It is unclear precisely at which momentum the 579 particle yield is dominated by jet production rather than 580 medium production. Moreover, most particles produced 581 in jets are at low momenta even though the jet momen- 582 tum itself is dominated by the contribution of a few high 583 p_T particles. Particularly if jets are modified by processes 584 such as recombination, strangeness enhancement, or hy- 585 drodynamical flow, these low momentum particles pro- 586 duced in jets may carry critical information about their 587 parent partons’ interactions with the medium. Methods 588 employed to suppress and subtract background from jet 589 measurements are dependent on assumptions about the 590 background contribution and can change the sensitivity 591 of measurements to possible medium modifications. The 592 resulting biases in the measurements can be used as a tool 593 rather than treated as a weakness in the measurement; 594 however, they must be first understood.

595 The largest source of correlated background is due to 596 collective flow. The azimuthal distribution of particles 597 created in a heavy ion collision can be written as

$$\frac{dN}{d(\phi - \psi_R)} \propto 1 + \sum_{n=1}^{\infty} 2v_n \cos(n(\phi - \psi_R)) \quad (2)$$

598 where N is the number of particles, ϕ is the angle of a 599 particle’s momentum in azimuth in detector coordinates 600 and ψ_R is the angle of the reaction plane in detector coor- 601 dinates (Poskanzer and Voloshin, 1998). The Fourier co- 602 efficients v_n are thought to be dominantly from collective 603 flow at low momenta (Adams *et al.*, 2005b; Adcox *et al.*, 604 2005; Arsene *et al.*, 2005b; Back *et al.*, 2005), although 605 equation 2 is valid for any correlation because any distri- 606 bution can be written as its Fourier decomposition. The 607

598 magnitude of the Fourier coefficients v_n decreases with
 599 increasing order. The sign of the flow contribution to the
 600 first order coefficient v_1 is dependent on the incoming di-
 601 rection of the nuclei and changes sign when going from
 602 positive to negative pseudorapidities. For most measure-
 603 ments, which average over the direction of the incoming
 604 nuclei, v_1 due to flow is zero, although we note that there
 605 may be contributions to v_1 from global momentum con-
 606 servation.

607 The even v_n arise mainly from anisotropies in the aver-
 608 age overlap region of the incoming nuclei, considering the
 609 nucleons to be smoothly distributed in the nucleus with
 610 the density depending only on the radius. The odd v_n
 611 for $n > 1$ are generally understood to arise from the fluc-
 612 tuations in the positions of the nucleons within the nu-
 613 cleus. These fluctuations also contribute to the even v_n ,
 614 though these coefficients are dominated by the overall ge-
 615 ometry. Jets themselves can lead to non-zero v_n through
 616 jet quenching, complicating background subtraction for
 617 jet studies. At high momenta ($p_T \gtrsim 5\text{-}10 \text{ GeV}/c$) the v_n
 618 are thought to be dominated by jet production. Further-
 619 more, the v_n fluctuate event-by-event even for a given
 620 centrality class. This means that independent measure-
 621 ments, which differ in their sensitivity to jets, averaged
 622 over several events cannot be used blindly to subtract the
 623 correlated background due to flow.

624 To measure jets, experimentalists have to make some
 625 assumptions about the interplay between hard and soft
 626 particles and about the form of the background. With-
 627 out such assumptions, experimental measurements are
 628 nearly impossible. Some observables are more robust to
 629 assumptions about the background than others, however,
 630 these measurements are not always the most sensitive to
 631 energy loss mechanisms or interactions of jets with the
 632 medium. An understanding of data requires an under-
 633 standing of the measurement techniques and assumptions
 634 about the background. We therefore discuss the measure-
 635 ment techniques and their consequences in great detail in
 636 Section II before discussing the measurements themselves
 637 in Section III.

638 II. EXPERIMENTAL METHODS

639 This section focuses on different methods for probing
 640 jet physics including inclusive hadron measurements, di-
 641 hadron correlations, jet reconstruction algorithms and
 642 jet-particle correlations and a brief description of relevant
 643 detectors. In addition to explaining the measurement de-
 644 tails and how the effect of the background on the observ-
 645 able is handled for each, this section highlights strengths
 646 and weaknesses of these different methods which are im-
 647 portant for interpreting the results. We emphasize back-
 648 ground subtraction and suppression techniques because
 649 of potential biases they introduce.

TABLE I Collision systems, collision energies (\sqrt{s}) for $p+p$ collisions, collision energies per nucleon ($\sqrt{s_{NN}}$) for $A+A$ collisions, charged particle multiplicities ($dN/d\eta$) for central collisions, energy densities for central collisions, and the temperature compared to the critical temperature for formation of the QGP T/T_c for both RHIC and the LHC.

Collider	RHIC	LHC
Collisions	$p+p$, $d+\text{Au}$, $\text{Cu}+\text{Cu}$, $\text{Au}+\text{Au}$, $\text{U}+\text{U}$	$p+p$, $p+\text{Pb}$, $\text{Pb}+\text{Pb}$
\sqrt{s}	62–500 GeV	0.9–14 TeV
$\sqrt{s_{NN}}$	7.7–500 GeV	2.76–5.02 TeV
$dN/d\eta$	192.4 ± 16.9 687.4 ± 36.6 (Adare <i>et al.</i> , 2016e)	– (Adare <i>et al.</i> , 2016d)
ϵ	1.36 ± 0.14 GeV/fm^3 (Adare <i>et al.</i> , 2016e)	12.3 ± 1.0 GeV/fm^3 (Adam <i>et al.</i> , 2016i)
T/T_c^a	1.3	1.8–1.9

^a Calculated using $T = 196 \text{ MeV}$ at $\sqrt{s_{NN}} = 200 \text{ GeV}$, $T = 280 \text{ MeV}$ at $\sqrt{s_{NN}} = 2.76 \text{ TeV}$, and $T = 292 \text{ MeV}$ at $\sqrt{s_{NN}} = 5.02 \text{ TeV}$ from (Srivastava *et al.*, 2016) assuming that $T_c = 155 \text{ MeV}$ from the extrapolation of the chemical freeze-out temperature using comparisons of data to statistical models in (Floris, 2014).

650 A. Detectors

651 Measurements of heavy ion collisions often focus on
 652 midrapidity, with precision, particle identification, and
 653 tracking in a high multiplicity environment. Some mea-
 654 surements, such as those of single particles, are not sig-
 655 nificantly impacted by a limited acceptance, while the ac-
 656 ceptance corrections for reconstructed jets are more com-
 657 plicated when the acceptance is limited. We briefly sum-
 658 marize the colliders, RHIC and the LHC, and the most
 659 important features of each of their detectors for mea-
 660 surements of jets, referring readers to other publications for
 661 details.

662 The properties of the medium are slightly different at
 663 RHIC and the LHC, with the LHC reaching the highest
 664 temperatures and energy densities and RHIC providing
 665 the widest range of collision energies and systems. The
 666 relevant properties of each collider are summarized in
 667 Table I. Some properties of each detector are summarized
 in Table II.

668 The BRAHMS (Adamczyk *et al.*, 2003), PHENIX (Ad-
 669 amcox *et al.*, 2003), and PHOBOS (Back *et al.*, 2003) ex-
 670 periments are experiments which have completed their taking
 671 data at RHIC. The STAR (Ackermann *et al.*, 2003) ex-
 672 periment is taking data at RHIC and sPHENIX (Adare
 673 *et al.*, 2015) is a proposed upgrade at RHIC to be built
 674 in the existing PHENIX hall. STAR has full azimuthal
 675 acceptance and nominally covers pseudorapidities $|\eta| < 1$
 676 with a silicon inner tracker and a time projection cham-
 677 ber (TPC), surrounded by an electromagnetic calorime-
 678 ter.

TABLE II Summary of acceptance of detectors at RHIC and the LHC and when detectors took data. When not otherwise listed, azimuthal acceptance is 2π .

Collider	Detector	EMCal	HCal	Tracking	Taking data
RHIC	BRAHMS	N/A	N/A	$0 < \eta < 4$	2000–2006
	PHENIX	$ \eta < 0.35$	N/A	$ \eta < 0.35, 2 \times \Delta\phi = 90^\circ$	2000–2016
	PHOBOS	N/A	N/A	$0 < \eta < 2, 2 \times \Delta\phi = 11^\circ$	2000–2005
	STAR	$ \eta < 1.0$	N/A	$ \eta < 1.0$	2000–
	sPHENIX	$ \eta < 1.0$	$ \eta < 1.0$	$ \eta < 1.0$	future
LHC	ALICE	$ \eta < 0.7, \Delta\phi = 107^\circ$ and $\Delta\phi = 60^\circ$	N/A	$ \eta < 0.9$	2009–
	ATLAS	$ \eta < 4.9$	$ \eta < 4.9$	$ \eta < 2.5$	2009–
	CMS	$ \eta < 3.0$	$ \eta < 5.2$	$ \eta < 2.5$	2009–
	LHCb	N/A	N/A	$ \eta < 0.35$	2009–

ter (Ackermann *et al.*, 2003). An inner silicon detector was installed before the 2014 run. Particle identification is possible both through energy loss in the TPC and a time of flight (TOF) detector. STAR also has forward tracking and calorimetry. The PHENIX central arms cover $|\eta| < 0.35$ and are split into two azimuthal regions (Adcox *et al.*, 2003). They consist of drift and pad chambers for tracking, a TOF for particle identification, and precision electromagnetic calorimeters. There are both midrapidity and forward silicon for precision tracking and forward electromagnetic calorimeters. PHENIX also has two muon arms at forward rapidities ($-1.15 < |\eta| < -2.25$ and $1.15 < |\eta| < -2.44$) with full azimuthal coverage. The PHOBOS detector consists of a large acceptance scintillator with wide acceptance for multiplicity measurements ($|\eta| < 3.2$) and two spectrometer arms capable of both particle identification and tracking covering $0 < |\eta| < 2$ and split into two azimuthal regions (Back *et al.*, 2003). The BRAHMS detector has a spectrometer arm capable of particle identification with wide rapidity coverage ($0 \lesssim y \lesssim 4$) (Adamczyk *et al.*, 2003). sPHENIX will have full azimuthal acceptance and acceptance in pseudorapidity of approximately $|\eta| < 1$ with a TPC combined with precision silicon tracking and both electromagnetic and hadronic calorimeters (Adare *et al.*, 2015). sPHENIX is optimized for measurements of jets and heavy flavor at RHIC.

The LHC has four main detectors, ALICE, ATLAS, CMS, and LHCb. ALICE, which is primarily devoted to studying heavy ion collisions at the LHC, has a TPC, silicon inner tracker, and TOF covering $|\eta| < 0.9$ and full azimuth (Aamodt *et al.*, 2008). It has an electromagnetic calorimeter (EMCal) covering $|\eta| < 0.7$ with two azimuthal regions covering 107° and 60° in azimuth and a forward muon arm. Both ATLAS and CMS are multipurpose detectors designed to precisely measure jets, leptons and photons produced in pp and heavy ion collisions. The ATLAS detector's precision tracking is performed by a high-granularity silicon pixel detector, followed by the silicon microstrip tracker and complemented by the transition radiation tracker for the $|\eta| < 2.5$ region. The hadronic and electromagnetic calorimeters provide her-

metic azimuthal coverage in the $|\eta| < 4.9$ range. The muon spectrometer surrounds the calorimeters covering $|\eta| < 2.7$ with full azimuthal coverage (Aad *et al.*, 2008). The main CMS detectors are silicon trackers which measure charged particles within the pseudorapidity range $|\eta| < 2.5$, an electromagnetic calorimeter partitioned into a barrel region ($|\eta| < 1.48$) and two endcaps ($|\eta| < 3.0$), and hadronic calorimeters covering the range $|\eta| < 5.2$. All CMS detectors listed here have full azimuthal coverage (Chatrchyan *et al.*, 2008). LHCb focuses on measurements of charm and beauty at forward rapidities. The LHCb detector consists of a single spectrometer covering $1.6 < |\eta| < 4.9$ and full azimuth (Alves *et al.*, 2008). This spectrometer arm is capable of tracking and particle identification, however, tracking is limited to low multiplicity collisions.

B. Centrality determination

The impact parameter b , defined as the transverse distance between the centers of the two colliding nuclei, cannot be measured directly. Glancing interactions with a large impact parameter generally produce fewer particles while collisions with a small impact parameter generally produce more particles, with the number of final state particles increasing monotonically with the overlap volume between the nuclei. This correlation can be used to define the collision centrality as a fraction of the total cross section. High multiplicity events have a low average b and low multiplicity events have a large average b . The former are called central collisions and the latter are called peripheral collisions. In large collision systems, the variations in the number of particles produced due to fluctuations in the energy production by individual soft nucleon-nucleon collisions is small compared to the variations due to the impact parameter. The charged particle multiplicity, N_{ch} , can then be used to constrain the impact parameter.

Usually the correlation between the impact parameter and the multiplicity is determined using a Glauber model (Miller *et al.*, 2007). The distribution of nucleons

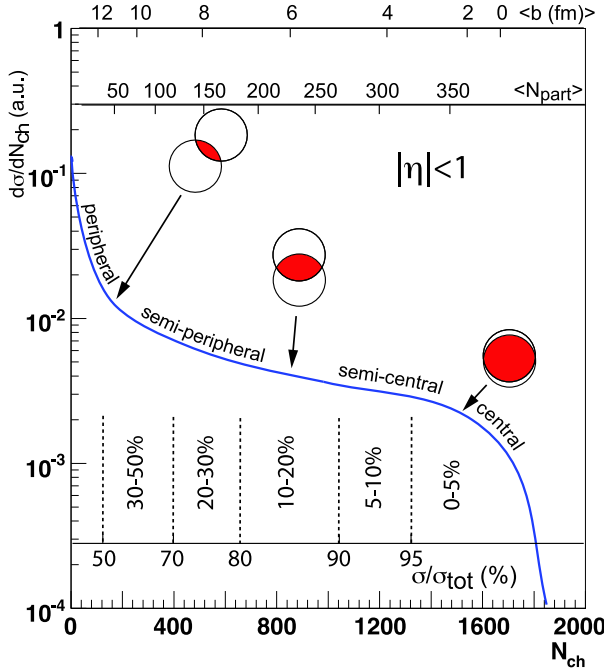


FIG. 4 Cartoon showing the correlation between the multiplicity N_{ch} , the impact parameter b , the number of binary nucleon-nucleon collisions N_{bin} , and the number of participating nucleons N_{part} . Figure from (Miller *et al.*, 2007) courtesy of Thomas Ullrich.

in the nucleus is usually approximated as a Fermi distribution in a Woods-Saxon potential and the multiplicity is assumed to be a function of the number of participating nucleons (N_{part}) and the binary number of interactions between nucleons (N_{bin}). The experimentally observed multiplicity is fit to determine a parametric description of the data and the data are binned by the fraction of events. For example, the 10% of all events with the highest multiplicity are referred to as 0-10% central. There are a few variations in technique which generally lead to consistent results (Abelev *et al.*, 2013c). Figure 4 illustrates this schematically. Centralities determined assuming that the distribution of impact parameters at a fixed multiplicity is Gaussian are consistent with those using a Glauber model (Das *et al.*, 2017).

The largest source of uncertainty from centrality determination in heavy ion collisions is due to the normalization of the multiplicity distribution at low multiplicities. In general an experiment identifies an anchor point in the distribution, such as identifying the N_{ch} where 90% of all collisions produce at least that multiplicity. Because the efficiency for detecting events with low multiplicity is low, the distribution is not measured well for low N_{ch} , so identification of this anchor point is model dependent. This inefficiency does not directly impact measurements of jets in 0-80% central collisions because these events are typically high multiplicity, however, it can lead to a

significant uncertainty in the correct centrality. This uncertainty is largest at low multiplicities, corresponding to more peripheral collisions.

As the phenomena observed in heavy ion collisions have been observed in increasingly smaller systems, this approach to determining centrality has been applied to these smaller systems as well. While the term “centrality” is still used, this is perhaps better understood as event activity, since the correlation between multiplicity and impact parameter is weaker in these systems and other effects may become relevant (Alvioli *et al.*, 2016, 2014; Alvioli and Strikman, 2013; Armesto *et al.*, 2015; Bzdak *et al.*, 2016; Coleman-Smith and Muller, 2014). The interpretation of the “centrality” dependence in small systems should therefore be done carefully.

803 C. Inclusive hadron measurements

Single particle spectra at high momenta, which are dominated by particles resulting from hard scatterings, can be used to study jets. To quantify any modifications to the hadron spectra in nucleus-nucleus ($A+A$) collisions, the nuclear modification factor was introduced. The nuclear modification factor in $A+A$ collisions is defined as

$$R_{AA} = \frac{\sigma_{NN}}{\langle N_{bin} \rangle} \frac{d^2 N_{AA}/dp_T d\eta}{d^2 \sigma_{pp}/dp_T d\eta} \quad (3)$$

where η is the pseudorapidity, p_T is the transverse momentum, $\langle N_{bin} \rangle$ is the average number of binary nucleon-nucleon collisions for a given range of impact parameter, and σ_{NN} is the integrated nucleon-nucleon cross section. N_{AA} and σ_{pp} in this context are the yield in $A+A$ collision and cross section in $p+p$ collisions for a particular observable. If nucleus-nucleus collisions were simply a superposition of nucleon-nucleon collisions, the high p_T particle cross-section should scale with the number of binary collisions and therefore $R_{AA} = 1$. An $R_{AA} < 1$ indicates suppression and an $R_{AA} > 1$ indicates enhancement. R_{AA} is often measured as a function of p_T and centrality class. Measurements of inclusive hadron R_{AA} are relatively straightforward as they only require measuring the single particle spectra and a calculation of the number of binary collisions for each centrality class based on a Glauber model (Miller *et al.*, 2007). Theoretically, hadron R_{AA} can be difficult to interpret, particularly at low momenta, because different physical processes that are not calculable in pQCD, such as hadronization, can change the interpretation of the result. Interpretation of R_{AA} usually focuses on high p_T , where calculations from perturbative QCD (pQCD) are possible. An alternative to R_{AA} is R_{CP} , where peripheral heavy ion collisions are used as the reference instead of $p+p$ collisions

$$R_{CP} = \frac{\langle N_{bin}^{peri} \rangle}{\langle N_{bin}^{cent} \rangle} \frac{d^2 N_{AA}^{cent}/dp_T d\eta}{d^2 N_{AA}^{peri}/dp_T d\eta} \quad (4)$$

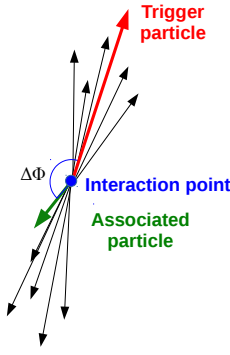


FIG. 5 Schematic diagram showing the identification of a high- p_T hadron in a $p+p$ collision and its use to define a coordinate system for dihadron correlations.

where *cent* and *peri* denote the values of $\langle N_{bin} \rangle$ and N_{AA} for central and peripheral collisions, respectively. This is typically done either when there is no $p+p$ reference available or the $p+p$ reference has much larger uncertainties than the $A+A$ reference. It does have the advantage that other nuclear effects could be present in the R_{CP} cross-section and cancel in the ratio, and that these collisions are recorded at the same time and thus have the same detector conditions. However, there can be QGP effects in peripheral collisions so this can make the interpretation difficult. The pQCD calculations used to interpret these results are sensitive in principle to hadronization effects, however, if the R_{AA} of hard partons does not have a strong dependence on p_T , the R_{AA} of the final state hadrons will not have a strong dependence on p_T . R_{AA} will therefore be relatively insensitive to the effects of hadronization and more theoretically robust.

D. Dihadron correlations

A hard parton scattering usually produces two partons that are separated by 180° in the transverse plane (commonly stated as back-to-back). In a typical dihadron correlation study (Aamodt *et al.*, 2012; Abelev *et al.*, 2009b; Adler *et al.*, 2003a, 2006d; Alver *et al.*, 2010), a high- p_T hadron is identified and used to define the coordinate system because its momentum is assumed to be a good proxy for the jet axis of the parton it arose from. This hadron is called the trigger particle. The azimuthal angle of other hadrons' momenta in the event is calculated relative to the momentum of this trigger particle. These hadrons are commonly called the associated particles. This is illustrated schematically in Figure 5. The associated particle is typically restricted to a fixed momentum range, also typically higher than the $\langle p_T \rangle$ of tracks in the event and lower than the momenta of trigger particles. The distribution of associated particles relative

to the trigger particle can be measured in azimuth ($\Delta\phi$), pseudorapidity ($\Delta\eta$), or both.

Figure 6 shows a sample dihadron correlation in $\Delta\phi$ and $\Delta\eta$ and its projection onto $\Delta\phi$ for trigger momenta $10 < p_T^t < 15$ GeV/c within pseudorapidities $|\eta| < 0.5$ and associated particles within $|\eta| < 0.9$ with momenta $1.0 < p_T^a < 2.0$ GeV/c in $p+p$ collisions at $\sqrt{s} = 2.76$ TeV in PYTHIA (Sjostrand *et al.*, 2006). The peak near 0° , called the near-side, is narrow in both $\Delta\phi$ and $\Delta\eta$ and results from associated particles from the same parton as the trigger particle. The peak near 180° , called the away-side, is narrow only in $\Delta\phi$ and is roughly independent of pseudorapidity. This peak arises from associated particles produced by the parton opposing the one which generated the trigger particle. The partons are back-to-back in the frame of the partons, but the rest frame of the partons is not necessarily the same as the rest frame of the incoming nuclei because the incoming partons may not carry the same fraction of the parent nucleons' momentum, x . Since most of the momenta of both the partons and the nucleons are in the direction of the beam (which is universally taken to be the z axis), a difference in pseudorapidity is observed, while the influence on the azimuthal position is negligible. This causes the away-side to be broad in $\Delta\eta$ without requiring modified fragmentation or interaction with the medium, as evident in Figure 6.

1. Background subtraction methods

Dihadron correlations typically have a low signal to background ratio, often less than 1:25. The raw signal in dihadron correlations is typically assumed to arise from only two sources, particles from jets and particles from the underlying event, which are correlated with each other due to flow. The production mechanisms of the signal and the background are assumed to be independent so they can be factorized. These assumptions are called the two source model (Adler *et al.*, 2006b). The correlation of two particles in the background due to flow is given by (Adler *et al.*, 2003a; Bielcikova *et al.*, 2004)

$$\frac{dN}{\pi d\Delta\phi} = B(1 + \sum_{n=1}^{\infty} 2v_n^t v_n^a \cos(n\Delta\phi)) \quad (5)$$

where B is a constant which depends on the normalization and the multiplicity of trigger and associated particles in an event, the v_n^t are the v_n for the trigger particle, the v_n^a are the v_n for the associated particle, and $\Delta\phi$ is the difference in azimuthal angle between the associated particle and the trigger. The v_n for the trigger particle may arise either from flow, if the trigger particle is not actually from a jet, or from jet quenching, since the path length dependence of partonic energy loss leads to a suppression of jets out-of-plane. Because dihadron cor-

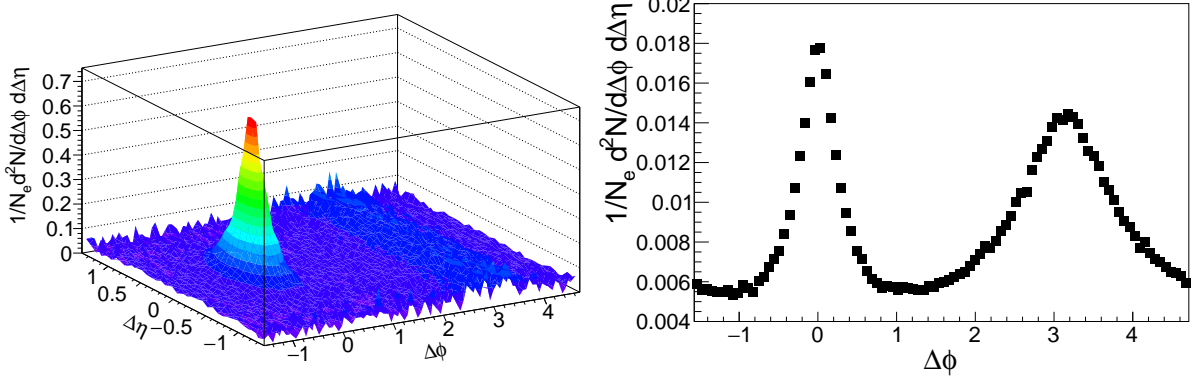


FIG. 6 Dihadron correlations for trigger momenta $10 < p_T^b < 15$ GeV/c and $1.0 < p_T^a < 2.0$ GeV/c within pseudorapidities $|\eta| < 0.5$ and associated particles within $|\eta| < 0.9$ in $p+p$ collisions at $\sqrt{s} = 2.76$ TeV in PYTHIA (Sjostrand *et al.*, 2006). The signal is normalized by the number of equivalent Pb+Pb collisions. Left: Correlation function as a function of $\Delta\phi$ and $\Delta\eta$. Right: Projection onto $\Delta\phi$.

relations are typically measured by averaging over positive and negative pseudorapidities, the average v_1 due to flow is zero and the $n = 1$ term is usually omitted. Global momentum conservation also leads to a v_1 signal which is approximately inversely proportional to the particle multiplicity (Borghini *et al.*, 2000). The momentum conservation term is typically assumed to be negligible, which may be valid for higher multiplicity events. The pseudorapidity range for both trigger and associated particles is typically restricted to a region where the v_n do not change dramatically so that the pseudorapidity dependence of $\frac{dN}{d\phi}$ is negligible. The azimuthal dependence of any additional sources of long range correlations could be expanded in terms of their Fourier coefficients without loss of generality.

There are two further assumptions commonly used in order to subtract this background: that the appropriate v_n are the same as the v_n measured in other analyses and that there is a region in $\Delta\phi$ near $\Delta\phi \approx 1$ where the signal is zero. The latter assumption is called the Zero-Yield-At-Minimum (ZYAM) method (Adams *et al.*, 2005a). Early studies of dihadron correlations fit the data near $\Delta\phi \approx 1$ to determine the background level (Adams *et al.*, 2004a; Adare *et al.*, 2007b,b; Adler *et al.*, 2003a, 2006c). Later studies typically use a few points around the minimum (Adler *et al.*, 2006b; Agakishiev *et al.*, 2010; Aggarwal *et al.*, 2010). An alternative to ZYAM for determining the background level, B in Equation 5, is the absolute normalization method (Sickles *et al.*, 2010). This method makes no assumption about the background level based on the shape of the underlying background but rather estimates the level of combinatorial pairs from the mean number of trigger and mean number of associated particles in all events as a function of event multiplicity.

It has been suggested that Hanbury-Brown-Twiss (HBT) correlations (Lisa and Pratt, 2008; Lisa *et al.*,

2005), quantum correlations between identical particles from the same source, may contribute to the near-side peak in some momentum regions. If the momenta of the trigger and associated particles are sufficiently different, these contributions are expected to be negligible. Distinguishing resonances from jet-like correlations is more difficult. A high momentum resonance can itself be considered a jet or part of a jet. The appropriate classification for lower momentum resonances is less clear, but functionally any short range correlations are considered part of the signal in dihadron correlations.

The background is then dominated by contributions from flow. However, this does not mean that the v_n measured in other analyses are necessarily the Fourier coefficients of the background for dihadron correlations. Methods for measuring v_n have varying sensitivities to non-flow (such as jets) and fluctuations (Voloshin *et al.*, 2008). Fluctuations in v_n may either increase or decrease the effective v_n , depending on their physical origin and its correlation with jet production. The correct v_n in equation 5 is also complicated by proposed decorrelations between the reaction planes for soft and hard processes, which would change the effective v_n (Aad *et al.*, 2014a; Jia, 2013). A recent method uses the reaction plane dependence of the background in equation 5 to extract the background level and shape from the correlation itself (Sharma *et al.*, 2016).

The majority of measurements of dihadron correlations in heavy ion collisions in the literature omit odd v_n since these studies were done before the odd v_n were observed and understood to arise due to collective flow. The first direct observation of the odd v_n was in high- p_T dihadron correlations, where subtraction of only the even v_n led to two structures called the ridge (on the near-side) (Abelev *et al.*, 2009b; Alver *et al.*, 2010) and the shoulder or Mach cone (on the away-side) (Abelev *et al.*,

949 2009b; Adare *et al.*, 2008a,a,d; Afanasiev *et al.*, 2008; 996
 950 Agakishiev *et al.*, 2010). This means that the majority 997
 951 of studies of dihadron correlations at low and interme- 998
 952 diate momenta ($p_T \lesssim 3$ GeV/c) do not take the odd 999
 953 v_n into account and therefore include distortions due to flow. 1000
 954 Exceptions are studies which used the $\Delta\eta$ dependence on 1001
 955 the near-side to subtract the ridge and focused on the 1002
 956 jet-like correlation (Abelev *et al.*, 2009b, 2010a, 2016; 1003
 957 Agakishiev *et al.*, 2012c). An understanding of the low 1004
 958 momentum jet components is important because many of 1005
 959 medium modifications of the jet manifest as differences in 1006
 960 distributions at low momenta. While some of the iconic 1007
 961 RHIC results showing jet quenching did not include odd 1008
 962 v_n (Adams *et al.*, 2004a) and the complex structures at 1009
 963 low and intermediate momenta are now understood to 1010
 964 arise due to flow rather than jets (Nattrass *et al.*, 2016), 1011
 965 some of the broad conclusions of these studies are robust, 1012
 966 and studies at sufficiently high momenta ($p_T \gtrsim 3$ GeV/c) 1013
 967 are still valid because the impact of the higher order v_n 1014
 968 is negligible. Section III focuses on results robust to the 1015
 969 omission of the odd v_n and more recent results.

970 E. Reconstructed jets

971 A jet is defined by the algorithm used to group final 1021
 972 state particles into jet candidates. In QCD any parton 1022
 973 may fragment into two partons, each carrying roughly 1023
 974 half of the energy and moving in approximately the same 1024
 975 direction. This is a difficult process to quantify theoreti- 1025
 976 cally and leads to divergencies in theoretical calculations. 1026
 977 A robust jet finding algorithm would find the same jet 1027
 978 with the same p_T regardless of the details of the fragmen- 1028
 979 tation and would thus be *collinear safe*. Additionally, 1029
 980 QCD allows for an infinite number of very soft partons 1030
 981 to be produced during the fragmentation of the parent 1031
 982 parton. All experiments have low momentum thresholds 1032
 983 for their acceptance so these particles cannot generally 1033
 984 be observed and the production of soft partons leads to 1034
 985 theoretical divergencies as well. A robust jet finding al- 1035
 986 gorithm will find the same jets, even in the presence of a 1036
 987 large number of soft partons and would thus be *infrared* 1037
 988 *safe*. In order for the jet definition to be robust, the 1038
 989 jet-finding algorithm must be both infrared and collinear 1039
 990 safe (Salam, 2010).

1038 Jet finding algorithms are generally characterized by a
 resolution parameter. In the case of a conical jet, this is
 the radius of the jets

$$R = \sqrt{\Delta\phi^2 + \Delta\eta^2} \quad (6)$$

991 where $\Delta\phi$ is the distance from the jet axis in azimuth and
 992 $\Delta\eta$ is the distance from the jet axis in pseudorapidity. A
 993 conical jet is symmetric in $\Delta\phi$ and $\Delta\eta$, although it is
 994 not theoretically necessary for jets to be symmetric. We 1039
 995 will focus the discussion on conical jets, since they are 1040

the most intuitive to understand. The most common jet-finding algorithm in heavy ion collisions, anti- k_T , usually reconstructs conical jets. The majority of jet measurements include corrections up to the energy of all particles in the jet, whether or not they are observed directly. The ALICE experiment also measures charged jets, which are corrected only up to the energy contained in charged constituents.

We emphasize that a measurement of a jet is not a direct measurement of a parton. A jet is a composite object comprising several final state hadrons. If the jet reconstruction algorithm applied to theoretical calculations and data is the same, experimental measurements of jets can be comparable to theoretical calculations of jets. However, even theoretically, it is unclear which final state particles should be counted as belonging to one parton. What the original parton's energy and momentum were before it fragmented is therefore an ill-posed question. The only valid comparisons between theory and experiment are between jets comprised of final state hadrons and reconstructed with the same algorithm. This understanding was the conclusion of the Snowmass Accord (Huth *et al.*, 1990). Ideally both the jet reconstruction algorithms and the treatment of the combinatorial background in heavy ion collisions would also be the same for theory and experiment.

1. Jet-finding algorithms

Infrared and collinear safe sequential recombination algorithms such as the k_T , anti- k_T and Cambridge/Aachen (CAMB) are encoded in *FastJet* (Cacciari *et al.*, 2011, 2008a,b, 2012; Salam, 2010). The *FastJet* (Cacciari *et al.*, 2012) framework takes advantage of advanced computing algorithms in order to decrease computational times for jet-finding. This is essential for jet reconstruction in heavy ion collisions due to the large combinatorial background. Due to the ubiquity of the anti- k_T jet-finding algorithm in studies of jets in heavy ion collisions, it is worth describing this algorithm in detail. The anti- k_T algorithm is a sequential recombination algorithm, which means that a series of steps for grouping particles into jet candidates is repeated until all particles in an event are included in a jet candidate. The steps are:

1. Calculate

$$d_{ij} = \min(1/p_{T,i}^2, 1/p_{T,j}^2) \frac{(\eta_i - \eta_j)^2 + (\phi_i - \phi_j)^2}{R^2} \quad (7)$$

and

$$d_i = 1/p_{T,i}^2 \quad (8)$$

for every pair of particles where $p_{T,i}$ and $p_{T,j}$ are the momenta of the particles, η_i and η_j are the

1041 pseudorapidities of the particles, and ϕ_i and ϕ_j are ¹⁰⁹⁵
 1042 the azimuthal angles of the particles. ¹⁰⁹⁶

1043 2. Find the minimum of the d_{ij} and d_i . If this mini- ¹⁰⁹⁷
 1044 mum is a d_{ij} , combine these particles into one jet ¹⁰⁹⁸
 1045 candidate, adding their energies and momenta, and ¹⁰⁹⁹
 1046 return to the first step.

1047 3. If the minimum is a d_i , this is a final state jet can- ¹¹⁰⁰
 1048 didate. Remove it from the list and return to the ¹¹⁰¹
 1049 first step. Iterate until no particles remain. ¹¹⁰²

1050 The original implementation of the anti- k_T used rapidity ¹¹⁰³
 1051 rather than pseudorapidity (Cacciari *et al.*, 2008a), how- ¹¹⁰⁴
 1052 ever, in practice most experiments cannot identify parti- ¹¹⁰⁵
 1053 cles to high momenta and the difference is negligible at ¹¹⁰⁶
 1054 high momenta so pseudorapidity is used in practice. ¹¹⁰⁷

2. Dealing with the background

1055 The anti- k_T algorithm has a few notable features for ¹¹⁰⁸
 1056 jet reconstruction in heavy ion collisions. Since d_{ij} is ¹¹⁰⁹
 1057 smallest for pairs of high- p_T particles, the anti- k_T al- ¹¹¹⁰
 1058 gorithm starts clustering high- p_T particles into jets first ¹¹¹¹
 1059 and forms a jet around these particles. The anti- k_T algo- ¹¹¹²
 1060 rithm creates jets which are approximately symmetric in ¹¹¹³
 1061 azimuth and pseudorapidity, at least for the highest en- ¹¹¹⁴
 1062 ergy jets. Particularly in heavy ion collisions, it must be ¹¹¹⁵
 1063 recognized that the “jets” from a jet-finding algorithm ¹¹¹⁶
 1064 are not necessarily generated by hard processes. Since ¹¹¹⁷
 1065 all final state particles are grouped into jet candidates, ¹¹¹⁸
 1066 some jet candidates will comprise only particles whose ¹¹¹⁹
 1067 production was not correlated because they were created ¹¹²⁰
 1068 in the same hard process but which randomly happen ¹¹²¹
 1069 to be in the same region in azimuth and pseudorapidity. ¹¹²²

1070 These jet candidates are called fake or combinatorial jets. ¹¹²³
 1071 Particles that are correlated through a hard process will ¹¹²⁴
 1072 be grouped into jet candidates, which will also contain ¹¹²⁵
 1073 background particles. Care must therefore be used when ¹¹²⁶
 1074 interpreting the results of a jet-finding algorithm as it is ¹¹²⁷
 1075 possible to have jet candidates in an analysis that come ¹¹²⁸
 1076 from processes that may not be included in the calcula- ¹¹²⁹
 1077 tion used to interpret the results. ¹¹³¹

1078 There are two important additional points to be made ¹¹³²
 1079 with regard to jet-finding algorithms as applied to heavy ¹¹³³
 1080 ion collisions. While jet-finding algorithms have been ¹¹³⁴
 1081 optimized for measurements in small systems such as ¹¹³⁵
 1082 $e^+ + e^-$ and $p + p$ collisions, these algorithms are computa- ¹¹³⁶
 1083 tionally efficient and well-defined both theoretically and ¹¹³⁷
 1084 experimentally. Although we may want to consider how ¹¹³⁸
 1085 we use these algorithms, there is no need for further de- ¹¹³⁹
 1086 velopment of jet-finding algorithms for use in heavy ion ¹¹⁴⁰
 1087 collisions. However, there is a difference between jet- ¹¹⁴¹
 1088 finding in principle and in practice. While these jet- ¹¹⁴²
 1089 finding algorithms are infrared and collinear safe *if all* ¹¹⁴³
 1090 *particles are input into the jet-finding algorithm*, most ex- ¹¹⁴⁴
 1091 perimental measurements restrict the momenta and ener- ¹¹⁴⁵
 1092 gies of the tracks and calorimeter clusters input into the ¹¹⁴⁶
 1093 jet-finding algorithms. Some apply other selection cri- ¹¹⁴⁷
 1094 teria to the population of jets, such as requiring a high ¹¹⁴⁸

1095 momentum track, which are not infrared or collinear safe. ¹⁰⁹⁶
 1096 These techniques are not necessarily avoidable, especially ¹⁰⁹⁷
 1097 in the high background environment of heavy ion colli- ¹⁰⁹⁸
 1098 sions, however, they must be considered when interpret- ¹⁰⁹⁹
 1099 ing the results.

1095 Combinatorial jets and distortions in the reconstructed ¹¹⁰⁰
 1096 jet energy due to background need to be taken into ac- ¹¹⁰¹
 1097 count in order to interpret a measured observable. This ¹¹⁰²
 1098 can be done either in the measurement, or in theoreti- ¹¹⁰³
 1099 cal calculations that are compared to the measurement. ¹¹⁰⁴
 1100 The latter is particularly difficult in a heavy ion environ- ¹¹⁰⁵
 1101 ment because the background has contributions from all ¹¹⁰⁶
 1102 particle production processes.

1103 While it is impossible to know which particles in a ¹¹⁰⁷
 1104 jet candidate come from hard processes and which come ¹¹⁰⁸
 1105 from the background, and indeed it is even ambiguous ¹¹⁰⁹
 1106 to make this distinction on theoretical level, differences ¹¹¹⁰
 1107 between particles in the signal and the background on av- ¹¹¹¹
 1108 erage can be used to reduce the impact of particles from ¹¹¹²
 1109 the background and calculate the impact of the remain- ¹¹¹³
 1110 ing background on an ensemble of jet candidates. As ¹¹¹⁴
 1111 mentioned in Section I, the average momentum of parti- ¹¹¹⁵
 1112 cles in the background is much lower than that of those ¹¹¹⁶
 1113 in the signal. Figure 7 shows a comparison of HYDJET ¹¹¹⁷
 1114 to STAR data (Lokhtin *et al.*, 2009b) and the particles ¹¹¹⁸
 1115 produced by hard and soft processes in HYDJET. At ¹¹¹⁹
 1116 sufficiently high p_T , particle production is dominated by ¹¹²⁰
 1117 hard processes. HYDJET has been tuned to match fluc- ¹¹²¹
 1118 tuations and v_n from heavy ion collisions, so this qualita- ¹¹²²
 1119 tive conclusion should be robust. Jets themselves can ¹¹²³
 1120 contribute to background for the measurement of other ¹¹²⁴
 1121 jets, however, the probability of multiple jets overlapping ¹¹²⁵
 1122 spatially and fragmenting into several high momentum ¹¹²⁶
 1123 particles is low. Therefore, introducing a minimum ¹¹²⁷
 1124 momentum for particles to be used in jet-finding reduces ¹¹²⁸
 1125 the number of background particles in the jet candi- ¹¹²⁹
 1126 dates. This also reduces the number of combinatorial ¹¹³⁰
 1127 jets, since there are very few high momentum particles ¹¹³¹
 1128 which were not created from a hard process. While this ¹¹³²
 1129 selection criterion reduces the background contribution, ¹¹³³
 1130 it is not collinear safe. Additionally, as most of the mod- ¹¹³⁴
 1131 ification of the jet fragmentation function is observed for ¹¹³⁵
 1132 constituents with $p_T < 3$ GeV, this could remove the ¹¹³⁶
 1133 modification signature for particular observables.

1134 The effect of the background can also be reduced by fo- ¹¹³⁵
 1135 cusing on smaller jets or higher energy jets. For a conical ¹¹³⁶
 1136 jet, the jet area is $A_{jet} = \pi R^2$. The average number of ¹¹³⁷
 1137 background particles in the jet candidate is proportional ¹¹³⁸
 1138 to the area. The background energy scales with the area ¹¹³⁹
 1139 of the jet, but is independent of the jet energy (assuming ¹¹⁴⁰
 1140 that the signal and background are independent), so the ¹¹⁴¹
 1141 fractional change in the reconstructed jet energy due to ¹¹⁴²

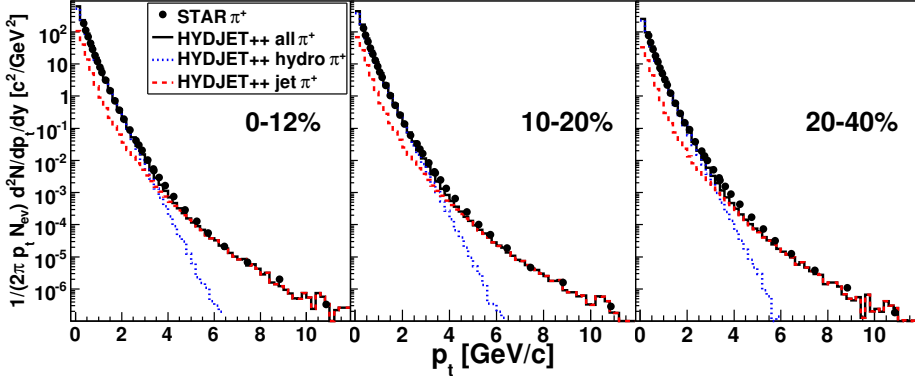


FIG. 7 Figure from (Lokhtin *et al.*, 2009b) comparing HYDJET (Lokhtin *et al.*, 2009a) calculations to STAR data (Abelev *et al.*, 2006). Particle production in HYDJET is separated into those from hard and soft processes. This shows that at sufficiently high momenta, particle production is dominated by hard processes.

background is smaller for higher energy jets as the majority of the jet energy is focused in the core of the jet. Furthermore, in elementary collisions, the distribution of final state particles in the jet as a function of the fraction of the jet energy carried by the particle is approximately independent of the jet energy. This means that the difference in the average momentum for signal particles versus background particles is larger for high energy jets. Since jets that interact with the medium are expected to lose energy and become broader, studies of high momentum, narrow jets alone cannot give a complete picture of partonic energy loss in the QGP. Furthermore, even in $p+p$ collisions, theoretical calculations are more difficult for jets with smaller cone sizes because they are sensitive to the details of the hadronization (Abelev *et al.*, 2013d).

The fraction of combinatorial jet candidates can also be reduced by requiring additional evidence of a hard process, such as requiring that the candidate jet has at least one particle above a minimum threshold, requiring that the jet candidate have a hard core, or identifying a heavy flavor component within the jet candidate. We note that the distinction between fake jets and the background contribution in jets from hard processes is ambiguous, particularly for low momentum jets, however, the corrections for these effects are generally handled separately. Below we review methods for addressing the impact of background particles on the jet energy and corresponding methods for dealing with any remaining combinatorial jets. Each of these methods have strengths and weaknesses, and may lead to biases in the surviving jet population.

There are five classes of methods for background subtraction in the four experiments which have published jet measurements in heavy ion collisions. ALICE and STAR use measurements of the average background energy/momentum density in the event to subtract the background contribution from jet candidates. ATLAS uses an iterative procedure, first finding jet candidates,

then omitting them from the calculation of the background energy distribution, and then using this background distribution to find new jet candidates. CMS subtracts background before jet finding, omitting jet candidates from the background subtraction. In addition, an event mixing method was recently applied to STAR data to estimate the average contribution from the background to both the jet energy and combinatorial jets. Constituent subtraction refers to corrections to account for background before jet finding. Each of these are described in greater detail below.

ALICE/STAR In this method the background contribution to a jet candidate is assumed to be proportional to the area of that candidate. The area of each jet is estimated by filling an event with many very soft, small area particles (ghost particles), rerunning the jet-finder, and then counting how many are clustered into a given jet. The background energy/momentum density per unit area (ρ) is measured by either using randomly oriented jet cones or the k_T jet-finding algorithm and calculating the momentum over the area of the cone or k_T jet. The median of the energy per unit area of the collection is used to reduce the impact from real jets in the event on the determination of the background density. The two highest energy jets in the event are omitted from the distribution of jets used to determine the background energy density. Since the background has a p_T modulation that is correlated with the reaction plane, an event plane dependent ρ can be determined as well (Adam *et al.*, 2016b).

This method was proposed in (Cacciari *et al.*, 2008b) for measurements in $p+p$ collisions under conditions with high pile up and its feasibility in heavy ion collisions demonstrated in (Abelev *et al.*, 2012a). The strength of this method is that it can be used even with jets clustered with low momentum constituents. However, the energy of individual jets is not known precisely since only the

average background contribution is subtracted, but the background itself could fluctuate which smears the measurement of the jet energy and momentum. Additionally measurements of the background energy density can include some contribution from real jets. Subtracting the average contribution to a jet candidate due to the background may not fully take into account the tendency of jet-finding algorithms to form combinatorial jets around hot spots in the background.

ATLAS We outline the approach in (Aad *et al.*, 2013b). We note that the details of the analysis technique are optimized for each observable. ATLAS measures both calorimeter and track jets. Track jets are reconstructed using charged tracks with $p_T > 4 \text{ GeV}/c$. The high momentum constituent cut strongly suppresses combinatorial jets, and ATLAS estimates that a maximum of only 4% of all $R = 0.4$ anti- k_T track jet candidates in 0-10% central Pb+Pb collisions contain a 4 GeV/c background track. For calorimeter jet measurements, ATLAS estimates the average background energy per unit area and the v_2 using an iterative procedure (Aad *et al.*, 2013b). In the first step, jet candidates with $R = 0.2$ are reconstructed. The background energy is estimated using the average energy modulated by the v_2 calculated in the calorimeters, excluding jet candidates with at least one tower with $E_T > \langle E_T \rangle$. Jets from this step with $E_T > 25 \text{ GeV}$ and track jets with $p_T > 10 \text{ GeV}/c$ are used to calculate a new estimate of the background and a new estimate of v_2 , excluding all clusters within $\Delta R < 0.4$ of these jets. This new background modulated by the new v_2 and jets with $E_T > 20 \text{ GeV}$ were considered for subsequent analysis.

Combinatorial jets are further suppressed by an additional requirement that they match a track jet with high momentum (e.g. $p_T > 7 \text{ GeV}/c$ (Aad *et al.*, 2013b)) or a high energy cluster (e.g. $E_T > 7 \text{ GeV}$ (Aad *et al.*, 2013b)) in the electromagnetic calorimeter. These requirements strongly suppress the combinatorial background, however, they may lead to fragmentation biases and may suppress the contribution from jets which have lost a considerable fraction of their energy in the medium. These biases are likely small for the high energy jets which have been the focus of ATLAS studies, however, the bias is stronger near the 20 GeV lower momentum threshold of ATLAS studies.

CMS In measurements by CMS the background is subtracted from the event before the jet-finding algorithm is run. The average energy and its dispersion is calculated as a function of η . Tower energies are recalculated by subtracting the mean energy plus the mean dispersion. Negative energies after this step are set to zero. These tower energies are input into a jet-finding algorithm and the

background is recalculated, omitting towers contained in the jets. The tower energies are again calculated by subtracting the mean energy plus the dispersion and setting negative values to zero.

Event Mixing The goal of event mixing is to generate the combinatorial background – in the case of jet studies, fake jets. In STAR, the fraction of combinatorial jets in an event class is generated by creating a mixed event where every track comes from a different event (Adamczyk *et al.*, 2017c). The data are binned in classes of multiplicity, reconstructed event plane, and z-vertex position so that the mixed event accurately reflects the distribution of particles in the background. Jet candidates are reconstructed using this algorithm in order to calculate the contribution from combinatorial jets, which can then be subtracted from the ensemble. This is a very promising method, particularly for low momentum jets, but we note that it is sensitive to the details of the normalization at low momenta. It is also computationally intensive, which may make it impractical, and it is unclear how to apply it to all observables.

Constituent Subtraction The constituent background subtraction method was first developed to remove pile-up contamination from LHC based experiments, where it is not unusual to have contributions from multiple collisions in a single event. Unlike the area based subtraction methods described above, the constituent method subtracts the background constituent-by-constituent. The intention is to correct the 4-momentum of the particles, and thus correct the 4-momentum of the jet (Berta *et al.*, 2014). It is necessary to consider the jet 4-momentum for some of the new jet observables that will be described in this paper, such as jet mass. The process is an iterative scheme that utilizes the ghost particles, which are nearly zero momentum particles with a very small area on the order of 0.005 which are embedded into the event by many jet finding algorithms. The jet finder is then run on the event, and the area is determined by counting the number of ghost particles contained within the jet. Essentially the local background density is determined and then subtracted from the constituents, which are thrown out if they reach zero momentum. The effect of this background scheme on the applicable observables is under study and it is not clear as of yet what its effect is compared to the more traditional area based background subtraction schemes.

F. Particle Flow

The particle flow algorithm was developed in order to use the information from all available sub-detectors

1324 in creating the objects that are then clustered with a 1380 jet-finding algorithm. Many particles will leave signals 1381 in multiple sub-detectors. For instance a charged pion 1326 will leave a track in a tracker and shower in a hadronic 1327 calorimeter. If information from both detectors is used, 1382 this would double count the particle. However, excluding 1329 a particular sub-detector would remove information 1383 about the energy flow in the collision as well. Tracking 1384 detectors generally provide better position information 1385 while hadronic calorimeters are sensitive to more particles 1386 but whose positions are altered by the high magnetic field 1387 necessary for tracking. The goal is to use the best information 1388 available to determine a particle's energy and 1389 position simultaneously.

1390 The particle flow algorithm operates by creating stable 1391 particles from the available detectors. Tracks from the 1392 tracker are extrapolated to the calorimeters – in the case 1393 of CMS, an electromagnetic calorimeter and a hadronic 1394 calorimeter (CMS, 2009). If there is a cluster in the as- 1395 sociated calorimeter, it is linked to the track in question. 1396 Only the closest cluster to the track is kept as a charged 1397 particle should only have a single track. The energy and 1398 momentum of the cluster and track are compared. If the 1399 energy is low enough compared to the momentum, only 1400 a single hadron with momentum equal to a weighted average 1401 of the track and calorimeter is created. The exact 1402 threshold should depend on the details of the detector 1403 and its energy resolution. If the energy is above a certain 1404 threshold, neutral particles are then created out of 1405 the excess energy. If that excess is only in an electromagnetic 1406 calorimeter, the neutral particle is assumed to be a photon. If the excess is in a hadronic calorimeter, the neutral particle is assumed to be a hadron. If there is some combination, multiple neutral particles may be created, with the photon given preference in terms of "using up" the excess energy.

1412 By grouping the information into individual particles, the particle flow algorithm reduces the sensitivity of the measurement of the jet energy to the jet fragmentation pattern. This is a correction that can be done prior to unfolding, which is described below. The particle flow algorithm can be a powerful tool, however, it depends on the details of the sub-detectors that are available, their energy resolution, and their granularity. For example, the ALICE detector has precision tracking detectors and an electromagnetic calorimeter but no hadronic calorimeter. The optimal particle flow algorithm for the ALICE detector is to use the tracking information when available and only use information from the electromagnetic calorimeter if there is no information from the tracking detectors. Additionally, the magnetic field strength plays a role, as this will dictate how much the charge particle paths diverge from one another before reaching the calorimeter and how far charged particles are deflected before reaching the calorimeters. To fully utilize this algorithm, the energy resolution of all calorimeters must

be known precisely, and the distribution of charged and neutral particles must be known.

G. Unfolding

1383 Before comparing measurements to theoretical calculations or other measurements, they must be corrected for both detector effects and smearing due to background fluctuations. Both the jet energy scale (JES) and the jet energy resolution (JER) need to be considered in any correction procedure. The jet energy scale is a correction to the jet to recover the true 4-vector of the original jet (and not of the parton that created it). The background subtraction methods described above are examples of corrections to the jet energy scale due to the addition of energy from the underlying background. Precision measurements of the energy scale, as done by the ATLAS collaboration (ATL, 2015a), are an important step in understanding the detector response and necessary to reduce the systematic uncertainties. The jet energy resolution is a measure of the width of the jet response distribution. An example from the ALICE experiment can be seen in Figure 8. In heavy-ion collisions there are two components, the increase in the distribution due to the fluctuating background that will be clustered into the jet, and due to detector effects.

1384 In most measurements of reconstructed jets, the jet energy resolution is on the order of 10-20% for the high momentum jets, where detector effects dominate. This can be understood because even a hadronic calorimeter is not equally efficient at observing all particles. In particular, the measurement of neutrons, antineutrons, and the K_L^0 is difficult. The high magnetic field necessary for measuring charged particle momentum leads to a lower threshold on the momenta of reconstructed particles and can sweep charged particles in or out of the jet. As a result, even an ideal detector has a limited accuracy for measuring jets. The large fluctuations in the measured jet energy due to these effects distort the measured spectrum. This is qualitatively different from measurements of single particle observables, where the momentum resolution is typically 1% or better, often negligible compared to other uncertainties. This means that measurements of jet observables must be corrected for fluctuations due to the finite detector resolution if they will be compared to theoretical calculations or to measurements of the same observable in a different detector, or even from the same detector with different running conditions. Fluctuations in the background in $A+A$ collisions lead to further distortions in the reconstructed jet energy. Correcting for these effects is generally referred to as unfolding in high energy physics, although it is called unsmeared or deconvolution in other fields.

1385 Here we summarize unfolding methods, based on the discussion in (Adye, 2011; Cowan, 2002). If the true value

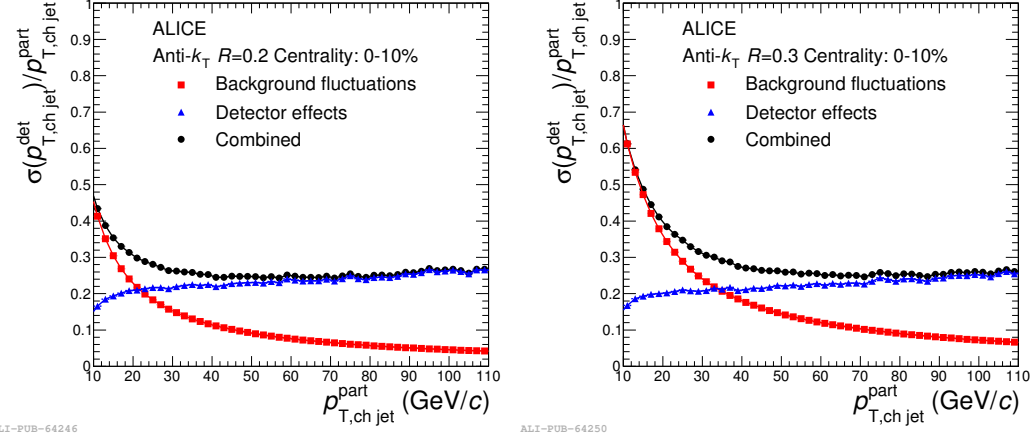


FIG. 8 Figure from ALICE (Abelev *et al.*, 2014a). On the left is the standard deviation of the combined jet response (black circles) for $R=0.2$ anti- k_T jets, including background fluctuations (red squares) and detector effects (blue triangles) for 0-10% central Pb+Pb events. On the right is the standard deviation of the combined jet response (black circles) for $R=0.3$ anti- k_T jets, including background fluctuations (blue triangles) and detector effects (red squares) for 0-10% central Pb-Pb events. The background effects increase the jet energy resolution more for larger jets, as can be seen from the difference in the background distributions in both plots. For high momentum jets, where the momentum of the jet is much larger than background fluctuations, the jet energy resolution will be dominated by detector effects.

of an observable in a bin i is given by y_i^{true} , then the observed value in bin j , y_j^{reco} , is given by

$$y_j^{reco} = \sum_{i=0}^N R_{ij} y_i^{true} \quad (9)$$

where R_{ij} is the response matrix relating the true and reconstructed values.

The response matrix is generally determined using Monte Carlo models including particle production, propagation of those particles through the detector material and simulation of its response, and application of the measurement algorithm, although sometimes data-driven corrections are incorporated into the response matrix. As an example, we consider the analysis of jet spectra. The truth result (y_i^{true}) is usually generated by an event generator such as PYTHIA (Sjostrand *et al.*, 2006) or DPM-JET (Ranft, 1999). The jet finding algorithm to be used in the analysis is run on this truth event, which generates the particle level jets comprising y_i^{true} . The truth event is then run through a simulation of the detector response. It is common to include a simulated background from a generator such as HIJING (X.-N. Wang, and M. Gyulassy, 1991), but not required. This creates the reconstructed event, and as before, the jet finding algorithm used in the analysis is run on this event to create the detector level jets that make up y_j^{reco} . Next, the particle level jets must be matched to detector level jets to build the response matrix, with unmatched jets determining the reconstruction efficiency. There are several ambiguities in this method. The first is that it comes with an assumption of the spectra shape and fragmentation pat-

tern of the jets from the simulation. The second is that there is not always a one-to-one correspondence between the truth and detector level jets. The detector response may cause the energy of a particular truth jet to be split into two detector level jets. However, the response matrix requires a one-to-one correspondence, which necessitates a choice.

If one could simply invert the response matrix, it would be possible to determine $y_i^{true} = \sum_{i=0}^N R_{ij}^{-1} y_j^{reco}$. However, response matrices for jet observables are generally ill-conditioned and not invertible. The further the jet response matrix is from a diagonal matrix, the more difficult the correction procedure is. This is one reason the background subtraction methods outlined in the preceding section are employed. By correcting the jet energy scale on a jet-by-jet basis, the response matrix is much closer to a diagonal matrix, however this is not a sufficient correction. The process of unfolding is thus required to determine y_i^{true} given the information in Equation 9.

One of the main challenges in unfolding is that it is an ill-posed statistical inverse problem which means that even though the mapping of y_i^{true} to y_j^{reco} is well-behaved, the inverse mapping of y_j^{reco} to y_i^{true} is unstable with respect to statistical fluctuations in the smeared observations. This is a problem even if the response matrix is known with precision. The issue is that within the statistical uncertainties, the smeared data can be explained by the actual physical solution, but also by a large family of wildly oscillating unphysical solutions. The smeared observations alone cannot distinguish among these alternatives, so additional a priori information about physically plausible solutions needs to

be included. This method of imposing physically plausible solutions is called regularization, and it essentially is a method to reduce the variance of the unfolded truth points by introducing a bias. The bias generally comes in the form of an assumption about the smoothness of the observable, however, this assumption always results in a loss of information.

If an observable is described well by models, it may be possible to correct the measurement using the ratio of the observed to the true value in Monte Carlo:

$$\gamma_j^{true} = \frac{\gamma_j^{true,MC}}{y_j^{reco,MC}} y_j^{reco} \quad (10)$$

where γ_j^{true} is the estimate of the true value, $\gamma_j^{true,MC}$ is the true value in the Monte Carlo model, and $y_j^{reco,MC}$ is the measurement predicted by the model. This approach is called a bin-by-bin correction. It is also satisfactory when the response matrix is nearly diagonal which is generally true when the bin width is wider than the resolution in the bin. In this circumstance, the inversion of the response matrix is generally stable and the measurement is not affected significantly by statistical fluctuations in the measurement or the response matrix. For example, bin-by-bin efficiency corrections to measurements of single particle spectra may be adequate as long as the momentum resolution is fairly good and the input spectra have roughly the same shape as the true spectra. This approach can work for measurements of reconstructed jets in systems such as $p+p$ collisions [e.g. fragmentation function measurements]. Unfortunately, for typical jet measurements, the desired binning is significantly narrower than the jet energy resolution, and fluctuations in the response matrix then lead to instabilities if the response matrix is inverted. Additionally, the high background environment of heavy ion collisions leads to lower energy resolution, and Monte Carlo models generally do not describe the data well. Bin-by-bin corrections are therefore usually inadequate for measurements in heavy ion collisions.

Several algorithms have been developed to solve equation 9. The two most commonly used algorithms are Single Value Decomposition (SVD) (Hocker and Kartvelishvili, 1996) and Bayesian Unfolding (D'Agostini, 1995). Bayesian unfolding uses a guess, which is called the prior of the true distribution, usually from a Monte Carlo model, as the start of an iterative procedure. This method is regularized by choosing how many iterations to use, where choosing an early iteration will result in a distribution that is closer to the prior, and thus more regularized. As the number of iterations increase there is a positive feedback which is driven by fluctuations in the response matrix and spectra, that makes the asymptotically unfolded spectrum diverge sharply from reality. The SVD formalism is a way by which to factorize a matrix into a set of matrices. This is used to write the

'unfolding' equation as a set of linear equations, with the assumption that the response matrix R can be decomposed into three matrices such that $R = USV^T$ where U and V are orthogonal and S is diagonal. The regularization method for using SVD formalism in unfolding uses a damped least squares method to couple all the linear equations that come out of the process and solve them. One then chooses a parameter, k , which corresponds to the k^{th} singular value of the decomposed matrix, and suppresses the oscillatory divergences in the solution.

It is worth noting that for any approach, there is a trade off between potential bias imposed on the results by the input from the Monte Carlo and the uncertainty in the final result. In practice, different methods and different training for Bayesian unfolding are compared for determination of the systematic uncertainties. For measurements where models describe the data well or where the resolution leads to minimal bin-to-bin smearing, bin-by-bin corrections are often preferred, both because of the potential bias and because of the difficulty of unfolding.

In order to confirm whether a particular algorithm used in unfolding is valid, it is necessary to perform closure tests, demonstrations that the method leads to the correct value when applied to a Monte Carlo model. The most simple tests are to convolute the Monte Carlo truth distribution with the response matrix to form a simulated detector distribution. This distribution can then be unfolded and compared to the original truth distribution. For this test, one should use roughly the same statistical precision as will be available in the data given how strongly the unfolding procedure is driven by statistics. However, this does not test the validity of the response matrix, or of the choice of spectral shape for the input distribution, or of the effect of combinatorial jets that will appear in the measured data. A more rigorous closure test can be done by embedding the detector level jets into minimally biased data, and performing the background and unfolding procedures on the embedded data to compare with the truth distribution.

Another approach is to "fold" the reference to take detector effects into account. For example, the initial measurements of the dijet asymmetry did not correct for the effect of background or detector resolution in $\text{Pb}+\text{Pb}$ but instead embedded $p+p$ jets in a $\text{Pb}+\text{Pb}$ background in order to smear the $p+p$ by an equivalent amount (Aad *et al.*, 2010; Chatrchyan *et al.*, 2011b). This may lead to a better comparison between data and a particular theory, but since the response matrix is generally not made available outside of the collaboration, it can only be done by experimentalists at the time of the publication. However, this would be an important cross-check for any model as it removes the mathematical uncertainty due to the ill posed inverse problem.

1592 H. Comparing different types of measurements

1593 The ultimate goal of measurements of jets in heavy ion 1642
 1594 collisions is not to learn about jets but to learn about 1643
 1595 the QGP. Measurements of jets in $e^+ + e^-$ and $p + p$ colli- 1644
 1596 sions are already complicated and the addition of a large 1645
 1597 combinatorial background in heavy ion collisions imposes 1646
 1598 greater experimental challenges. Suppressing and sub- 1647
 1599 tracting the background imposes biases on the resultant 1648
 1600 jet collections. Additionally, selection criteria applied 1649
 1601 to the collection of jet candidates in order to remove 1650
 1602 the combinatorial contribution will also impose a bias. 1651
 1603 The exact bias imposed by these assumptions cannot be 1652
 1604 known without a complete understanding of the QGP, 1653
 1605 which is what we are trying to gain by studying jets. Oc- 1654
 1606 casionally various methods are claimed to be “unbiased”, 1655
 1607 but is unclear what this means precisely since every mea- 1656
 1608 surement is biased towards a subset of the population of 1657
 1609 jets created in heavy ion collisions. Any particular mea- 1658
 1610 surement may have several types of bias. We discuss a 1659
 1611 few types of bias below.

1612 *Survivor bias* As jets interact with the medium and lose 1663
 1613 energy to the medium, they may begin to look more like 1664
 1614 the medium. There are fluctuations in how much energy 1665
 1615 each individual parton will lose in the medium, and se- 1666
 1616 lecting jets which look like jets in a vacuum may skew 1667
 1617 our measurements towards partons which have lost less 1668
 1618 energy in the medium.

1619 *Fragmentation bias* Many measurement techniques select 1673
 1620 jets which have hard fragments, which may lead to a 1674
 1621 survivor bias since interactions with the medium are ex- 1675
 1622 pected to soften the fragmentation function. Some mea- 1676
 1623 surements may preferentially select jets which fragment 1677
 1624 into a particular particle, such as a neutral pion or a 1678
 1625 proton. This in turn can bias the jet population to- 1679
 1626 wards quark or gluon jets. If fragmentation is modified 1680
 1627 in the medium, it could also bias the population towards 1681
 1628 jets which either have or have not interacted with the 1682
 1629 medium.

1630 *Quark bias* Even in $e^+ + e^-$ collisions, quark and gluon 1683
 1631 jets have different structures on average, with gluon 1684
 1632 jets fragmenting into more, softer particles at larger 1685
 1633 radii (Abreu *et al.*, 1996; Akers *et al.*, 1995). A 1686
 1634 bias may also be imposed by the jet-finding algorithm. 1687
 1635 OPAL found that gluon jets reconstructed with the k_T 1688
 1636 jet finding algorithm generally contained more parti- 1689
 1637 cles than those reconstructed with the cone algorithm 1690
 1638 in (Abe *et al.*, 1992) and that gluon jets contain more 1691
 1639 baryons (Ackerstaff *et al.*, 1999).

1640 The measurement techniques described above gener-
 1641 ally focus on higher momentum jets which fragment
 1642 into harder constituents and have narrower cone radii.
 1643 This surely induces a bias towards quark jets. Since
 1644 gluon jets are expected to outnumber quark jets signifi-
 1645 cantly (Pumplin *et al.*, 2002), this may not be quantita-
 1646 tively significant overall, depending on the measurement
 1647 and the collision energy. In some measurements, sur-
 1648 vivor bias is used as a tool. For instance measurements of
 1649 hadron-jet correlations select a less modified jet by iden-
 1650 tifying a hard hadron and then look for its partner jet on
 1651 the away-side (Adam *et al.*, 2015c). Correlations requir-
 1652 ing a trigger on both the near and away sides select jets
 1653 biased to be near the surface of the medium (Agakishiev
 1654 *et al.*, 2011). These biases are inherently unavoidable
 1655 and they must be understood in order to properly inter-
 1656 pret data. However, once they are well understood, the
 1657 biases can be engineered to purposefully select particu-
 1658 lar populations of jets, for instance to select jets biased
 1659 towards the surface in order to increase the probability
 1660 that the away side jet has traversed the maximum possi-
 1661 ble medium.

1662 As our experience with the v_n modulated background
 1663 in dihadron correlations shows, the issue is not merely
 1664 which measurements are most sensitive to the properties
 1665 of the medium but the possibility that our current under-
 1666 standing of the background may be incomplete. However,
 1667 the potential error introduced varies widely by the mea-
 1668 surement – single particle spectra, dihadron correlations,
 1669 and reconstructed jets all have completely different biases
 1670 and assumptions about the background. Our certainty in
 1671 the interpretation of the results is therefore enhanced if
 1672 the same conclusions can be drawn from measurements
 1673 of multiple observables. We therefore discuss a variety of
 1674 different measurements in Section III and demonstrate
 1675 that they all lead to the same conclusions – partons lose
 1676 energy in the medium and their constituents are broad-
 1677 ened and softened in the process.

1678 III. OVERVIEW OF EXPERIMENTAL RESULTS

1679 RHIC and the LHC have provided a wealth of data
 1680 which enhance our understanding of the properties of
 1681 the QGP. This section of the article reviews experimen-
 1682 tal results available at the time of publication, and
 1683 is organized according to the physics addressed by the
 1684 measurement rather than according to observable to
 1685 focus on the implications of the measurements. Therefore
 1686 the same observable may appear in multiple subsections.
 1687 The questions that jet studies attempt to answer to un-
 1688 derstand the QGP are: Are there cold nuclear matter ef-
 1689 fects which must be taken into consideration in order to
 1690 interpret results in heavy ion collisions? Do partons lose
 1691 energy in the medium and how much? How do partons
 1692 fragment in the medium? Is fragmentation the same as

in vacuum or is it modified? Where does the lost energy go and how does it influence the medium? Finally, in the next section we will discuss how well these questions have been answered and the questions that remain.

1697 A. Cold nuclear matter effects

1698 Cold nuclear matter effects refer to observed differences
 1699 between $p+p$ and $p+A$ or $d+A$ collisions where a hot
 1700 medium is not expected, but the presence of a nucleus
 1701 in the initial state could influence the production of the
 1702 final observable. These effects may result from coherent
 1703 multiple scattering within the nucleus (Qiu and Vitev,
 1704 2006), gluon shadowing (Gelis *et al.*, 2010), or partonic
 1705 energy loss within the nucleus (Bertocchi and Treleani,
 1706 1977; Vitev, 2007; Wang and Guo, 2001). While such
 1707 effects are interesting in their own right, if present, they
 1708 would need to be taken into account in order to interpret
 1709 heavy ion collisions correctly. Studies of open heavy fla-
 1710 vor at forward rapidities through spectra (Adare *et al.*,
 1711 2012a) and correlations (Adare *et al.*, 2014b) of leptons
 1712 from heavy flavor decays indicate that heavy flavor is
 1713 suppressed in cold nuclear matter. The J/ψ is also sup-
 1714 pressed at forward rapidities (Adare *et al.*, 2013d). Re-
 1715 cent studies have also indicated that there may be col-
 1716 lective effects for light hadrons in $p+A$ collisions (Aad
 1717 *et al.*, 2014d; Adam *et al.*, 2016h; Khachatryan *et al.*,
 1718 2015a) and even high multiplicity $p+p$ events (Aad *et al.*,
 1719 2016b; Khachatryan *et al.*, 2017b). Studies of jet produc-
 1720 tion in $p+A$ or $d+A$ collisions are necessary to quantify
 1721 the cold nuclear matter effects and decouple which effects
 1722 observed in $A+A$ data come from interactions with the
 1723 medium.

1724 Measurements of inclusive hadron R_{dAu} at $\sqrt{s_{NN}} =$
 1725 200 GeV (Abelev *et al.*, 2010b; Adler *et al.*, 2007b) and
 1726 R_{pPb} at $\sqrt{s_{NN}} = 5.02$ TeV (ATL, 2016; Aad *et al.*,
 1727 2016c; Abelev *et al.*, 2013e; Khachatryan *et al.*, 2015b,
 1728 2017a) are consistent with one within the systematic un-
 1729 certainties of these measurements, indicating that the
 1730 large hadron suppression observed in $A+A$ collisions can
 1731 not be due to cold nuclear matter effects. This is shown in
 1732 Figure 9. We note here that the CMS results shown here
 1733 were updated with a $p+p$ reference measured at $\sqrt{s_{NN}} =$
 1734 5.02 TeV (Khachatryan *et al.*, 2017a), which is also
 1735 consistent with an R_{pPb} of one.

1737 2. Reconstructed jets

1738 Measurements of reconstructed jets in $d+A$ collisions
 1739 at $\sqrt{s_{NN}} = 200$ GeV and $p+p$ collisions at 5.02 TeV in-
 1740 dicate that the minimum bias R_{dAu} (Adare *et al.*, 2016b)
 1741 and R_{pPb} (Aad *et al.*, 2015a; Adam *et al.*, 2016c), re-
 1742 spectively, are also consistent with one. Figure 10 shows
 1743 R_{pPb} measured by the CMS experiment and compared
 1744 to theoretical predictions.

1. Inclusive charged hadrons

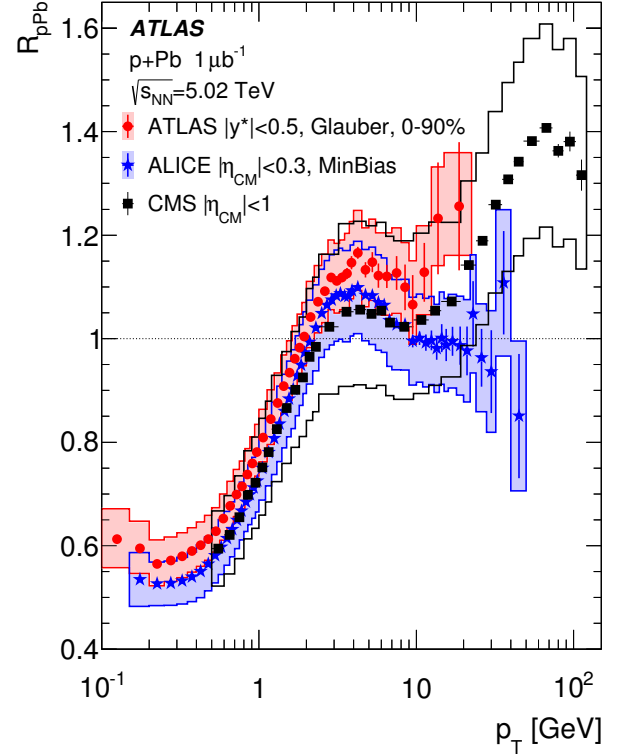


FIG. 9 Figure from ATLAS (Aad *et al.*, 2016c). The nuclear modification factor of charged hadrons in $p+Pb$ collisions at $\sqrt{s_{NN}} = 5.02$ TeV measured by the ALICE (Abelev *et al.*, 2013e), ATLAS (Aad *et al.*, 2016c), and CMS (Khachatryan *et al.*, 2015b) experiments. The data in this figure used an extrapolation of $p+p$ data from $\sqrt{s_{NN}} = 2.76$ TeV and 7 TeV as there was not a $p+p$ reference at the same energy available at this time. This shows that R_{pPb} is consistent with one within uncertainties for high p_T hadrons.

with NLO calculations including cold nuclear matter effects. The theoretical predictions and the experimental measurements in Figure 10 show that cold nuclear matter effects are small for jets for all p_T and pseudorapidity measured at the LHC. A centrality dependence at midrapidity in 200 GeV $d+A$ and 5.02 TeV $p+Pb$ collisions which cannot be fully explained by the biases in the centrality determination as studied in (Aad *et al.*, 2016a; Adare *et al.*, 2014a) is observed. It has been proposed that the forward multiplicities used to determine centrality are anti-correlated with hard processes at midrapidity (Armesto *et al.*, 2015; Bzdak *et al.*, 2016) or that the rare high- x parton configurations of the proton which produce high-energy jets have a smaller cross-section for inelastic interactions with nucleons in the nucleus (Alvioli *et al.*, 2016, 2014; Alvioli and Strikman, 2013; Coleman-Smith and Muller, 2014). The latter suggests that high p_T jets may be used to select proton configurations with

1762 varying sizes due to quantum fluctuations. While this 1810 is interesting in its own right and there may be initial 1811 state effects, there are currently no indications of large 1812 partonic energy loss in small systems, thus scaling the 1813 production in $p+p$ with the number of binary nucleon- 1814 nucleon collisions as a reference appears to valid for com- 1815 parison to larger systems. 1768

1769 3. Dihadron correlations

1770 Detailed studies of the jet structure in d +Au and com- 1771 parisons to both PYTHIA and $p+p$ collisions using di- 1772 hadron correlations at $\sqrt{s_{NN}} = 200$ GeV found no evi- 1773 dence for modification of the jet structure at midrapidity 1774 in cold nuclear matter (Adler *et al.*, 2006d). Stud- 1775 ies of correlations between particles at forward rapidities 1776 ($1.4 < \eta < 2.0$ and $-2.0 < \eta < -1.4$) in order to search 1777 for fragmentation effects at low x also found no evidence 1778 for modified jets in cold nuclear matter (Adler *et al.*, 1779 2006a). However, jet-like correlations with particles at 1780 higher rapidities ($3.0 < \eta < 3.8$) indicated modifications 1781 of the correlation functions in d +Au collisions at 1782 $\sqrt{s_{NN}} = 200$ GeV (Adare *et al.*, 2011d). This indicates that nu- 1783 clear effects may have a strong dependence on x and that 1784 studies of cold nuclear matter effects for each observable 1785 are important in order to demonstrate the validity of the 1786 baseline for studies in hot nuclear matter. While there is 1787 little evidence for effects at midrapidity, observables at 1788 forward rapidities may be influenced by effects already 1789 present in cold nuclear matter. Searches for acoplanarity 1790 in jets in p +Pb collisions observed no difference between 1791 jets in p +Pb and $p+p$ collisions (Adam *et al.*, 2015b).

1792 4. Summary of cold nuclear matter effects for jets

1793 Based on current evidence from p +Pb and d +Au colli- 1794 sions, $p+p$ collisions are an appropriate reference for jets, 1795 however, since numerous cold nuclear matter effects have 1796 been documented, each observable should be measured in 1797 cold nuclear matter in order to properly interpret data 1798 in hot nuclear matter. We therefore conclude that, based 1799 on the current evidence, p +Pb and d +Au collisions are 1800 appropriate reference systems for hard processes in $A+A$ 1801 collisions, although caution is needed, particularly at 1802 large rapidities and high multiplicities, and future studies 1803 in small systems may lead to different conclusions.

1804 B. Partonic energy loss in the medium

1805 Electroweak probes such as direct photons, which do 1861 not interact via the strong force, are expected to es- 1862 cape the QGP unscathed while probes which interact 1863 strongly lose energy in the medium and are suppressed at 1864 high momenta. Figure 11 shows a compilation of results 1865

1810 from PHENIX demonstrating that colored probes (high- 1811 p_T final state hadrons) are suppressed while electroweak 1812 probes (direct photons) are not at RHIC energies. Fig- 1813 ure 12 shows a similar compilation of results from the 1814 LHC, demonstrating that this is also true at higher ener- 1815 gies. This observed suppression in charged hadron spec- 1816 tra was the first indication of jet quenching in heavy ion 1817 collisions. The lowest value of the nuclear modification 1818 factor R_{AA} for light hadrons is about 0.2 in collisions 1819 at $\sqrt{s_{NN}} = 200$ GeV (Adams *et al.*, 2003b; Adler *et al.*, 1820 2003b; Back *et al.*, 2004) and about 0.1 in Pb+Pb colli- 1821 sions at LHC for $\sqrt{s_{NN}} = 2.76$ TeV and $\sqrt{s_{NN}} = 5.02$ 1822 TeV (CMS, 2016a; Aamodt *et al.*, 2011b; Chatrchyan 1823 *et al.*, 2012e). The R_{AA} of the charged hadron spectra 1824 appears to reach unity at $p_T \approx 100$ GeV/c (CMS, 2016a). 1825 This is expected from all QCD-inspired energy loss mod- 1826 els that at some point R_{AA} must reach one, because 1827 at leading order the differential cross section for inter- 1828 actions with the medium is proportional to $1/Q^2$ (Levai 1829 *et al.*, 2002). Studies of R_{CP} as a function of collision 1830 energy indicate that suppression sets in somewhere between 1831 $\sqrt{s_{NN}} = 27$ and 39 GeV (Adamczyk *et al.*, 2017a). At 1832 intermediate p_T the shape of R_{AA} with p_T is mass depen- 1833 dent with heavier particles approaching the light particle 1834 suppression level at higher momenta (Agakishiev *et al.*, 1835 2012a). However, even hadrons containing heavy quarks 1836 are suppressed at levels similar to light hadrons (Abelev 1837 *et al.*, 2012b).

1838 QCD-motivated models are generally able to describe 1839 inclusive single particle R_{AA} qualitatively, however, for 1840 each model the details of the calculations make it dif- 1841 ficult to compare results between models directly and 1842 extract quantitative information about the properties 1843 of the medium from such comparisons (Adare *et al.*, 1844 2008b). The JET collaboration was formed explic- 1845 itely to make such comparisons between models and 1846 data and their extensive studies determined that for 1847 a 10 GeV/c hadron the jet transport coefficient is 1848 $\hat{q} = 1.2 \pm 0.3$ GeV 2 in Au+Au collisions at $\sqrt{s_{NN}} = 200$ 1849 GeV and $\hat{q} = 1.9 \pm 0.7$ GeV 2 in Pb+Pb collisions at 1850 $\sqrt{s_{NN}} = 2.76$ TeV (Burke *et al.*, 2014).

1851 These detailed comparisons between data and energy 1852 loss models are one of the most important results in heavy 1853 ion physics and are one of the few results that directly 1854 constrain the properties of the medium. We emphasize 1855 that these constraints came from a careful comparison of 1856 a straightforward observable to various models. While 1857 we discuss measurements of more complicated observ- 1858 ables later, this highlights the importance of both pre- 1859 cision measurements of straightforward observables and 1860 careful, systematic comparisons of data to theory. Similar 1861 approaches are likely needed to further constrain the 1862 properties of the medium.

1863 It is remarkable that the R_{AA} values for hadrons at 1864 RHIC and the LHC are so similar since one would 1865 expect energy loss to increase with increased energy density

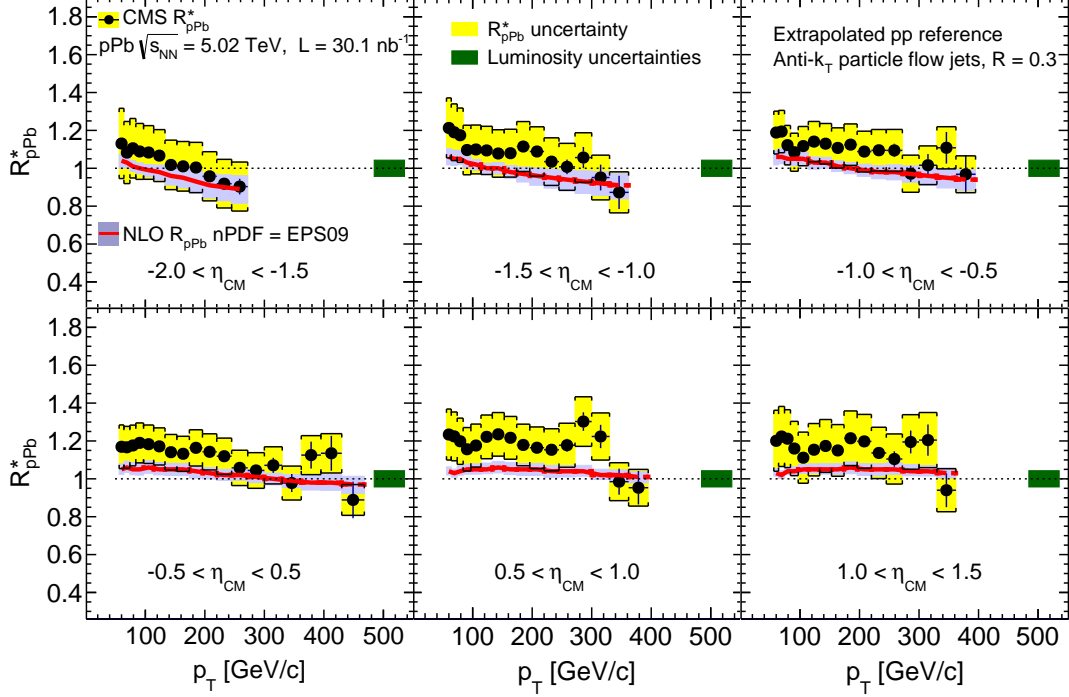


FIG. 10 Figure from CMS (Khachatryan *et al.*, 2016b). The nuclear modification factor of jets in $p+Pb$ collisions measured by the CMS experiment in various rapidity bins. This shows that cold nuclear matter effects are small for jets.

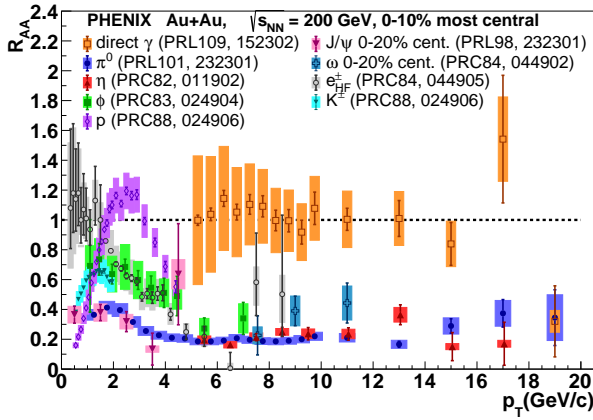


FIG. 11 R_{AA} from PHENIX for direct photons (Afanasiev *et al.*, 2012), π^0 (Adare *et al.*, 2008c), η (Adare *et al.*, 2010c), ϕ (Adare *et al.*, 2016c), p (Adare *et al.*, 2013e), J/ψ (Adare *et al.*, 2007a), ω (Adare *et al.*, 2011c), e^\pm from heavy flavor decays (Adare *et al.*, 2011a), and K^\pm (Adare *et al.*, 2013e). This demonstrates that colored probes (high- p_T final state hadrons) are suppressed while electroweak probes (direct photons) are not at RHIC.

pear at a lower p_T , so it is useful to study the shift of the hadron p_T spectrum in $A+A$ collisions to $p+p$ collisions rather than the ratio of yields. Note that the spectral shape also depends on the collisional energy. Spectra generally follow a power law trend described by $\frac{dN}{dp_T} \propto p_T^{-n}$ at high momenta. The spectra of hadrons is steeper in 200 GeV than in 2.76 TeV collisions ($n \approx 8$ and $n \approx 6.0$ respectively for the p_T range 7-20 GeV/c) (Adare *et al.*, 2012b, 2013c). Therefore, for R_{AA} , greater energy loss at the LHC could be counteracted by the flatter spectral shape. To address this, another quantity, the fractional momentum loss, (S_{loss}) has also been measured to better probe a change in the fractional energy loss of partons $\Delta E/E$ as a function of collision energy. This quantity is defined as

$$S_{loss} \equiv \frac{\delta p_T}{p_T} = \frac{p_T^{pp} - p_T^{AA}}{p_T^{pp}} \sim \left\langle \frac{\Delta E}{E} \right\rangle, \quad (11)$$

where p_T^{AA} is the p_T of the $A+A$ measurement. p_T^{pp} is determined by first scaling p_T spectrum measured in $p+p$ collisions by the nuclear overlap function, T_{AA} of the corresponding $A+A$ centrality class and then determining the p_T at which the yield of the scaled spectrum matches the yield measured in $A+A$ at the p_T^{AA} point of interest. This procedure is illustrated pictorially in Figure 13.

which should result in a lower R_{AA} at the LHC with its higher collision energies. However, the hadrons in a particular p_T range are not totally quenched but rather ap-

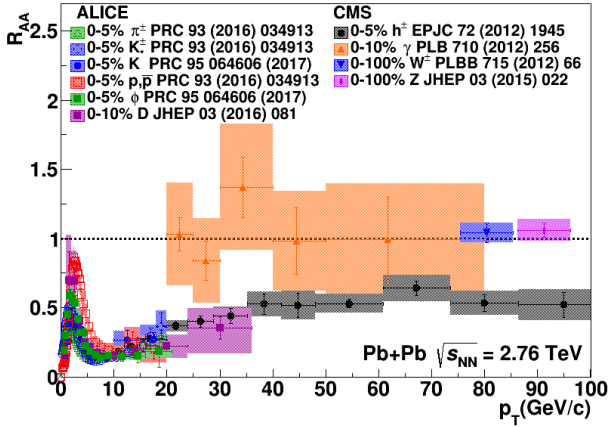


FIG. 12 R_{AA} from ALICE for identified π^\pm , K^\pm , and p (Adam *et al.*, 2016e) and D mesons (Adam *et al.*, 2016k) and CMS for charged hadrons (h^\pm) (Chatrchyan *et al.*, 2012e), direct photons (Chatrchyan *et al.*, 2012b), W bosons (Chatrchyan *et al.*, 2012f), and Z bosons (Chatrchyan *et al.*, 2011c). The W and Z bosons are shown at their rest mass and identified through their leptonic decay channel. This demonstrates that colored probes (high- p_T final state hadrons) are suppressed while electroweak probes (direct photons, W, Z) are not at the LHC.

Indeed a greater fractional momentum loss was observed for the most central 2.76 TeV Pb+Pb collisions compared to the 200 GeV Au+Au collisions (Adare *et al.*, 2016d). The analysis found that S_{loss} scales with energy density related quantities such as multiplicity ($dN_{ch}/d\eta$), as shown in Figure 13, and $dE_T/dy/A_T$ where A_T is the transverse area of the system. The latter quantity can be written in terms of Bjorken energy density, ϵ_{B_j} and the equilibrium time, τ_0 such that $dE_T/dy/A_T = \epsilon_{B_j} \tau_0$ and has been shown to scale with $dN_{ch}/d\eta$ (Adare *et al.*, 2016e). On the other hand, S_{loss} does not scale with system size variables such as N_{part} . Assuming that S_{loss} is a reasonable proxy for the mean fractional energy loss of the partons the scaling observations implies that fractional energy loss of partons scales with the energy density of the medium for these collision energies.

1. Jet R_{AA}

Measurements of hadronic observables blur essential physics due to the complexity of the theoretical description of hadronization and the sensitivity to non-perturbative effects. In principle, measurements of reconstructed jets are expected to be less sensitive to these effects. Next to leading order calculations demonstrate the sensitivity of R_{AA} measurements to the properties of the medium-induced gluon radiation (Vitev *et al.*, 2008). These measurements can differentiate between competing models of parton energy loss mechanisms, re-

ducing the large systematic uncertainties introduced by different theoretical formalisms (Majumder, 2007b). Figure 14 shows the reconstructed anti- k_T jet R_{AA} from ALICE (Adam *et al.*, 2015d) with $R = 0.2$ for $|\eta| < 0.5$, ATLAS (Aad *et al.*, 2015b) with $R = 0.4$ for $|\eta| < 2.1$, and CMS (Khachatryan *et al.*, 2017c,c) with $R = 0.2$, 0.3, and 0.4 for $|\eta| < 2.0$. At lower momenta, the ALICE data are consistent with the CMS data for all radii, while the ATLAS R_{AA} is higher than that of ALICE. At higher momenta, all measurements of jets from all three experiments agree within the experimental uncertainties of the jet measurements.

A jet is defined by the parameters of the jet finding algorithm and selection criteria such as those that are used to identify background jets due to fluctuations in heavy ion events. When making comparisons of jet observables between different experiments and to theoretical predictions, not only jet definitions but also the effects of selection criteria need to be considered carefully. While the difference between the pseudorapidity coverage is unlikely to lead to the difference between the ATLAS and ALICE results given the relatively flat distribution at mid-rapidity, the resolution parameter R as well as the different selection criteria could cause a difference as observed at low transverse momenta. The ATLAS approach to the combinatorial background, which favors jets with hard constituents, may bias the jet sample to unmodified jets, particularly at low momenta where the ATLAS and ALICE measurements overlap. ATLAS and CMS jet measurements agree at high momenta where jets are expected to be less sensitive to the measurement details. We therefore interpret the difference between the jet R_{AA} measured by the different experiments not as an inconsistency, but as different measurements due to different biases. We implore the collaborations to construct jet observables using the same approaches to background subtraction and suppression of the combinatorial background so that the measurements could be compared directly. Ultimately the overall consistency of R_{AA} at high p_T , even with widely varying jet radii and inherent biases in the jet sample, indicate that more sensitive observables are required to understand jet quenching quantitatively.

Although, the observation of jet quenching through R_{AA} was a major feat, it still leaves several open questions about hard partons' interactions with the medium. *How do jets lose energy?* Through collisions with the medium, gluon bremsstrahlung, or both? Where does that energy go? Are there hot spots or does the energy seem to be distributed isotropically in the event? Few experimental observables can compete with R_{AA} for overall precision, however, more differential observables may be more sensitive to the energy loss mechanism.

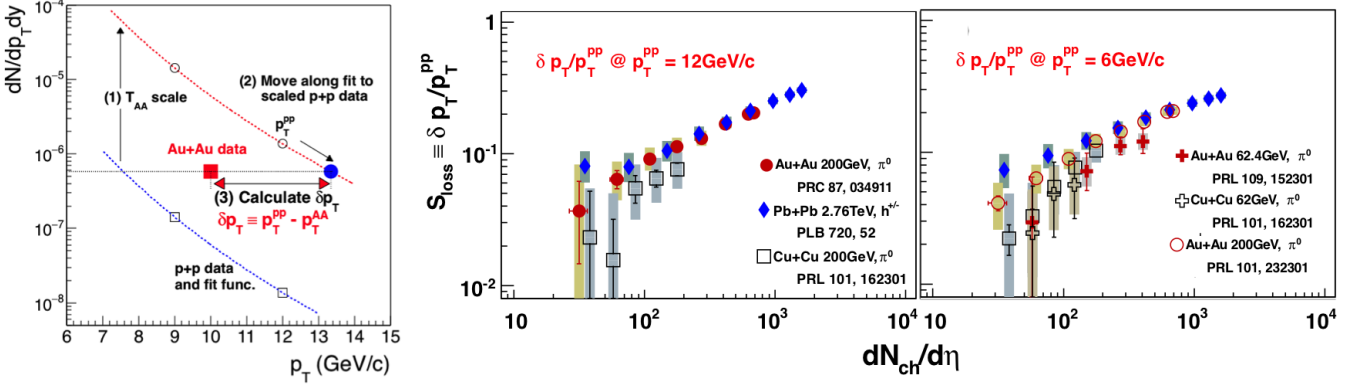


FIG. 13 Figure is a modified presentation of plots from PHENIX (Adare *et al.*, 2016d). The first plot (left) is a cartoon demonstrating how δp_T is determined. The fractional energy loss, S_{loss} measured as a function of the multiplicity, $dN_{ch}/d\eta$ is plotted for several heavy ion collision energies for hadrons with p_T^{pp} of 12 GeV (middle) and 6 GeV/c (right) where p_T^{pp} refers to the transverse momentum measured in $p+p$ collisions. The Pb+Pb data are from ALICE measured over $|\eta| < 0.8$ while all other data are from PHENIX which measures particle in the range $|\eta| < 0.35$. These results indicate that the fractional energy loss scales with the energy density of the system.

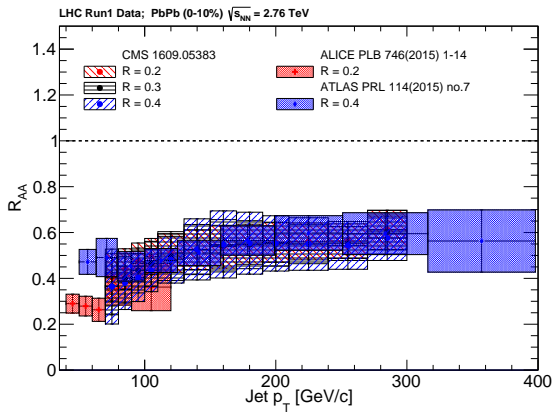


FIG. 14 Reconstructed anti- k_T jet R_{AA} from ALICE (Adam *et al.*, 2015d) with $R = 0.2$ for $|\eta| < 0.5$, ATLAS (Aad *et al.*, 2015b) with $R = 0.4$ for $|\eta| < 2.1$, and CMS (Khachatryan *et al.*, 2017c) with $R = 0.2, 0.3$ and 0.4 for $|\eta| < 2.0$. The ALICE and CMS data are consistent within uncertainties while the ATLAS data are higher. This may be due to the ATLAS technique, which could impose a survivor bias and lead to a higher jet R_{AA} at low momenta. Figure courtesy of Raghav Elayavalli Kunnawalkam.

1970 2. Dihadron correlations

1971 The precise mechanism responsible for modification 1992 of dihadron correlations cannot be determined based on 1993 these studies alone because there are many mechanisms 1994 which could lead to modification of the correlations. This 1995 includes not only energy loss and modification of jet 1996 fragmentation but also modifications of the underlying 1997 parton spectra. However, they are less ambiguous than 1998

1978 spectra alone because the requirement of a high momentum 1979 trigger particle enhances the fraction of particles 1980 from jets. Figure 15 shows dihadron correlations in $p+p$, 1981 $d+Au$, and $Au+Au$ at $\sqrt{s_{NN}} = 200$ GeV, demonstrating 1982 suppression of the away-side peak in central $Au+Au$ 1983 collisions. The first measurements of dihadron correlations 1984 showed complete suppression of the away-side peak 1985 and moderate enhancement of the near-side peak (Adams 1986 *et al.*, 2003a, 2004a; Adler *et al.*, 2003a). However, as 1987 noted above, a majority of dihadron correlation studies 1988 did not take the odd v_n due to flow into account, including 1989 those in Figure 15. A subsequent measurement with 1990 similar kinematic cuts including higher order v_n shows 1991 that the away-side is not completely suppressed, as shown 1992 in Figure 15, but rather that there is a visible but suppressed 1993 away-side peak (Nattrass *et al.*, 2016). Studies at 1994 higher momenta also see a visible but suppressed away-side 1995 peak (Adams *et al.*, 2006). 1996

The suppression is quantified by

$$1997 I_{AA} = Y_{AA}/Y_{pp}. \quad (12)$$

1998 where Y_{AA} is the yield in $A+A$ collisions and Y_{pp} is the 1999 yield in $p+p$ collisions. The yields must be defined over 2000 finite $\Delta\phi$ and $\Delta\eta$ ranges and are usually measured for 2001 a fixed range in associated momentum, p_T^a . Similar to 2002 R_{AA} , an I_{AA} greater than one means that there are more 2003 particles in the peak in $A+A$ collisions than in $p+p$ 2004 collisions and an I_{AA} less than one means that there are 2005 fewer. Gluon bremsstrahlung or collisional energy loss 2006 would result in more particles at low momenta and fewer 2007 particles at high momenta, leading to an I_{AA} greater than 2008 one at low momenta and an I_{AA} less than one at high 2009 momenta, at least as long as the lost energy does not 2010 reach equilibrium with the medium. Both radiative and 2011

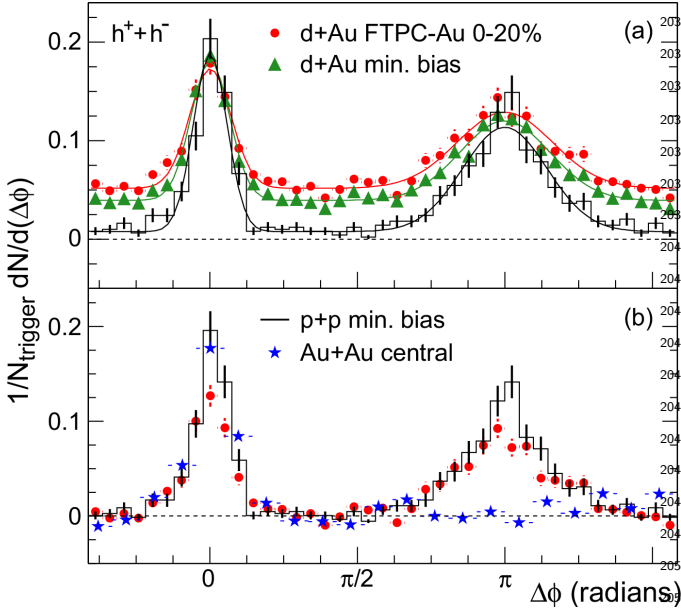


FIG. 15 Figure from STAR (Adams *et al.*, 2003a). (a) Dihadron correlations before background subtraction in $p+p$ and $d+Au$ and (b) Comparison of dihadron correlations after background subtraction in $p+p$, $d+Au$, and $Au+Au$ at $\sqrt{s_{\text{NN}}} = 200$ GeV for associated momenta $2.0 \text{ GeV}/c < p_T^a < p_T^b < p_T^c$ and trigger momenta $4 < p_T^t < 6 \text{ GeV}/c$. This measurement is now understood to be quantitatively incorrect because of erroneous assumptions in the background subtraction. We now see only partial suppression on the away-side (Nattrass *et al.*, 2016).

energy loss rather than a change in the underlying jet spectra since higher energy jets are both more collimated and contain more particles.

The away-side is suppressed at high momenta at both RHIC (Abelev *et al.*, 2010a; Adams *et al.*, 2006) and the LHC (Aamodt *et al.*, 2012). A reanalysis of reaction plane dependent dihadron correlations from STAR (Agakishiev *et al.*, 2010, 2014) at low momenta using a new background method which takes odd v_n into account (Sharma *et al.*, 2016) observed suppression on the away-side but no broadening, even though broadening was observed on the near-side at the same momenta (Nattrass *et al.*, 2016). This may indicate that the away-side width is less sensitive because the width is broadened by the decorrelation between the near- and away-side jet axes rather than indicating that these effects are not present. Reaction plane dependent studies can constrain the path length dependence of energy loss because, as shown in Figure 2, partons traveling in the reaction plane (in-plane) traverse less medium than those traveling perpendicular to the reaction plane (out-of-plane). The I_{AA} is highest for low momentum particles and is at a minimum for trigger particles at intermediate angles relative to the reaction plane rather than in-plane or out-of-plane. This likely indicates an interplay between the effects of surface bias and partonic energy loss.

Energy loss models are generally able to describe I_{AA} qualitatively, however, there has been no systematic attempt to compare data to models, as was done for R_{AA} . Simultaneous comparisons of R_{AA} and I_{AA} are expected to be highly sensitive to the jet transport coefficient \hat{q} (Jia *et al.*, 2011; Zhang *et al.*, 2007). Such a theoretical comparison is partially compounded by the wide range of kinematic cuts used in experimental measurements and the fact that most measurements neglected the odd v_n in the background subtraction.

3. Dijet imbalance

The first evidence of jet quenching in reconstructed jets at the LHC was observed by measuring the dijet asymmetry, A_J . This observable measures the energy or momentum imbalance between the leading and sub-leading or opposing jet in each event. Due to kinematic and detector effects, the energy of dijets will not be perfectly balanced, even in $p+p$ collisions. Therefore to interpret this measurement in heavy ion collisions, data from $A+A$ collisions must be compared to the distributions in $p+p$ collisions. Figure 16 shows the dijet asymmetry measurement from the ATLAS experiment where $A_J = \frac{E_{T1} - E_{T2}}{E_{T1} + E_{T2}}$ (Aad *et al.*, 2010). The left panel on the top row shows the A_J distribution for peripheral $Pb+Pb$ collisions and demonstrates that it is similar to that from $p+p$ collisions. However, dijets in central $Pb+Pb$ collisions are more likely to have a higher A_J value than dijets in $p+p$ collisions, con-

2009 collisional energy loss would lead to broader correlations. 2010 Partonic energy loss before fragmentation would lead to a 2011 suppression on the away-side but no modification on the 2012 near-side and no broadening because the near-side jet is 2013 biased towards the surface of the medium. Changes in 2014 the parton spectra can also impact I_{AA} because harder 2015 partons hadronize into more particles and higher energy 2016 jets are more collimated.

2017 No differences between $d+Au$ and $p+p$ collisions are 2018 observed on either the near- or away-side at midrapidity- 2019 (Adler *et al.*, 2006a,d), indicating that any modifi- 2020 cations observed are due to hot nuclear matter effects. 2021 The near-side yields at midrapidity in $A+A$, $d+Au$, and 2022 $p+p$ collisions are within error at RHIC (Abelev *et al.*, 2023 2010a; Adams *et al.*, 2006; Adare *et al.*, 2008a), even at 2024 low momenta (Abelev *et al.*, 2009b; Agakishiev *et al.*, 2025 2012c), indicating that the near-side jet is not substan- 2026 tially modified, although the data are also consistent 2027 with a slight enhancement (Nattrass *et al.*, 2016). A 2028 slight enhancement of the near-side is observed at the 2029 LHC (Aamodt *et al.*, 2012) and a slight broadening is 2030 observed at RHIC (Adare *et al.*, 2008a; Agakishiev *et al.*, 2031 2012c; Nattrass *et al.*, 2016). The combination of broad- 2032 ening and a slight enhancement favors moderate partonic 2033

sistent with expectations from energy loss. The bottom panel shows that these jets retain a similar angular correlation with the leading jet, even as they lose energy. The CMS measurement of $A_J = \frac{p_{T1}-p_{T2}}{p_{T1}+p_{T2}}$ (Chatrchyan *et al.*, 2011b) shows similar trends. The structure in the distribution of A_J is partially due to the 100 GeV lower limit on the leading jet and the 25 GeV lower limit on the subleading jet and partially due to detector effects and background in the heavy ion collision. These measurements are not corrected for detector effects or distortions in the observed jet energies due to fluctuations in the background. Instead the jets from $p+p$ collisions are embedded in a heavy ion event in order to take the effects of the background into account.

Recently ATLAS has measured A_J , and unfolded the distribution in order to take background and detector effects into account (ATL, 2015b), with similar conclusions. For jets above 200 GeV, the asymmetry is observed to be consistent with those observed in $p+p$, indicating that sufficiently high momentum jets are unmodified. This is consistent with observation that the R_{AA} consistent with one for hadrons at $p_T \approx 100$ GeV/c (CMS, 2016a), indicating that very high momentum jets are not modified.

Energy and momentum must be conserved, so the balance should be restored if jets can be reconstructed in such a way that the particles carrying the lost energy are included. For jets reconstructed with low momentum constituents, the background due to combinatorial jets is non-negligible, but requiring the jet to be matched to a jet constructed with higher momentum jet constituents, as well as a higher momentum jet will suppress the combinatorial jet background. STAR measurements of A_J using a high momentum constituent selection ($p_T > 2$ GeV/c) observed the same energy imbalance seen by ATLAS and CMS. However, the energy balance was recovered by matching these jets reconstructed with high p_T constituents, to jets reconstructed with low momentum constituents ($p_T > 150$ MeV/c) and then extracting A_J from the jets with the low momentum constituents (Adamczyk *et al.*, 2017b).

4. γ -hadron, γ -jet and Z -jet correlations

At leading order, direct photons are produced via Compton scattering, $q+g \rightarrow q+\gamma$, and quark-antiquark annihilation, as shown in the left two and right two Feynman diagrams in Figure 17, respectively. Due to the dearth of anti-quarks and abundance of gluons in the proton, Compton scattering is the dominant production mechanism for direct photons in $p+p$ and $A+A$ collisions. Therefore jets recoiling from a direct photon at midrapidity are predominantly quark jets. In the center of mass frame at leading order, the photon and recoil quark are produced heading precisely 180° away from each other in the transverse plane with the same mo-

mentum. At higher order, fragmentation photons and gluon emission impact the correlation such that the momentum is not entirely balanced and the back-to-back positions are smeared, even in $p+p$ collisions. Since photons do not lose energy in the QGP, the photon will escape the medium unscathed and the energy of the opposing quark can be determined from the energy of the photon. This channel is called the “Golden Channel” for jet tomography of the QGP because it is possible to calculate experimental observables with less sensitivity to hadronization and other non-perturbative effects than dihadron correlations and measurements of reconstructed jets. Additionally, direct photon analyses remove some of the ambiguity with respect to differences between quarks and gluons since the outgoing parton opposing the direct photon is predominantly a quark.

Correlations of direct photons with hadrons can be used to calculate I_{AA} , as for dihadron correlations. Studies of γ -h at RHIC led to similar conclusions to those reached by dihadron correlations, as shown in Figure 18, demonstrating suppression of the away-side jet (Abelev *et al.*, 2010c; Adamczyk *et al.*, 2016; Adare *et al.*, 2009, 2010b). In addition, γ -h correlations can measure the fragmentation function of the away-side jet assuming the jet energy is the photon energy. This is discussed in Section III.C.2. It should be noted that nonzero photon v_2 and v_3 have been observed (Adare *et al.*, 2012c, 2016a), leading to a correlated background. The physical origin of this v_2 is unclear, since photons do not interact with the medium, so it is also unclear if v_3 and higher order v_n impact the background. Measurements at high momenta are robust because the background is small and the photon v_2 appears to decrease with p_T . In (Adare *et al.*, 2013b), the systematic uncertainty due to v_3 was estimated and included in the total systematic uncertainty. Since the direct photon-hadron correlations are extracted by subtracting photon-hadron correlations from decays (primarily from $\pi^0 \rightarrow \gamma\gamma$) from inclusive photon-hadron correlations, the impact of the v_n in the final direct photon-hadron correlations is reduced as compared to dihadron and jet-hadron correlations.

Direct photons can also be correlated with a reconstructed jet. In principle, this is a direct measurement of partonic energy loss. Figure 19(a) shows measurements of the energy imbalance between a photon with energy $E > 60$ GeV and a jet at least $\frac{7}{8}\pi$ away in azimuth with at least $E_{jet} > 30$ GeV. Even in $p+p$ collisions, the jet energy does not exactly balance the photon energy because of next-to-leading order effects and because some of the quark’s energy may extend outside of the jet cone. The lower limit on the energy of the reconstructed jet is necessary in order to suppress background from combinatorial jets, but it also leads to a lower limit on the fraction of the photon energy observed. Figure 19(a) demonstrates that the quark loses energy in $Pb+Pb$ collisions. Figure 19(b) shows the average fraction of isolated photons

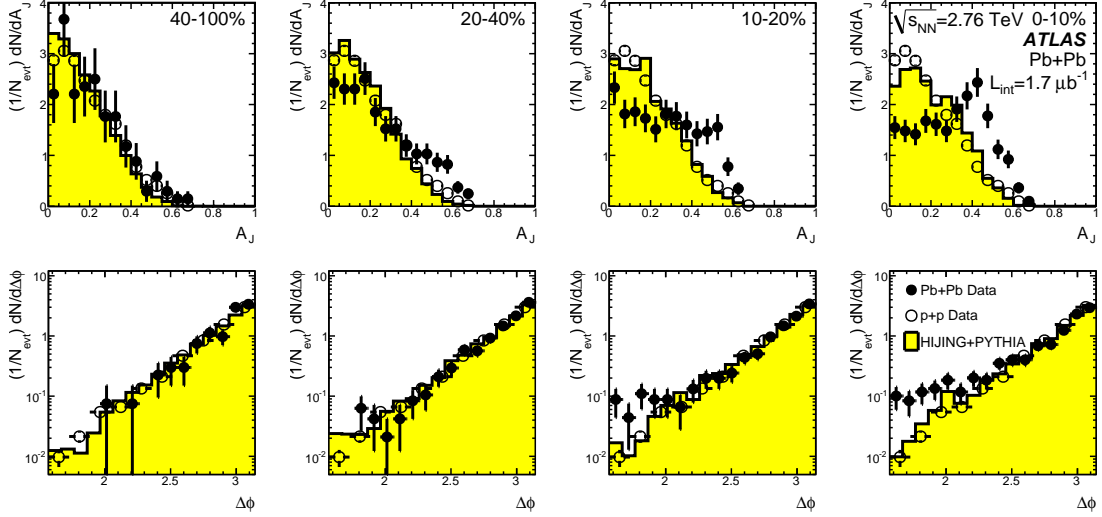


FIG. 16 Figure from ATLAS (Aad *et al.*, 2010). The top row shows comparisons of $A_J = (E_{T1} - E_{T2})/(E_{T1} + E_{T2})$ from $p+p$ and $Pb+Pb$ collisions at $\sqrt{s_{NN}} = 2.76$ TeV with leading jets above $p_T > 100$ GeV and subleading jets above 25 GeV. The bottom row shows the angular distribution of the jet pairs. This shows that the momenta of jets in jet pairs is not balanced in central $A+A$ collisions, indicating energy loss.



FIG. 17 Figure from PHENIX (Adare *et al.*, 2010b). The left two Feynman diagrams show direct photon production through Compton scattering and the right two diagrams show direct photon production through quark-antiquark annihilation. These are the leading order processes which contribute to the production of a gamma and a jet approximately 180° apart.

2195 matched to a jet, $R_{J\gamma}$. In $p+p$ collisions nearly 70% of
2196 all photons are matched to a jet, but in central $Pb+Pb$
2197 collisions only about half of all photons are matched to a
2198 jet. These measurements provide unambiguous evidence
2199 for partonic energy loss. However, the kinematic cuts
2200 required to suppress the background leave some ambiguity
2201 regarding the amount of energy that was lost. Some
2202 of the energy could simply be swept outside of the jet
2203 cone. The preliminary results of an analysis with higher
2204 statistics for the $p+p$ data and the addition of $p+Pb$ col-
2205 lisions also shows no significant modification, confirming
2206 that the $Pb+Pb$ imbalance does not originate from cold
2207 nuclear matter effects (Collaboration, 2013b).

2208 By construction, measurements of the process $q+g \rightarrow$
2209 $q+\gamma$ can only measure interactions of quarks with the
2210 medium. Since there are more gluons in the initial state
2211 and quarks and gluons may interact with the medium
2212 in different ways, studies of direct photons alone cannot
2213 give a full picture of partonic energy loss.

2214 With the large statistics data collected during the

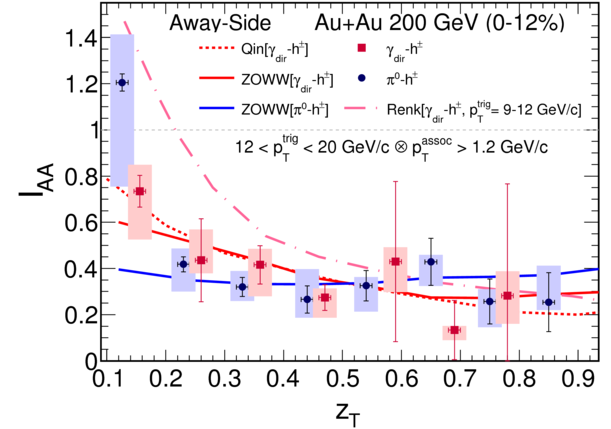


FIG. 18 Figure from STAR (Adamczyk *et al.*, 2016). The away-side I_{AA} for direct photon-hadron correlations (red squares) and π^0 -hadron correlations (blue circles) plotted as a function of $z_T = p_{T,h}/p_{T,trig}$ as measured by STAR in central 200 GeV Au+Au collisions. This shows the suppression of hadrons 180° away from a direct photon. The data are consistent with theory calculations which show the greatest suppression at high z_T and less suppression at low z_T . The curves are theory calculations from Qin (Qin *et al.*, 2009), Renk (Renk, 2009) and ZOWW (Chen *et al.*, 2010; Zhang *et al.*, 2009).

2215 2015 $Pb+Pb$ running of the LHC at 5 TeV, another
2216 “Golden Probe” for jet tomography of the QGP, the
2217 coincidences of a Z^0 and a jet, became experimentally ac-
2218 cessible (Neufeld *et al.*, 2011; Wang and Huang, 1997).
2219 While this channel has served as an essential calibrator

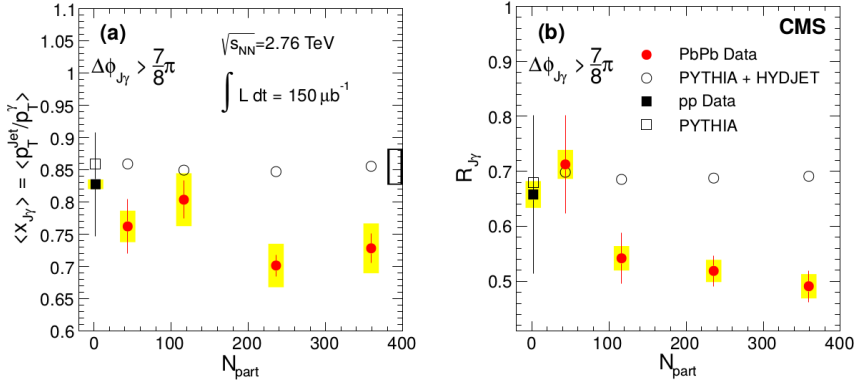


FIG. 19 Figure from CMS (Chatrchyan *et al.*, 2013b) for isolated photons with $p_T > 60$ GeV/c and associated jets with $p_T > 30$ GeV/c. (a) Average ratio of jet transverse momentum to photon transverse momentum, $\langle x_{J\gamma} \rangle$, as a function of the number of participating nucleons N_{part} . (b) Average fraction of isolated photons with an associated jet above 30 GeV/c, $R_{J\gamma}$, as a function of N_{part} . This demonstrates that the quark jet 180° away from a direct photon loses energy, with the energy loss increasing with increasing centrality.

of jet energy in TeV $p+p$ collisions, in heavy ion collisions it can be used to calibrate in-medium parton energy loss as the Z^0 carries no color charge and is expected to escape the medium unattenuated like the photon. However, photon measurements at higher momentum are limited due to the large background from decay photons in experimental measurements. Recent measurements of Z boson tagged jets in Pb+Pb collisions at $\sqrt{s_{NN}} = 5.02$ TeV (Sirunyan *et al.*, 2017c) show that angular correlations between Z bosons and jets are mostly preserved in central Pb+Pb collisions. However, the transverse momentum of the jet associated with that Z boson appears to be shifted to lower values with respect to the observations in $p+p$ collisions, as expected from jet quenching.

5. Hadron-jet correlations

Correlations between a hard hadron and a reconstructed jet were measured to overcome the downside of an explicit bias imposed by the background suppression techniques described in Section II.E. Similar to dihadron correlations, a reconstructed hadron is selected and the yield of jets reconstructed within $|\pi - \Delta\phi| < 0.6$ relative to that hadron is measured in (Adam *et al.*, 2015c). For sufficiently hard hadrons, a large fraction of the jets correlated with those hadrons would be jets that originated from a hard process, however, for low momentum hadrons, the yield will be dominated by combinatorial jets. The yield of combinatorial jets should be independent of the hadron momentum, so the difference between the yields, Δ_{recoil} , is calculated to subtract the background from the ensemble of jet candidates. This difference in yields is then compared to the same measurement in $p+p$ collisions.

Since the requirement of a hard hadron is opposite the

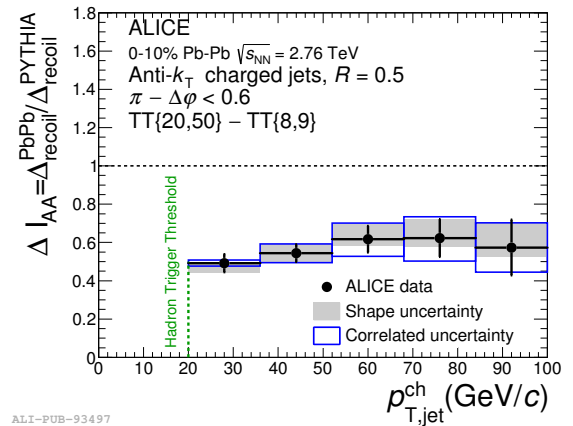


FIG. 20 Figure from ALICE (Adam *et al.*, 2015c). $\Delta I_{AA} = \Delta_{PbPb}^{recoil}/\Delta_{PYTHIA}^{recoil}$ where Δ_{recoil} is the difference between the number of jets within $\pi - \Delta\phi < 0.6$ of a hadron with $20 < p_T < 50$ GeV/c and a hadron with $8 < p_T < 9$ GeV/c. The green line indicates the momentum of the higher momentum hadron, an approximate lower threshold on the jet momentum. This demonstrates the suppression of a jet 180° away from a hard hadron.

jet being studied, no fragmentation bias is imposed on the reconstructed jet. Therefore, this measurement may be more sensitive to modified jets than observables that require selection criteria on the jet candidates themselves. Figure 20 shows the ratio of Δ_{recoil} in Pb+Pb collisions to that in $p+p$ collisions, $\Delta I_{AA} = \Delta_{PbPb}^{recoil}/\Delta_{PYTHIA}^{recoil}$. PYTHIA is used as a reference rather than data due to limited statistics available in the data at the same collision energy. PYTHIA agrees with the data from $p+p$ collisions at $\sqrt{s} = 7$ TeV. These data demonstrate that there is substantial jet suppression, consistent with the

2264 results discussed above.

2265 Measurements of hadron-jet correlations by 2266 STAR (Adamczyk *et al.*, 2017c) used a novel mixed 2267 event technique for background subtraction in order to 2268 extend the measurement to low momenta. The condi- 2269 tional yield correlated with a high momentum hadron 2270 was clearly suppressed in central Au+Au collisions 2271 relative to that observed in peripheral collisions, though 2272 substantially less so at the lowest momenta. A benefit 2273 of this method is that, in principle, the conditional yield 2274 of jets correlated with a hard hadron can be calculated 2275 with perturbative QCD.

2276 6. Path length dependence of inclusive R_{AA} and jet v_n

2277 The azimuthal asymmetry shown in Figure 2 provides 2278 a natural variation in the path length traversed by hard 2279 partons and the orientation of the reaction plane can be 2280 reconstructed from the distribution of final state hadrons. 2281 The correlations with this reaction plane can therefore 2282 be used to investigate the path length of partonic energy 2283 loss. The reaction plane dependence of inclusive particle 2284 R_{AA} demonstrates that energy loss is path length de- 2285 pendent (Adler *et al.*, 2007a), as expected from models. 2286 The path length changes with collision centrality, system 2287 size, and angle relative to the reaction plane, however, the 2288 temperature and lifetime of the QGP also change when 2289 the centrality and system size are varied. When particle 2290 production is studied relative to the reaction plane an- 2291 gle, the properties of the medium remain the same while 2292 only the path length is changed. Because the eccentric- 2293 ity of the medium and therefore the path length can only 2294 be determined in a model, any attempt to determine the 2295 absolute path length is model dependent. Attempts to 2296 constrain the path length dependence of R_{AA} were ex- 2297 plored in (Adler *et al.*, 2007a). While these studies were 2298 inconclusive, they showed that R_{AA} is constant at a fixed 2299 mean path length and that there is no suppression for a 2300 path length below $L = 2$ fm, indicating that there is ei- 2301 ther a minimum time a hard parton must interact with 2302 the medium or there must be substantial effects from 2303 surface bias. More conclusive statements would require 2304 more detailed comparisons to models.

2305 At high p_T , the single particle v_n in equation 2 are 2306 dominated by jet production and a non-zero v_2 indi- 2307 cates path length dependent jet quenching. Above 10 2308 GeV/c, a non-zero v_2 is observed at RHIC (Adare *et al.*, 2309 2013a) and the LHC (Abelev *et al.*, 2013a; Chatrchyan 2310 *et al.*, 2012a) and can be explained by energy loss mod- 2311 els (Abelev *et al.*, 2013a). Above 10 GeV/c, v_3 in central 2312 collisions is consistent with zero (Abelev *et al.*, 2013a). 2313 The v_n of jets themselves can be measured directly, how- 2314 ever, only jet v_2 has been measured (Aad *et al.*, 2013a; 2315 Adam *et al.*, 2016b). Figure 21 compares jet and charged 2316 particle v_2 from ATLAS and ALICE. ALICE measure-

2317 ments are of charged jets, which are only constructed 2318 with charged particles and not corrected for the neutral 2319 component, with $R = 0.2$ and $|\eta| < 0.7$ and ATLAS mea- 2320 surements are reconstructed jets with $R = 0.2$ and $|\eta| <$ 2321 2.1. The v_2 observed by ALICE is higher than that ob- 2322 served by ATLAS, although consistent within the large 2323 uncertainties. The ALICE measurement is unfolded to 2324 correct for detector effects, but it is not corrected for 2325 the neutral energy contribution. Both measurements use 2326 methods to suppress the background which could lead to 2327 greater surface bias or bias towards unmodified jets. The 2328 ALICE measurement requires a track above 3 GeV/c in 2329 the jet to reduce the combinatorial background. The AT- 2330 LAS measurement requires the calorimeter jets used in 2331 the measurement to be matched to a 10 GeV track jet or 2332 to contain a 9 GeV calorimeter cluster. Because of the 2333 higher momentum requirement the ATLAS measurement 2334 has a greater bias than the ALICE sample of jets.

2335 These measurements provide some constraints on the 2336 path length dependence, however, this is not the only rel- 2337 evant effect. Theoretical calculations indicate that both 2338 event-by-event initial condition fluctuations and jet-by- 2339 jet energy loss fluctuations play a role in v_n at high 2340 p_T (Betz *et al.*, 2017; Noronha-Hostler *et al.*, 2016; Zapp, 2341 2014a). This is perhaps not surprising, analogous to the 2342 importance of fluctuations in the initial state for mea- 2343 surements of the v_n due to flow. However, it does indi- 2344 cate that much more insight into which observables are 2345 most sensitive to path length dependence and the role of 2346 fluctuations in energy loss is needed from theory.

2347 7. Heavy quark energy loss

2348 The jet quenching due to radiative energy loss is ex- 2349 pected to depend upon the species of the fragmenting 2350 parton (Horowitz and Gyulassy, 2008). The simplest ex- 2351 ample is gluon jets, which are expected to lose more en- 2352 ergy in the medium than quark jets due to their larger 2353 color factor. Similarly, the mass of the initial parton also 2354 plays a role and the interpretation of this effect depends 2355 on the theoretical treatment of parton-medium inter- 2356 actions. Strong coupling calculations based on AdS/CFT 2357 correspondence predict large mass effects at all trans- 2358 verse momenta and in weak-coupling calculations based 2359 on pQCD mass effects may arise from the “dead-cone” ef- 2360 fect (Dokshitzer and Kharzeev, 2001), the suppression of 2361 gluon emission at small angles relative to a heavy quark, 2362 but may be limited to a small range of heavy-quark trans- 2363 verse momenta comparable to the heavy-quark mass. 2364 However, the relevance of the dead-cone effect in heavy 2365 ion collisions is debated (Aurenche and Zakharov, 2009).

2366 Searches for a decreased suppression of heavy flavor 2367 using single particles are still inconclusive due to large 2368 uncertainties, although they indicate that heavy quarks 2369 may indeed lose less energy in the medium. As shown

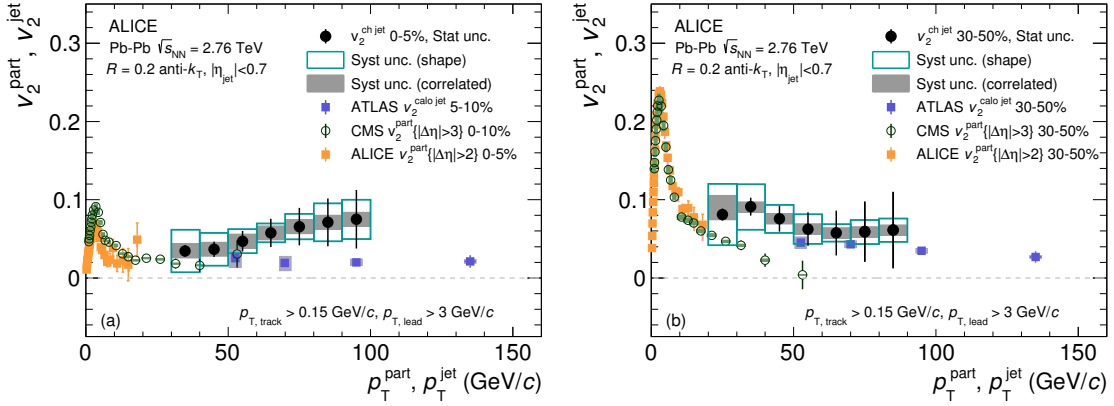


FIG. 21 Figure from ALICE (Adam *et al.*, 2016b). Jet v_2 from charged jets by ALICE (Adam *et al.*, 2016b) and calorimeter jets by ATLAS (Aad *et al.*, 2013a) compared to the charged hadron v_2 for 5–10% (left) and 30–50% collisions (Abelev *et al.*, 2013a; Chatrchyan *et al.*, 2012a). This demonstrates that partonic energy loss is path length dependent.

in Figure 11, the R_{AA} of single electrons from decays of heavy flavor hadrons is within uncertainties of that of hadrons containing only light quarks. Measurements of single leptons are somewhat ambiguous because of the difference between the momentum of the heavy meson and the decay lepton. Since the mass effect is predicted to be momentum dependent with negligible effects for $p_T \gg m$, the decay may wash out any mass effect. The R_{AA} of D mesons is within uncertainties of the light quark R_{AA} (Adam *et al.*, 2015a, 2016k; Adamczyk *et al.*, 2014b). Particularly at the LHC, these results may be somewhat ambiguous because D mesons may also be produced in the fragmentation of light quark or gluon jets. B mesons are much less likely to be produced by fragmentation. Preliminary measurements of B meson R_{AA} show less suppression than for light mesons, although the uncertainties are large and prohibit strong conclusions (CMS, 2016b).

Experimentally, heavy flavor jets are primarily identified using the relative long lifetimes of hadrons containing heavy quarks, resulting in decay products significantly displaced from the primary vertex. A variant of the secondary vertex mass, requiring three or more charged tracks, is also used to extract the relative contribution of charm and bottom quarks to various heavy flavor jet observables. However these methods cannot discriminate between heavy quarks from the original hard scattering, which then interact with the medium and lose energy, and those from a parton fragmenting into bottom or charm quarks (Huang *et al.*, 2013). A requirement of an additional B-meson in the event could ensure a purer sample of bottom tagged jets (Huang *et al.*, 2015), however, this is not currently experimentally accessible due to the limited statistics. Figure 22 shows a compilation of all current measurements of heavy flavor jets at LHC (Chatrchyan *et al.*, 2014a; Khachatryan *et al.*, 2016d; Sirunyan *et al.*, 2017b). The R_{AA} of bottom quark tagged jets is

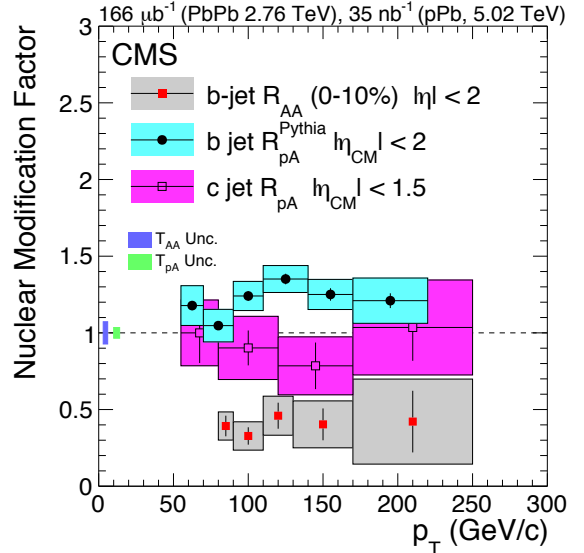


FIG. 22 The R_{AA} and R_{pPb} of heavy flavor associated jets measured by the CMS Collaboration (Chatrchyan *et al.*, 2014a; Khachatryan *et al.*, 2016d; Sirunyan *et al.*, 2017b). This shows that b quarks lose energy in the medium. Figure courtesy of Kurt Jung.

measured utilizing the Pb+Pb and $p+p$ data collected at $\sqrt{s_{NN}} = 2.76$ TeV. Bottom tagged jet measurements in $p+Pb$ collisions are also performed to study cold nuclear matter effects in comparison to expectations from PYTHIA at the 5 TeV center of mass energy (Khachatryan *et al.*, 2016d). Jets which are associated with the charm quarks in $p+Pb$ collisions are also studied with a variant of the bottom tagging algorithm (Sirunyan *et al.*, 2017b). A strong suppression of R_{AA} of jets associated with bottom quarks is observed in Pb+Pb collisions while the R_{pPb} is consistent with unity. These CMS measure-

ments demonstrate that jet quenching does not have a strong dependence on parton mass and flavor, at least in the jet p_T range studied (Chatrchyan *et al.*, 2014a; Khachatryan *et al.*, 2017c). The charm jet R_{pPb} also shows consistent results with negligible cold nuclear matter effects when compared with the measurements from $p+p$ collisions.

8. Summary of experimental evidence for partonic energy loss in the medium

Partonic energy loss in the medium is demonstrated by numerous measurements of jet observables. To date, the most precise quantitative constraints on the properties of the medium come from comparisons of R_{AA} to models by the JET collaboration (Burke *et al.*, 2014).

The interpretation of R_{AA} as partonic energy loss is confirmed by measurements of dihadron, gamma-hadron, jet-hadron, hadron-jet, and jet-jet correlations. The assumption about the background contribution and the biases of these measurements vary widely, so the fact that they all lead to a coherent physical interpretation strengthens the conclusion that they are due to partonic energy loss in the medium. This energy loss scales with the energy density of the system rather than the system size.

Reaction plane dependent inclusive particle R_{AA} , inclusive particle v_2 , and jet v_2 indicate that this energy loss is path length dependent, perhaps requiring a parton to traverse a minimum of around 2 fm of QGP to lose energy. Comparison of jet v_n to models indicates that jet-by-jet fluctuations in partonic energy loss impacts action plane dependent measurements significantly, however, this is not yet fully understood theoretically.

Measurements of heavy quark energy loss are consistent with expectations from models, however, they are also consistent with the energy loss observed for gluons and light quarks. Studies of heavy quark energy loss will improve substantially with the slated increases in luminosity and detector upgrades. The STAR heavy flavor tracker has already enabled higher precision measurements of heavy flavor at RHIC and one of the core goals of the proposed detector upgrade, sPHENIX, is precision measurements of heavy flavor jets. Run 3 at the LHC will enable higher precision measurements of heavy flavor, including studies of heavy flavor jets in the lower momentum region which may be more sensitive to mass effects.

The key question for the field is how to constrain the properties of the medium further. The Monte Carlo models the Jetscape collaboration is developing will include both hydrodynamics and partonic energy loss and the Jetscape collaboration plans Bayesian analyses similar to (Bernhard *et al.*, 2016; Novak *et al.*, 2014) incorporating jet observables. These models will also enable

the exact same analysis techniques and background subtraction methods to be applied to data and theoretical calculations. We propose including single particle R_{AA} (including particle type dependence), jet R_{AA} (with experimental analysis techniques applied), high momentum single particle v_2 , jet v_2 , hadron-jet correlations, and I_{AA} from both γ -hadron and dihadron correlations. The analysis method for all of these observables should be replicable in Monte Carlos. We omit A_J because a majority of these measurements are not corrected for detector effects. Bayesian analyses comparing theoretical calculations to data may be the best avenue for constraining the properties of the medium using measurements of jets. This is likely to improve our understanding of which observables are most useful for constraining models.

C. Influence of the medium on the jet

Section III.B examined the evidence that partons lose energy in the medium, but did not examine how partons interact with the medium. Understanding modifications of the jet by the medium requires a bit of a paradigm shift. As highlighted in Section II, a measurement of a jet is not a measurement of a parton but a measurement of final state hadrons generated by the fragmentation of the parton. Final state hadrons are grouped into the jet (or not) based on their spatial correlations with each other (and therefore the parton). Whether or not the lost energy retains its spatial correlation with the parent parton depends on whether or not the lost energy has had time to equilibrate in the medium. If a bremsstrahlung gluon does not reach equilibrium with the medium, when it fragments it will be correlated with the parent parton. Interactions with the medium shift energy from higher momentum final state particles to lower momentum particles and broadens the jet. Similar apparent modifications could occur if partons from the medium become correlated with the hard parton through medium interactions (Casalderrey-Solana *et al.*, 2017). Whether or not this lost energy is reconstructed as part of a jet depends on the jet finding algorithm and its parameters.

Whereas the observation that energy is lost is relatively straightforward, there are many different ways in which the jet may be modified, and we cannot be sure which mechanisms actually occur in which circumstances until we have measured observables designed to look for these effects. There are several different observables indicating that jets are indeed modified by the medium, each with different strengths and weaknesses. We distinguish between mature observables – those which have been measured and published, usually by several experiments – and new observables – those which have either only been published recently or are still preliminary. Mature observables largely focus on the average properties of jets as a function of variables which we can either mea-

sure directly or are straightforward to calculate, such as momentum and the position of particles in a jet. This includes dihadron correlations (h-h); correlations of a direct photon or Z with either a hadron or a reconstructed jet (γ -h and γ -jet); the jet shape ($\rho(r)$); the dijet asymmetry (A_J); the momentum distribution of particles in a reconstructed jet, called the fragmentation function ($D_{jet}(z)$), where $z = p_T/E_{jet}$); identification of constituents (PID), and heavy flavor jets (HF jets). Where our experimental measurements of these observables have limited precision, this is either due to the limited production cross section (heavy flavor jets and correlations with direct photons) or due to limitations in our understanding of the background (identified particles).

Our improving understanding of the parton-medium interactions has largely motivated the search for new, more differential observables. Partonic energy loss is a statistical process so ensemble measurements such as the average distribution of particles in a jet, or the average fractional energy loss, are important but can only give a partial picture of partonic energy loss. Just as fluctuations in the initial positions of nucleons must be understood to properly interpret the final state anisotropies of the medium, fluctuations play a key role in partonic interactions with the medium. The average shape and energy distribution of a jet is smooth, but each individual jet is a lumpy object. These new observables include the jet mass M_{jet} , subjetteness ($N_{subjetteness}$), LeSub, the splitting function z_g , the dispersion (p_T^D), and the girth (g). We leave the definitions of these variables to the following sections and we focus our discussion on observables which have been measured in heavy ion collisions, omitting those which have only been proposed to date. In general these observables are sensitive to the properties and structure of individual jets, and they are adapted from advances in jet measurements from particle physics. Investigations of new observables are important because they will allow access to well defined pQCD observables, which increases the sensitivity of our measurements to the properties of the QGP. The goal of each new observable is to construct something that is sensitive to properties of the medium that our mature observables are not sufficiently sensitive to, or to be able to disentangle physics processes that are not directly related to the medium properties, such as the difference in fragmentation between quark and gluon jets. Most measurements of these new observables are still preliminary and we therefore avoid drawing strong conclusions from them. Our understanding of these observables is still developing, particularly our understanding of how they are impacted by analysis cuts and the approach to the approach used to remove background effects. An observable which is highly effective for, say, distinguishing between quark and gluon jets in $p+p$ collisions, may not be as effective in heavy ion collisions.

We summarize the current status of observables sensitive to the medium modifications of jets in Table III. This list of observables also shows the evolution of the field.

Early on, due to statistical limitations, studies focused on dihadron correlations. These measurements are straightforward experimentally, however, they are difficult to calculate theoretically because all hadron pairs contribute and the kinematics of the initial hard scattering is poorly constrained. In contrast, as discussed in Section III.B.4, when direct photons are produced in the process $q+g \rightarrow q+\gamma$, the initial kinematics of the hard scattered partons are known more precisely. In some kinematic regions, these measurements are limited by statistics, and in others they are limited by the systematic uncertainty predominately from the subtraction of background photons from π^0 decay. Measurements of reconstructed jets are feasible over a wider kinematic region, but the kinematics of the initial hard scattering are not constrained as well. Nearly all measurements are biased towards quarks for the reasons discussed in Section II, however, it may be possible to tune the bias either using identified particles or by using new observables that select for particular fragmentation patterns.

Table III summarizes whether or not modifications, particularly broadening and softening, have been observed using each observable and which experiments have measured them. This table demonstrates that each measurement has strengths and weaknesses and that all observations contribute to our current understanding. Modifications to the jet structure have been observed for most observables, but not all. Since each observable is sensitive to different modifications, all provide useful input for differentiating between jet quenching models and understanding the effects of different types of initial and final state processes. We begin our discussion of measurements indicating modification of jets by the medium with mature observables. For each observable we revisit these issues in a discussion stating what we have learned from that observable.

1. Fragmentation functions with jets

Fragmentation functions are a measure of the distribution of final state particles resulting from a hard scattering and represent the sum of parton fragmentation functions, D_i^h , where i represents each parton type ($u, d, g, etc.$) contributing to the final distribution of hadrons, h . Typically, fragmentation functions are measured as a function of z or ξ where $z = p^h/p$ and $\xi = -\ln(z)$, where p is the momentum of parton produced by the hard scattering. Jet reconstruction can be used to determine the jet momentum, p^{jet} to approximate the parton momentum p , while the momentum of the hadrons, p^h , are measured for each hadron that is clustered into the jet by the jet reconstruction algorithm. In collider experiments, the transverse momentum, p_T , is

TABLE III Summary of measurements sensitive to fragmentation in heavy ion collisions. Preliminary measurements are denoted with a (P). New observables are separated from mature observables by a line. The first two columns after the observable describe biases inherent to the observable, while the next four columns refer to observations made from the measured results. We refer the readers to each section for details of measurements of each observable.

Observable	kinematics	q/g bias	evidence of modification	evidence of broadening	evidence of softening	measured by	Discussion
$D_{jet}(z)$	constrained	q bias	yes	insensitive	yes	CMS, ATLAS	III.C.1
γ -h	very well	q only	yes	yes	yes	STAR, PHENIX	III.C.2
γ -jet	very well	q only	yes	yes	yes	CMS	III.C.2
h-h	poor	unknown	yes	yes	yes	STAR, PHENIX, ALICE, CMS	III.C.3
jet-h	constrained	q bias	yes	yes	yes	ALICE(P), CMS, STAR	III.C.4
A_J	constrained	q bias	yes	insensitive	yes	STAR, ATLAS, CMS	III.C.5
$\rho(r)$	constrained	q bias	yes	yes	yes	CMS	III.C.6
identified h-h	poor	select	no			STAR, PHENIX	III.C.7
HF jets	constrained	q	yes			CMS	N/A
LeSub	constrained	unknown	no			ALICE(P)	III.C.8
p_T^D	constrained	select	yes			ALICE(P)	III.C.10
girth	constrained	select	yes			ALICE(P)	III.C.11
z_g	constrained	unknown	yes (CMS), no (STAR)			CMS, STAR(P)	III.C.12
τ_N	constrained	unknown	no			ALICE(P)	III.C.13
M_{jet}	constrained	unknown	no			ALICE	III.C.9

typically substituted for the total momentum p in the fragmentation function. It should be noted that this is not precisely the same observable as what is commonly referred to as the fragmentation function by theorists.

The fragmentation functions for jets in Pb+Pb collisions at $\sqrt{s_{NN}} = 2.76$ TeV have been measured by the ATLAS (Aad *et al.*, 2014c) and CMS (Chatrchyan *et al.*, 2012c, 2014c) Collaborations. The ratios of the fragmentation functions for several different centrality bins to the most peripheral centrality bin are shown in Figure 23. The most central collisions show a significant change in the average fragmentation function relative to peripheral collisions. At low z there is a noticeable enhancement followed by a depletion at intermediate z . This suggests that the energy loss observed for mid to high momentum hadrons is redistributed to low momentum particle production. We note that this corresponds to only a few additional particles and is a small fraction of the energy that R_{AA} , A_J and the other energy loss observables discussed in Section III.B indicate is lost. Arguably, this is the most direct observation of the softening of the fragmentation function expected from partonic energy loss in the medium. However, the definition of a fragmentation function in Equation 1 uses the momentum of the initial parton and, as discussed in Section II, a jet's momentum is not the same as the parent parton's momentum. Fragmentation functions measured with jets with large radii are approximately the same as the fragmentation functions in Equation 1, but this is not true for the jets with smaller radii measured in heavy ion collisions.

It is important to note that initial fragmentation measurements from the LHC used only dijets samples with

large momenta ($p_T > 4$ GeV/c) constituents, which indicated that there was no modification of fragmentation functions (Chatrchyan *et al.*, 2012c). With increased statistics and improved background estimation techniques these fragmentation measurements were re-measured later with inclusive jets with constituent tracks with $p_T > 1$ GeV/c utilizing the 2011 data. Figure 24 compares the measurements from CMS from two different measurements using 2010 and 2011 data. The initial 2010 analysis did not include lower momentum jet constituents due to the difficulty with background subtraction in that kinematic region and focused on leading and subleading jets. While the two measurements are consistent, the conclusion drawn from the 2010 data alone was that there was no apparent modification of the jet fragmentation functions. This highlights how critical biases are to the proper interpretation of measurements. The high momentum of these jets combined with the background subtraction and suppression techniques also means that the data in both Figure 23 and Figure 24 are likely biased towards quark jets.

2. Boson tagged fragmentation functions

As described previously, bosons can be used to tag the initial kinematics of the hard scattering. For fragmentation functions, this gives access to the initial parton momentum in the calculation of the fragmentation variable z . At the top Au+Au collision energy at RHIC, $\sqrt{s_{NN}} = 200$ GeV, there have been no direct measurements of fragmentation functions from reconstructed jets

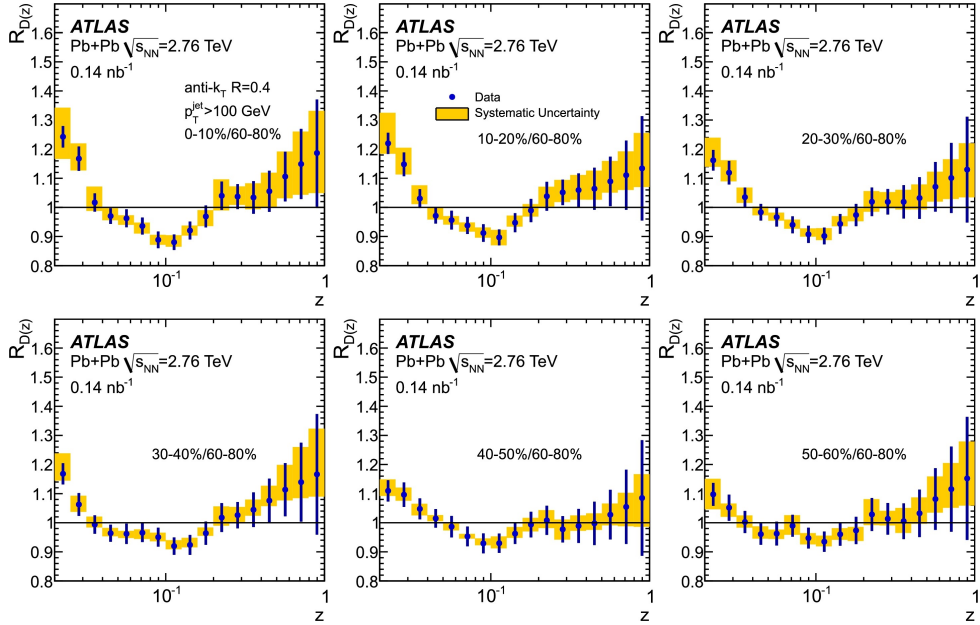


FIG. 23 Figure from ATLAS (Aad *et al.*, 2014c). Ratio of fragmentation functions from reconstructed jets measured by ATLAS for jets in Pb+Pb collisions at various centralities to those in 60-80% central collisions at $\sqrt{s_{NN}} = 2.76$ TeV. This shows that fragmentation functions are modified in $A+A$ collisions, with an enhancement at low momenta (low z) and a depletion at intermediate momenta (intermediate z), with the modification increasing from more peripheral to more central collisions.

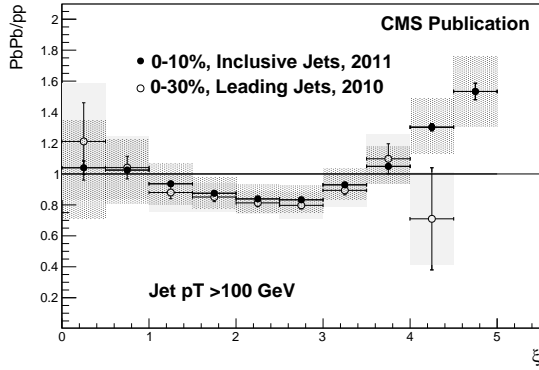


FIG. 24 Comparison of CMS measurements of fragmentation functions in Pb+Pb over pp from reconstructed jets for jets in Pb+Pb collisions at $\sqrt{s_{NN}} = 2.76$ TeV from 2010 and 2011 data (Chatrchyan *et al.*, 2012c, 2014c). Even though the two measurements are consistent, the 2010 data in isolation indicate that fragmentation is not modified while the 2011 data, which extend to lower momenta and use a less biased jet sample, clearly show modification at low momenta (high ξ). This highlights the difficulty in drawing conclusions from a single measurement, particularly when neglecting possible biases.

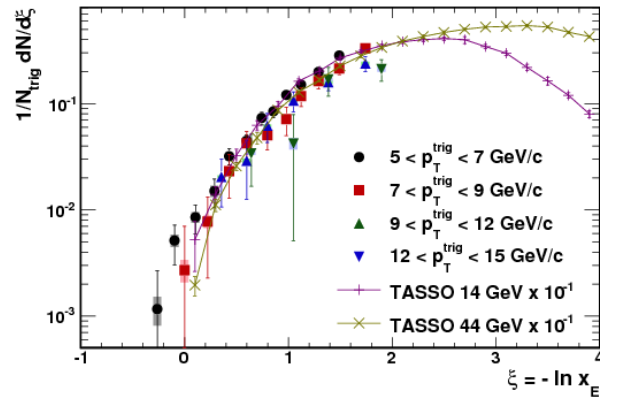


FIG. 25 Figure from PHENIX (Adare *et al.*, 2010b). $\xi = -\ln(x_E)$ distributions where $x_E = -|p_T^a/p_T^t| \cos(\Delta\phi) \approx z$ for isolated direct photon-hadron correlations for several photon p_T ranges from $p+p$ collisions at $\sqrt{s} = 200$ GeV compared to TASSO measurements in e^+e^- collisions at $\sqrt{s} = 14$ and 44 GeV. This demonstrates that direct photon measurements can be used reliably to extract quark fragmentation functions in $p+p$ collisions and that fragmentation functions are the same in e^+e^- and $p+p$ collisions.

2694 so far, however, γ -hadron correlations have been mea- 2698
 2695 sured both in $p+p$ and Au+Au collisions. The fragmen- 2699
 2696 tation function was measured in $p+p$ collisions at RHIC 2700
 2697 as a function of $x_E = -|\frac{p_T^a}{p_T^t}| \cos(\Delta\phi) \approx z$ (Adare *et al.*, 2701
 2698 2010b) and is shown in Figure 25. The $p+p$ results agree
 2699 well with the TASSO measurements of the quark frag-
 2700 mentation function in electron-positron collisions, which
 2701 is consistent with the production of a quark jet oppo-

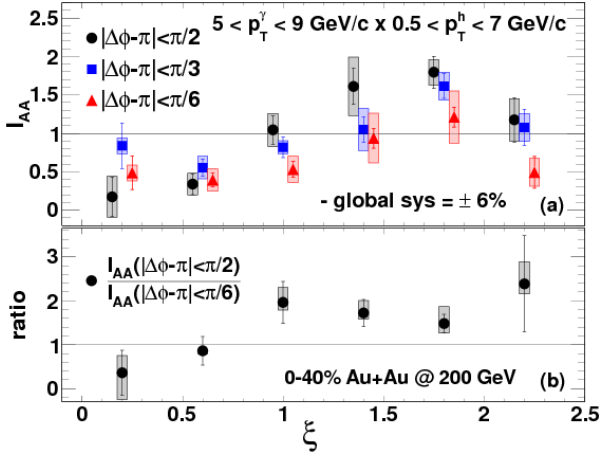


FIG. 26 Figure from PHENIX (Adare *et al.*, 2013b). The top panel shows I_{AA} for the away-side as a function of $\xi = \log(\frac{1}{z}) = \log(\frac{p_{T,jet}}{p_{T,had}})$. The points are shifted for clarity. The bottom panel shows the ratio of the I_{AA} for $|\Delta\phi - \pi| < \pi/2$ to $|\Delta\phi - \pi| < \pi/6$. This demonstrates the enhancement at low momentum combined with a suppression at high momentum, a shift consistent with expectations from energy loss models. The change is largest for wide angles from the direct photon.

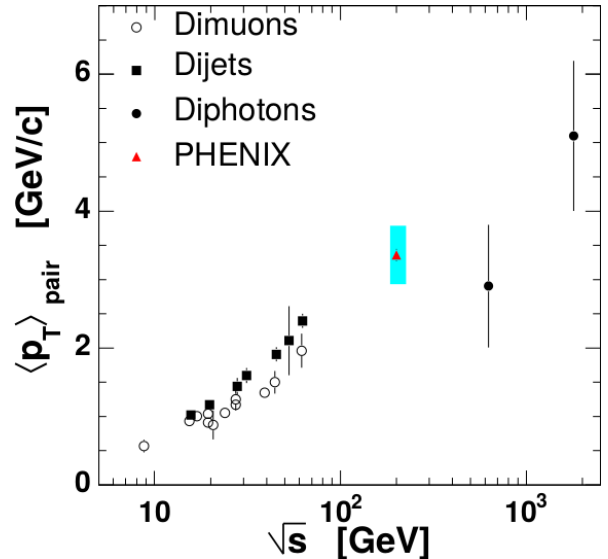


FIG. 27 Figure from PHENIX (Adler *et al.*, 2006c). Compilation of $\langle p_T \rangle_{pair} = \sqrt{2}k_T$ measurements where k_T is the acoplanarity momentum vector. Dihadron correlation measurements in $p+p$ collisions from PHENIX are consistent with the trend from dimuon, dijet and diphoton measurements at other collision energies. Dimuon and dijet measurements are from fixed target experiments and the diphoton measurements are from the Tevatron.

site the direct photon as expected in Compton scattering. Using the $p+p$ results as a reference, direct photon-hadron correlations were measured in Au+Au collisions at RHIC (Adare *et al.*, 2013b). The I_{AA} are shown in Figure 26. A suppression is observed for $\xi < 1$ ($z > 0.4$) while an enhancement is observed for $\xi > 1$ ($z < 0.4$). This suggests that energy loss at high z is redistributed to low z . Comparing these results to the results from STAR (Abelev *et al.*, 2010c; Adamczyk *et al.*, 2016) suggests that this is not a z_T dependent effect but rather a p_T dependent effect. STAR measured direct photon-hadron correlations for a similar z_T range but does not observe the clear enhancement exhibited in the PHENIX measurement. However, STAR is able to measure low values of z_T by increasing the trigger photon p_T , while PHENIX goes to low z_T by decreasing the associated hadron p_T . Preliminary PHENIX results as a function of photon p_T are consistent with the conclusion that modifications of fragmentation depend on associated particle p_T rather than z_T . Furthermore, STAR does observe an enhancement for jet-hadron correlations with hadrons of $p_T < 2$ GeV/c which is consistent with the PHENIX direct photon-hadron observation.

The direct photon-hadron correlations also suggest that the low p_T enhancement occurs at wide angles with respect to the axis formed by the hard scattered partons. Figure 26 shows the yield measured by PHENIX for different $\Delta\phi$ windows on the away-side. The enhancement is most significant for the widest window, $|\Delta\phi - \pi| < \pi/2$.

3. Dihadron correlations

Measurements of dihadron correlations are sensitive to modifications in fragmentation, although the interpretation is complicated because the initial kinematics of the hard scattering are poorly constrained. Differences observed in the correlations can either be due to medium interactions or due to changes in the parton spectrum. At high p_T , there are no indications of modification of the near- or away-side at midrapidity in d +Au collisions (Adler *et al.*, 2006a,d) so any effects observed in $A+A$ are hot nuclear matter effects and either d +Au or $p+p$ can be used as a reference for $A+A$ collisions.

The near-side peak can be used to study the angular distribution of momentum and particles around the triggered jet. The away-side peak is wider than the near-side due to the resolution of the triggered jet peak axis and the effect of the acoplanarity momentum vector, k_T . Dihadron correlations have been measured in $p+p$ collisions to determine the intrinsic k_T . Measurements of $\langle p_T \rangle_{pair} = \sqrt{2}k_T$ as a function of \sqrt{s} are shown in Figure 27.

The effect of the nucleus on k_T has been studied in d +Au collisions at 200 GeV (Adler *et al.*, 2006d) and in p +Pb collisions at 5.02 TeV (Adam *et al.*, 2015b) via dihadron correlations and reconstructed jets respectively. The dihadron measurements in d +Au are consistent with the PHENIX $p+p$ measurements shown in Figure 27,

2758 while the p +Pb dijet results agree with PYTHIA expectations. Since no broadening has been observed in p +Pb or d +Au collisions, any broadening of the away-side jet peak in $A+A$ collisions would be the result of modifications from the QGP. Assuming this is purely from radiative energy loss, the transport coefficient \hat{q} can be extracted directly from a measurement of k_T according to $\hat{q} \propto \langle k_T^2 \rangle$ (Tannenbaum, 2017).

2766 Figure 28 shows the widths in $\Delta\phi$ and $\Delta\eta$ on the near-side as a function of p_T^t , p_T^a , and the average number of participant nucleons, $\langle N_{\text{part}} \rangle$ for d +Au, Cu+Cu, and Au+Au collisions at $\sqrt{s_{\text{NN}}} = 62.4$ and 200 GeV (Agakishiev *et al.*, 2012c). The near-side is broader in both $\Delta\phi$ and $\Delta\eta$ in central collisions. This broadening does not have a strong dependence on the angle of the trigger particle relative to the reaction plane (Nattrass *et al.*, 2016). One interpretation of this is that the jet-by-jet fluctuations in partonic energy loss are more significant than path length dependence for this observable (Zapp, 2014a). Higher energy jets have higher particle yields and are more collimated, so if changes were due to an increase in the average parton energy the yield would increase but the width would decrease. In contrast, interactions with the medium would lead to broadening and the softening of the fragmentation function which would lead to more particles. The near-side yields are not observed to be modified (Agakishiev *et al.*, 2012c), although I_{AA} at RHIC (Nattrass *et al.*, 2016) is also consistent with the slight enhancement seen at the LHC (Aamodt *et al.*, 2012). This indicates that the increase in width is most likely due to medium interactions rather than changes in the parton spectra.

2790 Recent studies of the away-side do not indicate a measurable broadening (Nattrass *et al.*, 2016), at least for the low momenta in this study ($4 < p_T^t < 6$ GeV/ c , $1.5 \text{ GeV}/c > p_T^a$). This is in contrast to earlier studies which neglected odd v_n in the background subtraction, indicating dramatic shape changes. These earlier studies are discussed in greater detail in Section III.D.3 because the modifications observed were generally interpreted as an impact of the medium on the jet. We note that broadening is observed on the away-side for jet-hadron correlations, as discussed below. The current apparent lack of broadening in dihadron correlations may indicate that this is not the most sensitive observable because of the decorrelation between the trigger on the near-side and the angle of the away-side jet. It may also be a kinematic effect because modifications are extremely sensitive to momentum. The away-side I_{AA} decreases with increasing p_T^a , indicating a softening of the fragmentation function of surviving jets (Nattrass *et al.*, 2016).

2809 A large collection of experimental measurements in e^+e^- collisions show that jets initiated by gluons exhibit differences with respect to jets from light-flavor quarks (Abreu *et al.*, 1996; Acton *et al.*, 1993; Akers *et al.*, 1995; Barate *et al.*, 1998; Buskulic *et al.*, 1996).

2814 First, the charged particle multiplicity is higher in gluon jets than in light-quark jets. Second, the fragmentation functions of gluon jets are considerably softer than that of quark jets. Finally, gluon jets appeared to be less collimated than quark jets. These differences have already been exploited to differentiate between gluon and quark jets in p + p collisions (Collaboration, 2013a). The simplest and most studied variable used experimentally is the multiplicity, the total number of constituents of reconstructed jet. Since gluon hadronization produces jets which are ‘wider’ than jets induced by quark hadronization, jet shapes could be studied with jet width variables to distinguish quark and gluon jets.

2821 Since there are significant differences in baryon and meson production in $A+A$ collisions compared to p + p collisions, such differences may exist for jets. Furthermore, energy loss is different for quark and gluon jets, so species-dependent energy loss may mean that there are differences between jets with different types of leading hadrons. These differences may be observed through comparisons of jets with leading baryons and mesons or light and strange hadrons. The OPAL collaboration measured the ratio of K_0^S production in e^+e^- collisions in gluon jets to that in quark jets to be $1.10 \pm 0.02 \pm 0.02$ and the ratio of Λ production in gluon jets to that in quark jets to be $1.41 \pm 0.04 \pm 0.04$ (Ackerstaff *et al.*, 1999), meaning that jets containing a Λ or a proton are somewhat more likely to arise from gluon jets than jets which do not contain a baryon. This difference is small, however, a large difference in the interactions between quark and gluon jets in heavy ion collisions may be observable.

2845 Measurements of dihadron correlations with identified leading triggers may be sensitive to these effects. Studies of identified strange trigger particles found a somewhat higher yield in jets with a leading K_0^S than those with a leading unidentified charged hadron or Λ at the same momentum (Abelev *et al.*, 2016). This was also observed in d +Au collisions, indicating that the more massive leading Λ simply takes a larger fraction of the jet energy. The slight centrality dependence indicates there may be medium effects, however, these could arise from differences in quark and gluon jets or from strange and non-strange jets. Ultimately these data are inconclusive due to their low precision. Dihadron correlations with identified pion and non-pion triggers (Adamczyk *et al.*, 2015) shown in Figure 29 observed a higher yield in jets with a leading pion than those with a leading kaon or proton. This difference was larger in Au+Au collisions than in d +Au collisions, which (Adamczyk *et al.*, 2015) proposes may be impacted to fewer baryon trigger particles coming from jets due to recombination. Both of these results could be impacted by several effects – differences in quark and gluon jets in the vacuum, differences in energy loss in the medium for quark and gluon jets, and modified fragmentation in the medium. Since both stud-

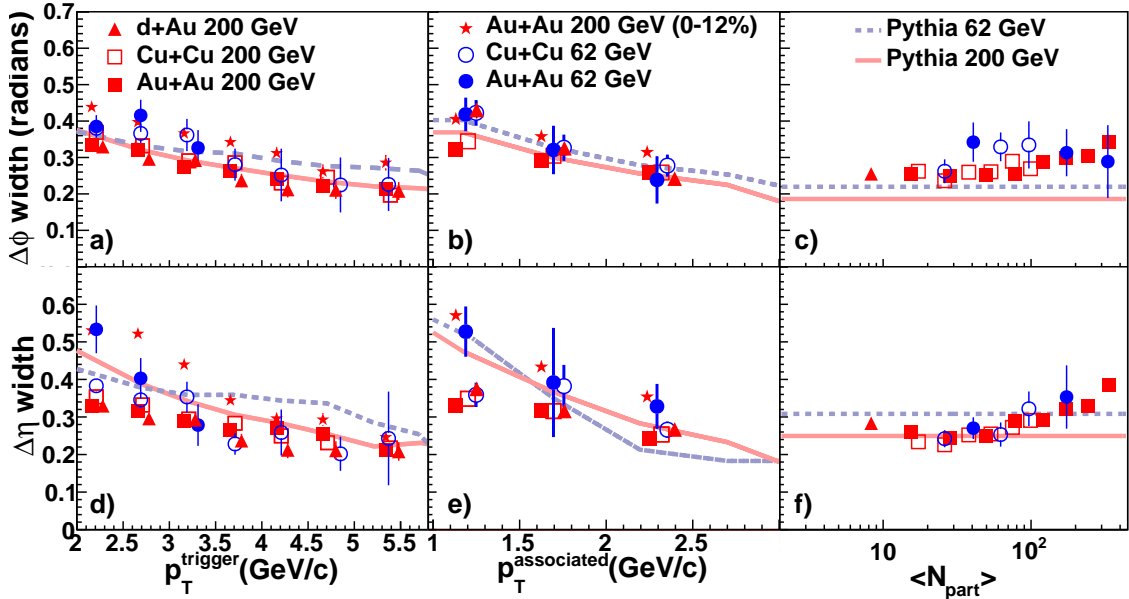


FIG. 28 Figure from STAR (Agakishiev *et al.*, 2012c). Dependence of the Gaussian widths in $\Delta\phi$ and $\Delta\eta$ on p_T^t for $1.5 \text{ GeV}/c < p_T^a < p_T^t < p_T^a$ for $3 < p_T^t < 6 \text{ GeV}/c$, and $\langle N_{\text{part}} \rangle$ for $3 < p_T^t < 6 \text{ GeV}/c$ and $1.5 \text{ GeV}/c < p_T^a < p_T^t$ for 0-95% d + Au , 0-60% Cu + Cu at $\sqrt{s_{\text{NN}}} = 62.4 \text{ GeV}$ and $\sqrt{s_{\text{NN}}} = 200 \text{ GeV}$, 0-80% Au + Au at $\sqrt{s_{\text{NN}}} = 62.4 \text{ GeV}$, and 0-12% and 40-80% Au + Au at $\sqrt{s_{\text{NN}}} = 200 \text{ GeV}$. This demonstrates that the correlation is broadened in central Au + Au collisions.

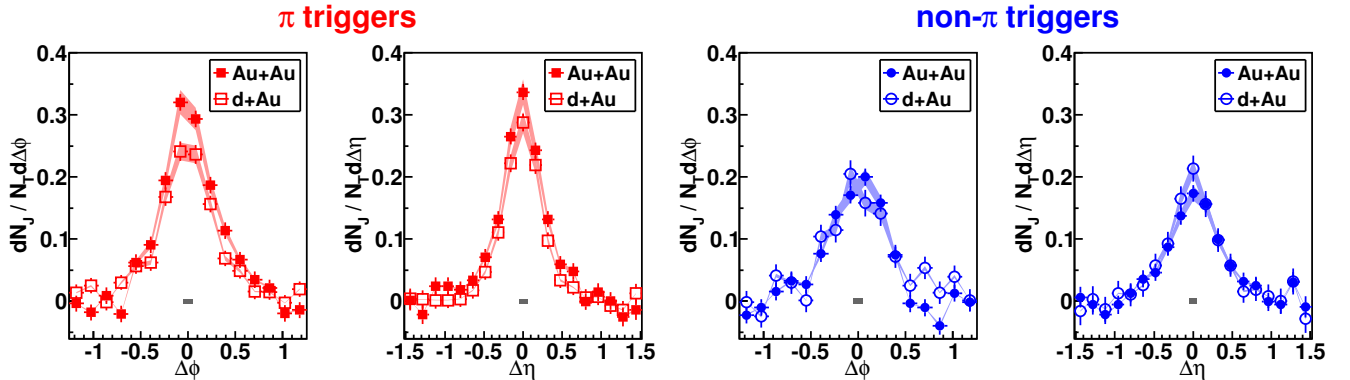


FIG. 29 Figure from STAR (Adamczyk *et al.*, 2015). The $\Delta\phi$ and $\Delta\eta$ projections of the correlation for $|\Delta\eta| < 0.78$ and $|\Delta\phi| < \pi/4$, respectively, for pion triggers (left two panels) and non-pion triggers (right two panels). Filled symbols show data from the 0-10% most central Au + Au collisions at $\sqrt{s_{\text{NN}}} = 200 \text{ GeV}$. Open symbols show data from minimum bias d + Au data at $\sqrt{s_{\text{NN}}} = 200 \text{ GeV}$. This figure shows that the yield is higher for pion trigger particles than non-pion trigger particles, which are mostly kaons and protons, and that there is a higher yield for pion trigger particles in central Au + Au collisions than in d + Au collisions. This may be an indication of differences in partonic energy loss for quarks and gluons in the medium.

ies observe differences, at least some of these effects are present in the data, however, the data cannot distinguish which effects are present.

4. Jet-hadron correlations

Measurements of jet-hadron correlations are sensitive to the broadening and softening of the fragmentation function, but have the advantage over dihadron correlations that the jet will be more closely correlated with the kinematics of its parent parton than a high p_T hadron.

Figure 30 shows jet-hadron correlations measured by CMS (Khachatryan *et al.*, 2016a) as a function of $\Delta\eta$ from the trigger jet. Not shown here are the results as a function of $\Delta\phi$ from the trigger jet, however the conclusions were quantitatively the same. The jets in this sample had a resolution parameter of $R = 0.3$ and a leading jet $p_T > 120 \text{ GeV}/c$ in order to reduce the effect of the background on the trigger jet sample. The background

sample had a resolution parameter of $R = 0.3$ and a leading jet $p_T > 120 \text{ GeV}/c$ in order to reduce the effect of the background on the trigger jet sample. The background

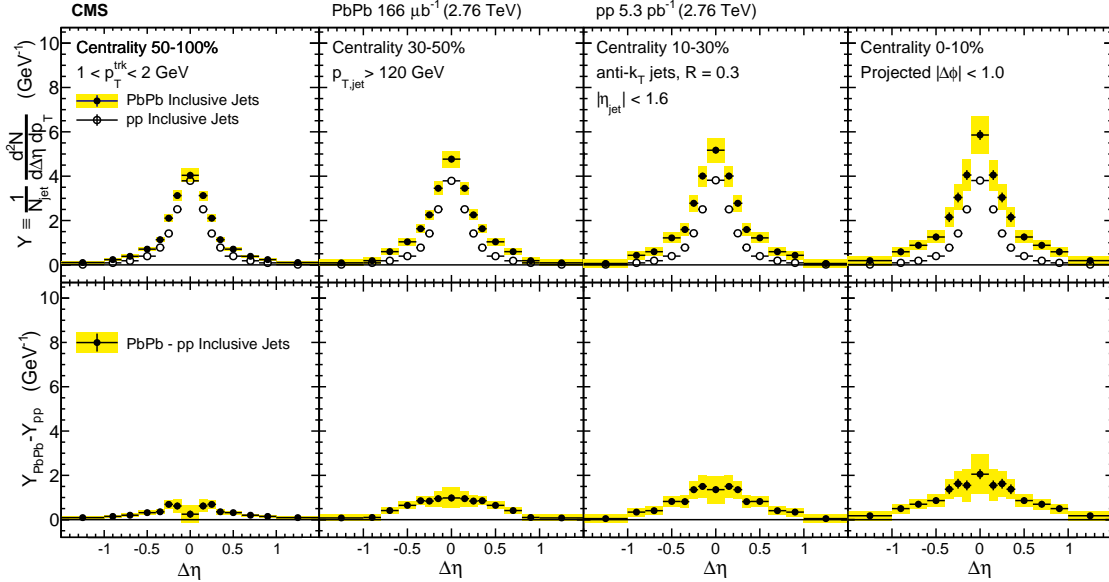


FIG. 30 Figure from CMS (Khachatryan *et al.*, 2016a). Symmetrized $\Delta\eta$ distributions correlated with Pb+Pb and $p+p$ inclusive jets with $p_T > 120$ GeV are shown in the top panels for tracks with $1 < p_T < 2$ GeV. The difference between per-jet yields in Pb+Pb and $p+p$ collisions is shown in the bottom panels. These measurements indicate that the jet is broadened and softened, as expected from energy loss models.

removal for the jets reconstructed in Pb+Pb was done high momenta was balanced by the enhancement at low via the HF/Voronoi method, which is described in (CMS, 2013), a slightly different method than described in Sec. II. The effect of the combinatorial background on the distribution of associated tracks was removed by a sideband method, in which the background is approximated by the measured two dimensional correlations in the range $1.5 < |\Delta\eta| < 3.0$. Jets in Pb+Pb are observed to be broader, with the greatest increase in the width for low momentum associated particles. This is consistent with expectations from partonic energy loss. These studies found that the subleading jet was broadened even more than the leading jet, indicating a bias towards selecting less modified jets as the leading jet.

Jet hadron correlations have also been studied at RHIC energies, where the width and yield of the away-side peak, rather than the associated particle correlations themselves, can be seen in Figure 31. This figure shows the away-side widths and

momenta, which means that this change in the jet structure likely comes from modification of the jet rather than modifications of the jet spectrum. This enhancement at low p_T is at the same associated momentum for both jet energies, which may indicate that the enhancement is not dependent on the energy of the jet but the momentum of the constituents.

5. Dijets

The LHC A_J measurements shown in Figure 16 show a significant energy imbalance for dijets due to medium effects in central collisions (Aad *et al.*, 2010; Chatrchyan *et al.*, 2011b) while RHIC A_J measurements suggest that energy imbalance observed for jet cones of $R=0.2$ can be recovered within a jet cone of $R=0.4$ for measurable dijet events (Adamczyk *et al.*, 2017b). The STAR measurements demonstrate that the energy imbalance is recovered when including low p_T constituents (Adamczyk *et al.*, 2017b), also indicating a softening of the fragmentation function. Comparing these two results is complicated since they have very different surface biases, both due to the experimental techniques and the different collision energies. In order to interpret such comparisons and draw definitive conclusions a robust Monte Carlo generator is required because the differences in these observables are not analytically calculable. To develop a better picture of the transverse structure of the jets, it

$$D_{AA} = Y_{Au+Au} \langle p_T^{assoc} \rangle_{Au+Au} - Y_{p+p} \langle p_T^{assoc} \rangle_{p+p} \quad (13)$$

where Y_{Au+Au} and Y_{p+p} are the number of particles in the away-side from (Adamczyk *et al.*, 2014a) for two different ranges of jet p_T . The width in $p+p$ is consistent with that in Au+Au within uncertainties, although the uncertainties are large due to the large uncertainties in the v_n . The D_{AA} shows that momentum is redistributed within the jet, with suppression ($D_{AA} < 0$) for $p_T < 2$ GeV/c associated particles and enhancement ($D_{AA} > 0$) for > 2 GeV/c. This indicates that the suppression at

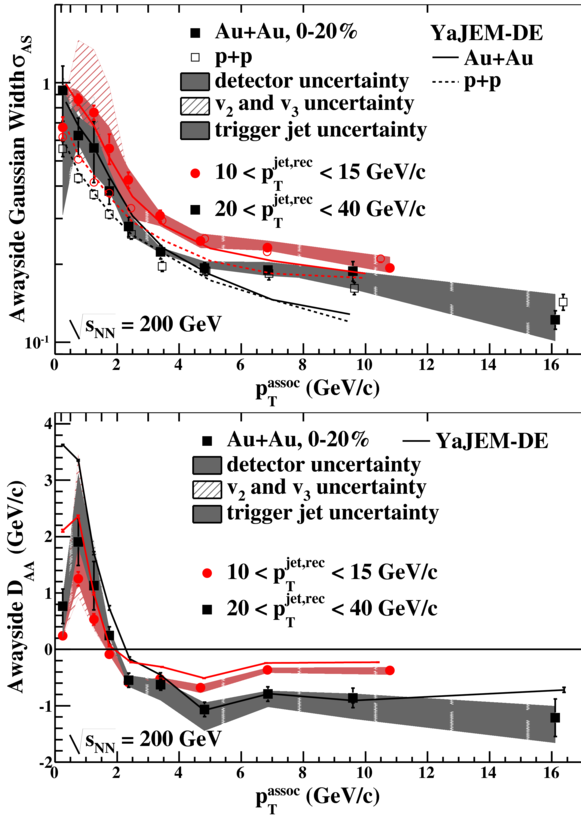


FIG. 31 Figure from STAR (Adamczyk *et al.*, 2014a). Gaussian widths of the away-side peaks (σ_{AS}) for $p+p$ collisions (open squares) and central $Au+Au$ collisions (solid squares) (upper) and away-side momentum difference D_{AA} as defined in Equation 13 (lower) are both plotted as a function of p_T^a . The widths (note the log scale on the y-axis) show no evidence of broadening in $Au+Au$ relative to $p+p$ due to the large uncertainties in the $Au+Au$ measurement. However, D_{AA} shows the suppression of high momentum particles associated with the jet is balanced by the enhancement of lower momentum associated particles. The point at which enhancement transitions to suppression appears to occur at the same associated particle's momentum and does not depend on the jet momentum. Data are for $\sqrt{s_{NN}} = 200$ GeV collisions and YaJEM-DE model calculations are from (Renk, 2013b).

is best to measure observables specifically designed to probe the transverse direction.

The effect on dijets along the direction transverse to the jet axis was studied by measuring the angular difference between the reconstructed jet axis of the leading and sub-leading jets (Aad *et al.*, 2010; Chatrchyan *et al.*, 2011b). These results are shown in Figure 16 and little change to the angular deflection of the sub-leading jet in central Pb+Pb collisions compared to $p+p$ collisions is observed. It is important to point out that the tails in the $p+p$ distribution may be due to 3-jet events while those pairs in Pb+Pb events are the results of dijets undergoing energy loss.

2950 6. Jet Shapes

Another observable that is related to the structure of the jet is the called the jet shape. This observable is constructed with the idea that the high energy jets we are interested in are roughly conical. First a jet finding algorithm is run to determine the axis of the jet, and then the sum of the transverse momentum of the tracks in concentric rings about the jet axis are summed together (and divided by the total transverse jet momentum). The differential jet shape observable $\rho(r)$ is thus the radial distribution of the transverse momentum:

$$\rho(r) = \frac{1}{\delta r} \frac{1}{N_{jet}} \sum_{jets} \frac{\sum_{tracks \in [r_a, r_b]} p_T^{track}}{p_T^{jet}} \quad (14)$$

2951 where the jet cone is divided rings of width δr which have
2952 an inner radius r_a and an outer radius r_b .

2953 The differential and integrated jet shape measurements
2954 measured by CMS are shown in Figure 32. For this CMS
2955 study, inclusive jets with $p_T > 100$ GeV/c, resolution
2956 parameter $R = 0.3$ and constituent tracks with $p_T > 1$
2957 GeV/c were used. The effect of the background on the
2958 signal jets was removed through the iterative subtraction
2959 technique described in Section II. The associated tracks
2960 were not explicitly required to be the constituent tracks,
2961 however given that the momentum selection criteria is
2962 the same and the conical nature of jets at this energy,
2963 they will essentially be the same. The effect of the back-
2964 ground on the distribution of the associated particles was
2965 removed via an η reflection method, where the analysis
2966 was repeated for an $R = 0.3$ cone with the opposite sign η
2967 but same ϕ . This preserves the flow effects in a model in-
2968 dependent way in the determination of the background.
2969 The differential jet shapes in the most central Pb+Pb
2970 collisions are broadened in comparison to measurements
2971 done in $p+p$ collisions at the same center of mass energy
2972 (Chatrchyan *et al.*, 2013a). As shown in other measure-
2973 ments, the effect is centrality dependent. These measure-
2974 ments demonstrate that there is an enhancement in the
2975 modification with increasing angle from the jet axis, in-
2976 dicating a broadening of the jet profile and a depletion
2977 near $r \approx 0.2$.

2978 7. Particle composition

Theory predicts higher production of baryons and strange particles in jets fragmenting in the medium relative to jets fragmenting in the vacuum (Sapeta and Wiedemann, 2008). The only published study searching for modified particle composition in jets in heavy ion collisions is the Λ/K_S^0 ratio in the near-side jet-like correlation of dihadron correlations in Cu+Cu collisions at $\sqrt{s_{NN}} = 200$ GeV by STAR (Abelev *et al.*, 2016) shown in Figure 33. This measurement indicated that particle

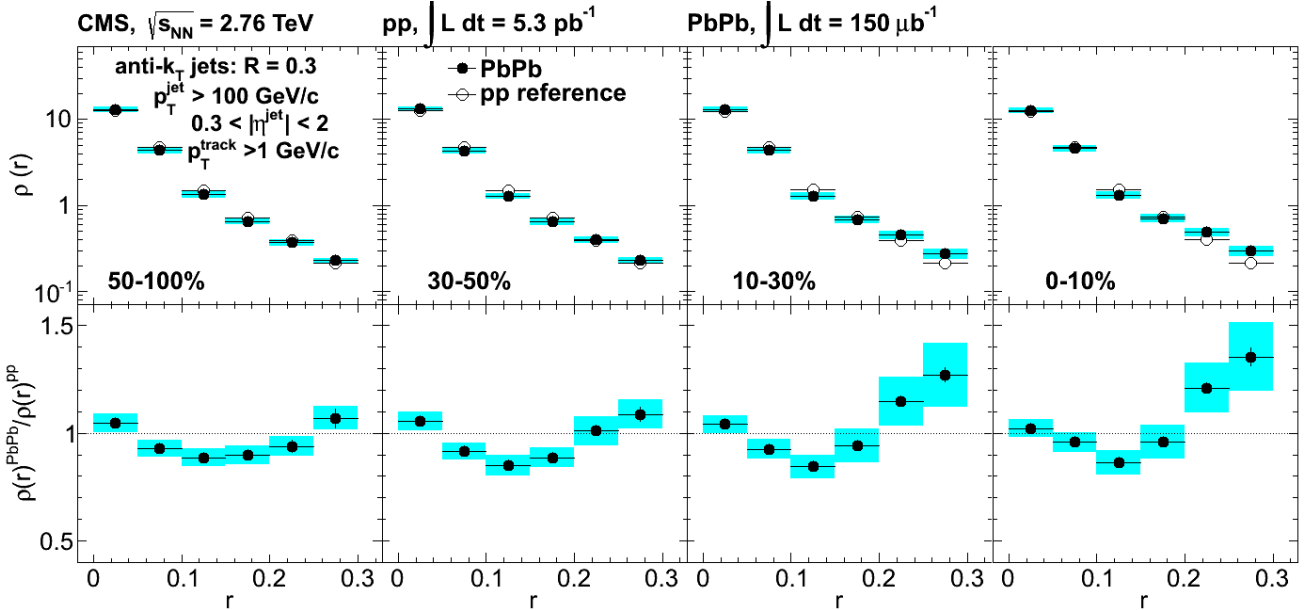


FIG. 32 Figure from CMS (Chatrchyan *et al.*, 2013a). Differential jet shapes in Pb+Pb and $p+p$ collisions for four Pb+Pb centralities. Each spectrum is normalized so that its integral is unity. This shows that there are more particles in jets in central collisions and these modifications are primarily at large angles relative to the jet axis, as expected from partonic energy loss.

2988 ratios in the near-side jet-like correlation are compara- 3014 8. LeSub
 2989 ble to the inclusive particle ratios in $p+p$ collisions. At 3015
 2990 high momenta, the inclusive particle ratios in $p+p$ col- 3016
 2991 lisions are expected to be dominated by jet fragmentation 3017
 2992 and therefore are a good proxy for direct observation of 3018
 2993 the particle ratios in reconstructed jets. PYTHIA studies 3019
 2994 show that the inclusive particle ratios in $p+p$ col- 3020
 2995 lisions are approximately the same as the particle ra- 3021
 2996 tios in dihadron correlations with similar kinematic cuts; 3022
 2997 differences are well below the uncertainties on the ex- 3023
 2998 perimental measurements. The consistency between the 3024
 2999 Λ/K_S^0 ratio in the jet-like correlation in Cu+Cu collisions 3025
 3000 and the inclusive ratio in $p+p$ collisions is therefore in- 3026
 3001 terpreted as evidence that the particle ratios in jets are 3027
 3002 the same in $A+A$ collisions and $p+p$ collisions, that at 3028
 3003 least the particle ratios are not modified. In contrast, the 3029
 3004 inclusive Λ/K_S^0 reaches a maximum near 1.6 (Agakishiev 3030
 3005 *et al.*, 2012b), a few times that in $p+p$ collisions. Prelim- 3031
 3006 inary measurements from both the STAR dihadron cor- 3032
 3007 relations (Suarez, 2012) and ALICE collaborations from 3033
 3008 both dihadron correlations (Veldhoen, 2013) and recon- 3034
 3009 structed jets (Kucera, 2016; Zimmermann, 2015) support 3035
 3010 this conclusion. However, experimental uncertainties are 3036
 3011 large and for studies in dihadron correlations, results are 3037
 3012 not available for the away-side and the near-side is known 3038
 3013 to be surface biased.

8. LeSub

One of the new observables constructed in order to attempt to create well defined QCD observables is LeSub, defined as:

$$\text{LeSub} = p_T^{\text{lead,track}} - p_T^{\text{sublead,track}} \quad (15)$$

LeSub characterizes the hardest splitting, so it should be insensitive to background, however, it is not colinear safe and therefore cannot be calculated reliably in pQCD. It agrees well with PYTHIA simulations of $p+p$ collisions and is relatively insensitive to the PYTHIA tune (Cunqueiro, 2016), which is not surprising as the hardest splittings in PYTHIA do not depend on the tune. LeSub calculated in PYTHIA agrees well with the data from Pb+Pb collisions for $R = 0.2$ charged jets. This indicates that the hardest splittings are likely unaffected by the medium. Modifications may depend on the jet momentum, as the ALICE results are for relatively low momentum jets at the LHC. The ALICE measurement is also for relatively small jets, which preferentially selects more collimated fragmentation patterns, but it indicates that observables that depend on the first splittings are insensitive to the medium.

9. Jet Mass

In a hard scattering the partons are produced off-shell, and the amount they are off-shell is the virtuality (Ma-

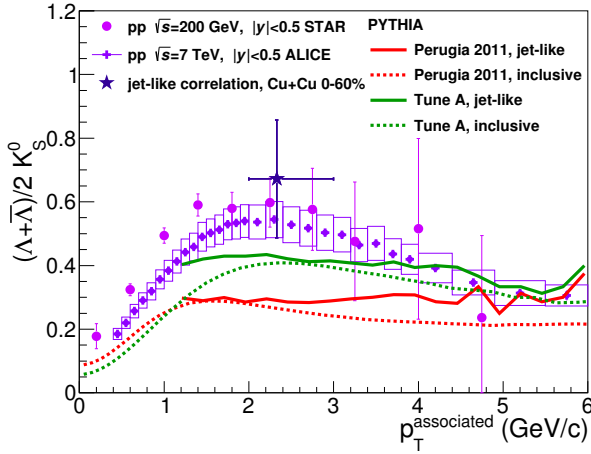


FIG. 33 Figure from STAR (Abelev *et al.*, 2016). Λ/K_S^0 ratio measured in jet-like correlations in 0-60% Cu+Cu collisions at $\sqrt{s_{NN}} = 200$ GeV for $3 < p_T^{\text{trigger}} < 6$ GeV/c and $2 < p_T^{\text{associated}} < 3$ GeV/c along with this ratio obtained from inclusive p_T spectra in $p+p$ collisions. Data are compared to calculations from PYTHIA (Sjostrand *et al.*, 2006) using the Perugia 2011 tunes (Skands, 2010) and Tune A (Field and Group, 2005). This shows that, within the large uncertainties, there is no indication that the particle composition of jets is modified in $A+A$ collisions, where Λ/K_S^0 reaches a maximum of 1.6 (Agakishiev *et al.*, 2012b).

jumder and Putschke, 2016). When a jet showers in vacuum, at each splitting the virtuality is reduced and momentum is produced transverse to the original scattered parton's direction, until the partons are on-shell and thus hadronize. For a vacuum jet, if the four vectors of all of the daughters from the original parton are combined, the mass calculated from the combination of the daughters would be precisely equal to the virtuality. The virtuality of hard scattered parton is important as it is directly related to how broad the jet itself is, as it is directly related to how much momentum transverse to the jet axis the daughters can have.

The mass of a jet might serve as a way to better characterize the state of the initial parton. It is important to construct observables where the only difference between $p+p$ collisions compared to heavy ion collisions is due to the effects of jet quenching, and not the result of biases in the jet selection. Jet mass may make a much closer comparison between heavy ion and $p+p$ observables by selecting more similar populations of parent partons than could be achieved by selecting differentially in transverse momentum alone. Secondly, the measured jet mass itself could be affected by in-medium interactions as the vir-

tuality of the jet can increase for a given splitting due to the medium interaction, unlike in the vacuum case.

Figure 34 shows the ALICE (Acharya *et al.*, 2017) jet mass measurement of charged jets for most central collisions. No difference is observed between PYTHIA Peru-

gia 2011 tune (Skands, 2010) and data from Pb+Pb collisions in all jet p_T bins indicating no apparent modification within uncertainties. In addition to PYTHIA, these distributions were compared to three different quenching models, JEWEL (Zapp, 2014a) with recoil on, JEWEL with recoil off, and Q-PYTHIA (Armesto *et al.*, 2009). Both Q-PYTHIA and JEWEL with the recoil on produced jets with a larger mass distribution than in the data, whereas JEWEL with the recoil off gives a slightly lower value than the data. This implies that jet mass as a distribution in these energy and momentum ranges is rather insensitive to medium effects, as JEWEL and Q-PYTHIA both incorporate medium effects whereas PYTHIA describes vacuum jets. The agreement between PYTHIA and data could also indicate that the jets selected in this analysis were biased towards those that fragmented in a vacuum-like manner. More differential measurements of jet mass are needed to determine the usefulness of jet mass variable.

10. Dispersion

Since quark jets have harder fragmentation functions, they are more likely to produce jets with hard constituents that carry a significant fraction of the jet energy.

This can be studied with $p_T^D = \sqrt{\sum_i p_{T,i}^2} / \sum_i p_{T,i}$. This observable was initially developed in order to distinguish between quark and gluon jets with quark jets yielding a larger mean p_T^D (Collaboration, 2013a). The ALICE experiment has measured p_T^D in Pb+Pb collisions, shown in Figure 35. The data from Pb+Pb collisions for $R = 0.2$ charged jets with transverse momentum between 40 and 60 GeV is compared to data from PYTHIA with the Perugia 11 tune. In Pb+Pb collisions, the mean p_T^D was found to be larger compared to the PYTHIA reference, which had been validated by comparisons with $p+p$ data. This may indicate either a selection bias towards quark jets or harder fragmenting jets.

11. Girth

The jet girth is another new observable describing the shape of a jet. The jet girth, g , is the p_T weighted width of the jet

$$g = \sum_i \frac{p_T^i}{p_T^{\text{jet}}} |r_i|, \quad (16)$$

where r_i is the angular distance between particle i and the jet axis. If jets are broadened by the medium, we would expect that g would be increased, and the converse would be that if jets were collimated than g would be reduced. While the distributions overlap, the gluon jets are broader and have a higher average g than quark

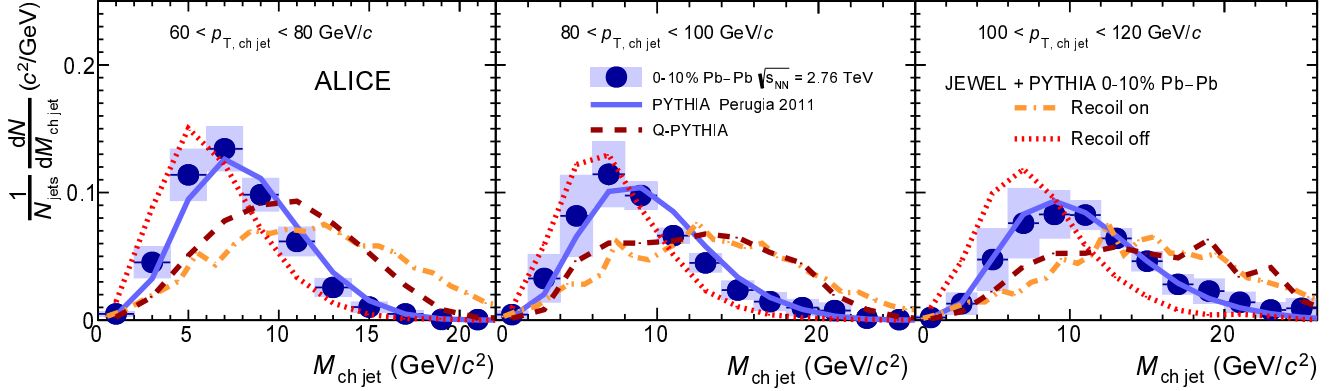


FIG. 34 Figure from ALICE (Acharya *et al.*, 2017). Fully-corrected jet mass distribution for anti- k_T jets with $R=0.4$ in the 10% most central Pb+Pb collisions compared to PYTHIA (Sjostrand *et al.*, 2006) with the Perugia 2011 tune (Skands, 2010) and predictions from the jet quenching event generators JEWEL (Zapp, 2014a) and Q-PYTHIA (Armesto *et al.*, 2009). No difference is observed between PYTHIA and the data. This shows that there is no modification of the jet mass within uncertainties.

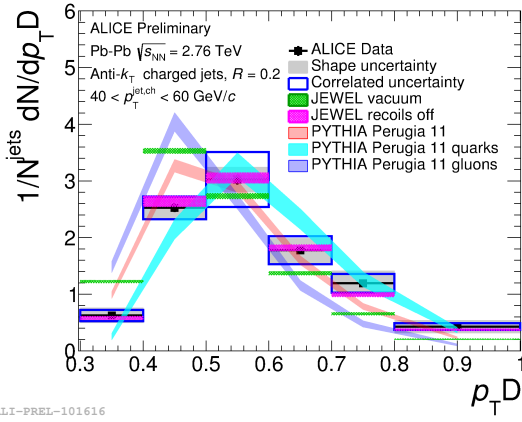


FIG. 35 Figure from ALICE (Cunqueiro, 2016). Unfolded p_T^D shape distribution in Pb+Pb collisions for $R=0.2$ charged jets with momenta between 40 and 60 GeV/c compared to PYTHIA simulations, to JEWEL calculations, and to q/g PYTHIA templates. This shows that the dispersion is larger in Pb+Pb collisions than in $p+p$ collisions. This may indicate either modifications or a quark bias.

3117 Figure 36. JEWEL includes partonic energy loss and
 3118 predicts little modification of the girth in heavy ion colli-
 3119 sions. PYTHIA calculations include inclusive jets, quark
 3120 jets, and gluon jets. The data are closest to PYTHIA
 3121 predictions for quark jets. This may be due to bias to-
 3122 wards quarks in surviving jets in Pb+Pb collisions.

3123 One of the unanswered questions regarding jets in
 3124 heavy ion collisions is whether jets start to fragment
 3125 while they are in the medium, or whether they simply
 3126 lose energy to the medium and then fragment similar to
 3127 fragmentation in vacuum after reaching the surface. If
 3128 the latter is true, jet quenching would be described as
 3129 a shift in parton p_T followed by vacuum fragmentation,
 3130 which would mean that jets shapes in Pb+Pb collisions
 3131 would be consistent with jet shapes in $p+p$ collisions. If g
 3132 is shifted, this would favor fragmentation in the medium
 3133 and if it is not, it would favor vacuum fragmentation.
 3134 These observations are qualitatively consistent with the
 3135 measurements of p_T^D discussed in Section III.C.6 and the
 3136 jet shape discussed in Section III.C.6.

3137 12. Grooming

3106 jets. The ALICE experiment has shown that distribu-
 3107 tions of g in $p+p$ collisions agree well with PYTHIA dis-
 3108 tributions, indicating that it is a reasonable probe and
 3109 that PYTHIA can be used as a reference. In Pb+Pb col-
 3110 lisions, the ALICE experiment found that g is slightly
 3111 shifted towards smaller values compared to the PYTHIA
 3112 reference for $R = 0.2$ charged jets (Cunqueiro, 2016),
 3113 although the significance of this shift is unclear. This in-
 3114 dicates that the core may appear to be more collimated
 3115 in Pb+Pb collisions than $p+p$ collisions. Measurements
 3116 are compared to JEWEL and PYTHIA calculations in

3138 Jet grooming algorithms (Butterworth *et al.*, 2008;
 3139 Dasgupta *et al.*, 2013; Ellis *et al.*, 2010; Krohn *et al.*,
 3140 2010) attempt to remove soft radiation from the lead-
 3141 ing partonic components of the jet, isolating the larger
 3142 scale structure. The motivation for algorithms such as
 3143 jet grooming was to develop observables which can be
 3144 calculated with perturbative QCD, and which are rela-
 3145 tively insensitive to the details of the soft background.
 3146 This allows us to determine whether the medium affects
 3147 the jet formation process from the hard process through
 3148 hadronization, or whether the parton loses energy to the

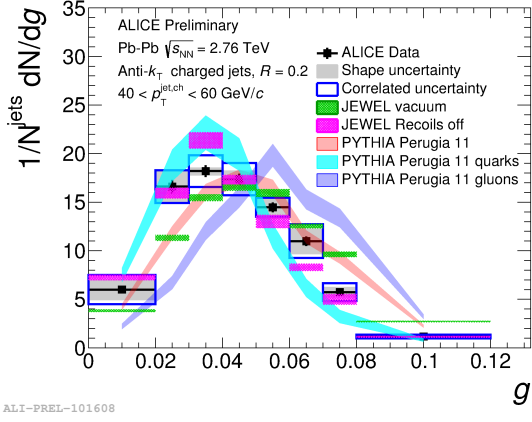


FIG. 36 Figure from ALICE (Cunqueiro, 2016). The girth g for $R=0.2$ charged jets in Pb+Pb collisions with jet p_T^{ch} between 40 and 60 GeV/c compared to a PYTHIA simulations, to JEWEL calculations, and to q/g PYTHIA templates. This shows that jets are somewhat more collimated in Pb+Pb collisions than in $p+p$ collisions. This may indicate a quark bias in surviving jets in Pb+Pb collisions.

3173 trality intervals for jets within the transverse momentum
 3174 range of 160–180 GeV/c (Sirunyan *et al.*, 2017a). While
 3175 the measured z_g distribution in peripheral Pb+Pb col-
 3176 lisions is in agreement with the expected $p+p$ measurement
 3177 within uncertainties, a difference becomes apparent in the
 3178 more central collisions. This observation indicates that
 3179 the splitting into two branches becomes increasingly more
 3180 unbalanced for more central collisions for the jets within
 3181 the transverse momentum range of 160–180 GeV/c . A
 3182 similar preliminary measurement by STAR observes no
 3183 modification in z_g (Kauder, 2017). The apparent modi-
 3184 fications seen by CMS were proposed to be due to a re-
 3185 striction to subjets with a minimum separation between
 3186 the two hardest subjets $R_{12} > 0.1$ (Milhano, 2017). This
 3187 indicates that there may be modifications of z_g limited
 3188 to certain classes of jets but not observed globally. This
 3189 dependence of modifications on jets may be a result of in-
 3190 teractions with the medium (Milhano *et al.*, 2017). While
 3191 grooming and measurements of the jet substructure are
 3192 promising, we emphasize the need for a greater under-
 3193 standing of the impact of the large combinatorial back-
 3194 ground and the bias of kinematic cuts on z_g .

3149 medium with fragmentation only affected at much later
 3150 stages. It is important to realize that the answers to these
 3151 questions will depend on the jet energy and momentum,
 3152 so there will not be a single definitive answer. Jet groom-
 3153 ing allows separation of effects of the length scale from
 3154 effects of the hardness of the interaction. Essentially this
 3155 will allow us to see whether we are scattering off of point-
 3156 like particles in the medium or scattering off of something
 3157 with structure. However, to properly apply this class of
 3158 algorithms to the data, a precision detector is needed.

The jet grooming algorithm takes the constituents of a jet, and recursively declusters the jet's branching history and discards the resulting subjets until the transverse momenta, $p_{T,1}, p_{T,2}$, of the current pair fulfills the soft drop condition (Larkoski *et al.*, 2014):

$$\frac{\min(p_{T,1}, p_{T,2})}{p_{T,1} + p_{T,2}} > z_{\text{cut}} \theta^{\beta} \quad (17)$$

3159 where θ is an additional measure of the relative angu-
 3200 lar distance between the two sub-jets and z_{cut} and θ^{β} are
 3201 parameters which can select how strict the soft drop con-
 3202 dition is. For the heavy-ion analyses conducted so far, β
 3203 has been set to zero and z_{cut} has been set to 0.1.

3204 A measurement of the first splitting of a parton in
 3205 heavy ion collisions is performed by the CMS collabora-
 3206 tion in Pb+Pb collisions at $\sqrt{s_{\text{NN}}} = 5 \text{ TeV}$. The splitting
 3207 function is defined as $z_g = p_{T,2}/(p_{T,1} + p_{T,2})$ with $p_{T,2}$ in-
 3208 dicating the transverse momentum of the least energetic
 3209 subjet and $p_{T,1}$ the transverse momentum of the most en-
 3210 ergetic subjet, applied to those jets that passed the soft
 3211 drop condition outlined above. Figure 37 shows the ratio
 3212 of z_g in Pb+Pb to that in $p+p$ from CMS for several cen-

3195 13. Subjettiness

The observable τ_N is a measure of how many hard
 3196 cores there are in a jet. This was initially developed to
 3197 tag jets from Higgs decays in high energy $p+p$ collisions.
 3198 A jet from a single parton usually has one hard core, but
 3199 a hard splitting or a bremsstrahlung gluon would lead to
 3200 an additional hard core within the jet. An increase in
 3201 the fraction of jets with two hard cores could therefore
 3202 be evidence of gluon bremsstrahlung.

The jet is reclustered into N subjets, and the following
 3203 calculation is performed over each track in the jet:

$$\tau_N = \frac{\sum_{i=1}^M (p_T^i \min(\Delta R_{1,i}, \Delta R_{2,i}, \dots, \Delta R_{N,i}))}{R_0 \sum_{i=1}^N p_T^i} \quad (18)$$

3204 where $\Delta R_{N,i}$ is the distance in $\eta-\phi$ between the i th track
 3205 and the axis of the N th subjet and the original jet has
 3206 resolution parameter R_0 . In the case that all particles
 3207 are aligned exactly with one of the subjets' axes, τ_N will
 3208 equal zero. In the case where there are more than N
 3209 hard cores, a substantial fraction of tracks will be far
 3210 from the nearest subjet axis, however, all tracks must
 3211 have $\min(\Delta R_{1,i}, \Delta R_{2,i}, \dots, \Delta R_{N,i}) \leq R_0$ because they are
 3212 contained within the original jet. The maximum value of
 3213 τ_N is therefore one, the case when all jet constituents are
 3214 at the maximum distance from the nearest subjet axis.

Jets that have a low value of τ_N are therefore more
 3215 likely to have N or fewer well defined cores in their sub-
 3216 structure, whereas jets with a high value are more likely
 3217 to contain at least $N+1$ cores. A shift in the distribu-
 3218 tion of τ_N in a jet population towards lower values can

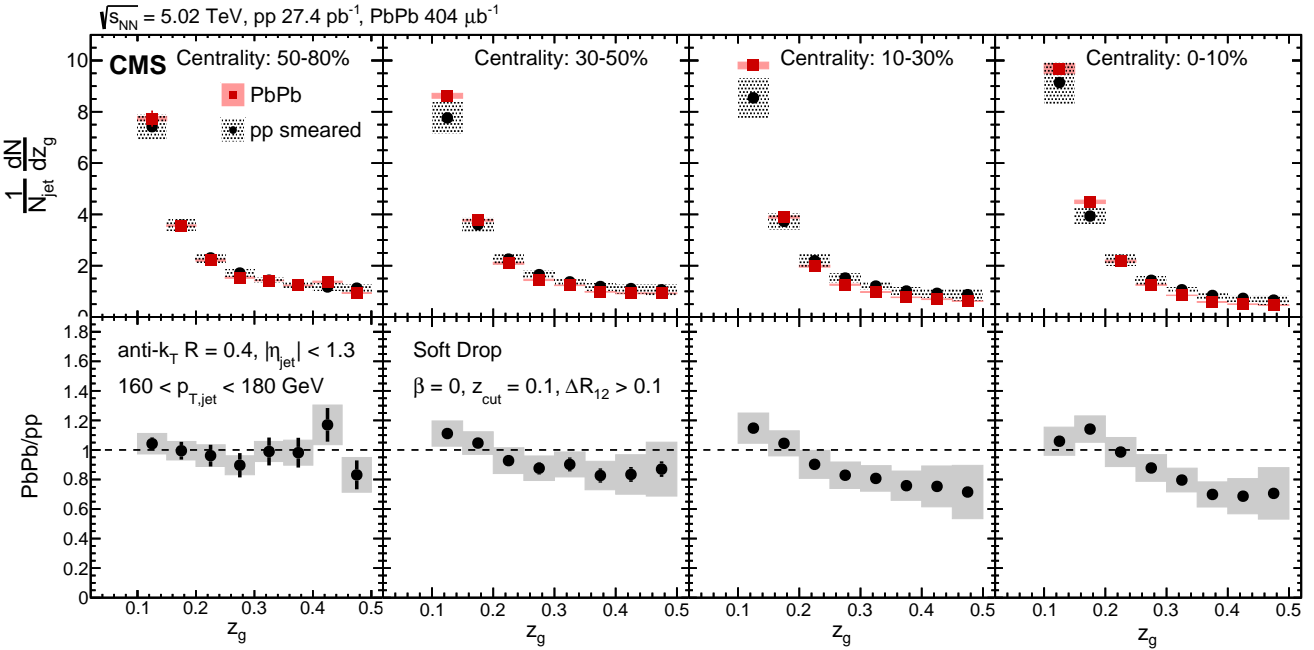


FIG. 37 Figure from CMS (Sirunyan *et al.*, 2017a). Ratio of the splitting function $z_g = p_{T2}/(p_{T1} + p_{T2})$ in Pb+Pb and $p+p$ collisions with the jet energy resolution smeared to match that in Pb+Pb for various centrality selections and $160 < p_{T,jet}^jet < 180$ GeV. This shows that the splitting function is modified in central Pb+Pb collisions compared to $p+p$ collisions, which may indicate either a difference in the structure of jets in the two systems or an impact of the background.

3220 indicate fewer subjets while a shift to higher τ_N can indicate
 3221 more subjets. The observable τ_2/τ_1 was constructed
 3222 by the ALICE experiment (Zardoshti, 2017). Similar to
 3223 the approach in (Adam *et al.*, 2015c; Adamczyk *et al.*,
 3224 2017c), background was subtracted using the coincidence
 3225 between a soft trigger hadron, which should have only a
 3226 weak correlation with jet production, and a high mo-
 3227 mentum trigger hadron, and can be seen in Figure 38. A
 3228 jet where this ratio is close to zero most likely has two
 3229 hard cores. This observable is relatively insensitive to
 3230 the fluctuations in the background, as it would have to
 3231 carry a significant fraction of the jet momentum to be
 3232 modified. The ALICE result shows that the structure of
 3233 the jets was unmodified for $R = 0.4$ charged jets with
 3234 $40 \leq p_{t,jet}^{ch} < 60$ GeV/c compared to PYTHIA cal-
 3235 culations. This implies that medium interactions do not lead to ex-
 3236 tra cores within the jet, at least for selection of jets in
 3237 this measurement. As for many jet observables, this ob-
 3238 servable may be difficult to interpret for low momentum
 3239 jets in a heavy ion environment.

3240 14. Summary of experimental evidence for medium 3241 modification of jets

3242 The broadening and softening of jets due to interac-
 3243 tions with the medium is demonstrated clearly by several
 3244 mature observables which measure the average properties
 3245 of jets. This includes fragmentation functions measured
 3246

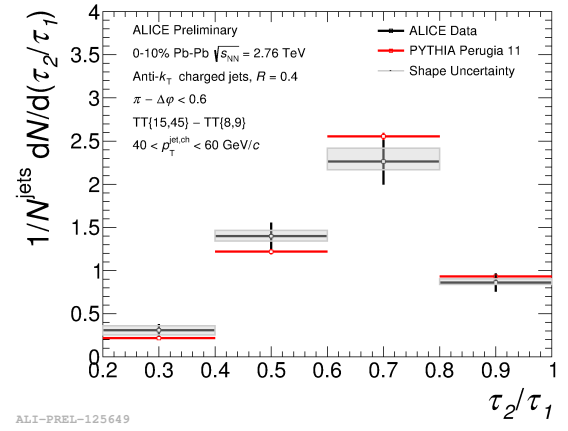


FIG. 38 Figure from (Zardoshti, 2017). τ_2/τ_1 fully corrected recoil $R=0.4$ jet shape in 0-10% Pb+Pb collisions at $40 \leq p_{t,jet}^{ch} < 60$ GeV/c. This shows that, at least for this kinematic selection, the subjettiness is not modified. The trigger tracks are 8-9 GeV/c for the background dominated region and 15-45 GeV/c for the signal dominated region.

3246 with both jets and bosons, widths of dihadron correlations, jet-hadron correlations, and measurements of the jet shape. On average, no change in the particle composition of jets in heavy ion collisions as compared to $p+p$ collisions is observed. There are some indications from

3251 dihadron correlations that quark and gluon jets do not 3207
 3252 interact with the medium in the same way. These observ- 3208
 3253 ables generally preferentially select quark jets over gluon 3209
 3254 jets, even in $p+p$ collisions. Some of the observables have 3210
 3255 a strong survivor bias due to the kinematic cuts that are 3211
 3256 applied in order to reduce the combinatorial background. 3212

3257 As our understanding of partonic energy loss has im- 3213
 3258 proved, the community has sought more differential ob- 3214
 3259 servables. This is motivated in part by an increased un- 3215
 3260 derstanding of the importance of fluctuations – while the 3216
 3261 average properties of jets are smooth, individual jets are 3217
 3262 lumpy, and by a desire construct well defined QCD ob- 3218
 3263 servables. These new observables give us access to dif- 3219
 3264 ferent properties of jets, such as allowing distinction be- 3220
 3265 tween quark and gluon jets, and therefore may be more 3221
 3266 sensitive to the properties of the medium. Since the ex- 3222
 3267 ploration of these observables is in its early stages, it 3223
 3268 is unclear whether we fully understand the impact of 3224
 3269 the background or kinematic cuts applied to the anal- 3225
 3270 yses. It is therefore unclear in practice how much addi- 3226
 3271 tional information these observables can provide about 3227
 3272 the medium, without applying the observables to Monte 3228
 3273 Carlo events with different jet quenching models. We en- 3229
 3274 courage cautious optimism and more detailed studies of 3230
 3275 these observables.

3276 For future studies to maximize our understanding
 3277 of the medium by the Jetscape collaboration using a 3331
 3278 Bayesian analysis, we propose first to produce compar-
 3279 isons between dihadron correlations, jet-hadron correla- 3332
 3280 tions, and γ -hadron correlations to insure that the mod- 3333
 3281 els have properly accounted for the path length depen- 3334
 3282 dence, initial state effects and the basics of fragmentation 3335
 3283 and hadronization. We do not list R_{AA} here as it is likely 3336
 3284 that this observable will be used to tune some aspects of 3337
 3285 the model, as it has been used in the past. For the most 3338
 3286 promising jet quenching models, we would propose that 3339
 3287 these studies would be followed by comparisons of ob- 3340
 3288 servables that depend more heavily on the details of the 3341
 3289 fragmentation, but are still based on the average distri- 3342
 3290 bution such as jet shapes, fragmentation functions, and 3343
 3291 particle composition. Finally, it would be useful to see 3344
 3292 the comparison of z_g to models. We urge that initial in- 3345
 3293 vestigations of the latter happen early so that the back- 3346
 3294 ground effect can be quantified. 3347

3295 We note that the same analysis techniques and selec- 3348
 3296 tion criteria must be used for analyses of the experiment 3349
 3297 and of the models in order for the comparisons to be 3350
 3298 valid. This is particularly true for studies using recon- 3351
 3299 structed jets where experimental criteria to remove the 3352
 3300 effects of the background can bias the sample of jets used 3353
 3301 in construction of the observables. We omit A_J from con- 3354
 3302 sideration because nearly any reasonable model gives a 3355
 3303 reasonable value, thus it is not particularly differential. 3356
 3304 We also omit heavy flavor jets because current data do 3357
 3305 not give much insight into modifications of fragmenta- 3358
 3306 tion, and it is not clear whether it will be possible exper- 3359

3307 imentally to measure jets with a low enough p_T that the
 3308 mass difference between heavy and light quarks is relevant.
 3309 Inclusion of new observables into these studies may
 3310 increase the precision with which medium properties can
 3311 be constrained, but it is critical to replicate the exact
 3312 analysis techniques.

3313 In order to compare experimental data, or to compare
 3314 experimental data with theory, not only is it necessary
 3315 for the analyses to be conducted the same way as it is
 3316 stated above, but they should be on the same footing.
 3317 Thus comparing unfolded results to uncorrected results
 3318 it not useful. In general, we urge extreme caution in
 3319 interpreting uncorrected results, especially for observables
 3320 created with reconstructed jets. Since it is unclear how
 3321 much the process of unfolding may bias the results, an im-
 3322 portant check would be to compare the raw results with
 3323 the folded theory. However, this requires complete docu-
 3324 mentation of the raw results and the response matrix on
 3325 the experimental side, and requires a complete treatment
 3326 of the initial state, background, and hadronization on the
 3327 theory side. This comparison, which we could think of
 3328 as something like a closure test, would still require that
 3329 the same jet finding algorithms with the same kinematic
 3330 elections are applied to the model.

D. Influence of the jet on the medium

3331 The preceding sections have demonstrated that hard
 3332 partons lose energy to the medium, most likely through
 3333 gluon bremsstrahlung and collisional energy loss. Often
 3334 an emitted gluon will remain correlated with the par-
 3335 ent parton so that the fragments of both partons are
 3336 spatially correlated over relatively short ranges ($R =$

$$\sqrt{\Delta\phi^2 + \Delta\eta^2} \lesssim 0.5$$
). Hadrons produced from the gluon
 3337 may fall inside or outside the jet cone of the parent par-
 3338 ton, depending on the jet resolution parameter. Whether
 3339 or not this energy is then reconstructed experimentally as
 3340 part of the jet depends on the resolution parameter and
 3341 the reconstruction algorithm. For sufficiently large reso-
 3342 lution parameters, the “lost” energy will still fall within
 3343 the jet cone, so that the total energy clustered into the
 3344 jet would remain the same. “Jet quenching” is then man-
 3345 ifest as a softening and broadening of the structure of the
 3346 jet. The evidence for these effects was discussed in the
 3347 previous section.

3348 If, however, a parton loses energy and that energy in-
 3349 teracts with or becomes equilibrated in the medium, it
 3350 may no longer have short range spatial correlations with
 3351 the parent parton. This energy would then be distributed
 3352 at distances far from the jet cone. Alternately, the en-
 3353 ergy may have very different spatial correlations with the
 3354 parent parton so that it no longer looks like a jet formed
 3355 in a vacuum, and a jet finding algorithm may no longer
 3356 group that energy with the jet that contains most of the
 3357 energy of its parent parton. Evidence for these effects is

3360 difficult to find, both because of the large and fluctuating background contribution from the underlying event, 3406 and because it is unclear how this energy would be different from the underlying event. We discuss both the 3407 existing evidence that there may be some energy which reaches equilibrium with the medium, and the ridge and 3411 the Mach cone, which are now understood to be features of the medium rather than indications of interactions of hard partons with the medium. We also discuss searches for direct evidence of Molière scattering off of partons in the medium. 3415

3416 1. Evidence for out-of-cone radiation

3417 The dijet asymmetry measurements demonstrate momentum imbalance for dijets in central heavy ion collisions, implying energy loss, but do not describe where that energy goes. To investigate this, CMS looked at the distribution of momentum parallel to the axis of a high momentum leading jet in three regions (Chatrchyan *et al.*, 3423 2011b), shown schematically in Figure 39. The jet reconstruction used in this analysis was an iterative cone algorithm with a modification to subtract the soft underlying event on an event-by-event basis, the details of which can be found in (Kodolova *et al.*, 2007). Each jet was selected with a radius $R = 0.5$ around a seed of minimum transverse energy of 1 GeV. Since energy can be deposited outside $R > 0.5$ even in the absence of medium effects and medium effects are expected to broaden the jet, the momenta of all particles within in a slightly larger region, $R < 0.8$, were summed, regardless of whether or not the particles were jet constituents or subtracted as background. This region is called in-cone and the region $R > 0.8$ is called out-of-cone. 3431

3440 CMS investigated these different regions of the events with a measurement of the projection of the p_T of reconstructed charged tracks onto the leading jet axis. For each event, this projection was calculated as

$$3445 p_T^{\parallel} = \sum_i -p_T^i \cos(\phi_i - \phi_{\text{Leading Jet}}), \quad (19) \quad 3446$$

3447 where the sum is over all tracks with $p_T > 0.5$ GeV/c. These results were then averaged over events to obtain $\langle p_T^{\parallel} \rangle$. This momentum imbalance in-cone and out-of-cone as a function of A_J , shown as black points in Figure 40. The momentum parallel to the jet axis in-cone is large, but should be balanced by the partner jet 180° away in the absence of medium effects. A large A_J indicates substantial energy loss for the away-side jet, while a small A_J indicates little interaction with the medium. This shows that the total momentum in the event is indeed balanced. For small A_J , the $\langle p_T^{\parallel} \rangle$ in the in-cone and out-of-cone regions is within zero as expected for balanced jets. For large A_J , the momentum in-cone is non-zero, balanced by the momentum out-of-cone. These events

were compared to PYTHIA+HYDJET simulations in order to understand which effects were simply due to the presence of a fluctuating background and which were due to jet quenching effects. In both the central Pb+Pb data and the Monte Carlo, an imbalance in jet A_J also indicated an imbalance in the p_T of particles within the cone of $R = 0.8$ about either the leading or subleading jet axes. To investigate further, CMS added up the momentum contained by particles in different momentum regions. The imbalance in the direction of the leading jet is dominated by particles with $p_T > 8$ GeV/c, but is partially balanced in the subleading direction by particles with momenta below 8 GeV/c. The distributions look very similar in both the data and the Monte Carlo for the in-cone particle distribution. The out-of-cone distributions indicated a slightly different story. For both the data and the Monte Carlo, the missing momentum was balanced by additional, lower momentum particles, in the subleading jet direction. The difference is that in the Pb+Pb data, the balance was achieved by very low momentum particles, between 0.5 and 1 GeV/c. In the Monte Carlo, the balance was achieved by higher momentum particles, mainly above 4 GeV/c, which indicates a different physics mechanism. In the Monte Carlo, the results could be due to semi-hard initial- or final-state radiation, such as three jet events. 3448

The missing transverse momentum analysis was recently extended by examining the multiplicity, angular, and p_T spectra of the particles using different techniques. As above, these results were characterized as a function of the Pb+Pb collision centrality and A_J (Khachatryan *et al.*, 2016c). This extended the results to quite some distance from the jet axes, up to a ΔR of 1.8. The angular pattern of the energy flow in Pb+Pb events was very similar to that seen in $p+p$ collisions, especially when the resolution parameter is small. This indicates that the leading jet could be getting narrower, and/or the subleading jet is getting broader due to quenching effects. For a given range in A_J , the in-cone imbalance in p_T in Pb+Pb collisions is found to be balanced by relatively low transverse momentum out-of-cone particles with $0.5 < p_T < 2$ GeV/c. This was quantitatively different than in $p+p$ collisions where most of the momentum balance comes from particles with p_T between $2 < p_T < 8$ GeV/c. This could indicate a softening of the radiation responsible for the p_T imbalance of dijets in the medium formed in Pb+Pb collisions. In addition, a larger multiplicity of associated particles is seen in Pb+Pb than in $p+p$ collisions. In every case, the difference between $p+p$ and Pb+Pb observations increased for more central Pb+Pb collisions. 3449

3450 However, some caution should be used in interpreting the result as these measurements make assumptions about the background, and require certain jet kinematics, which may limit how robust the conclusions are. It is unlikely that the medium would focus the leading jet

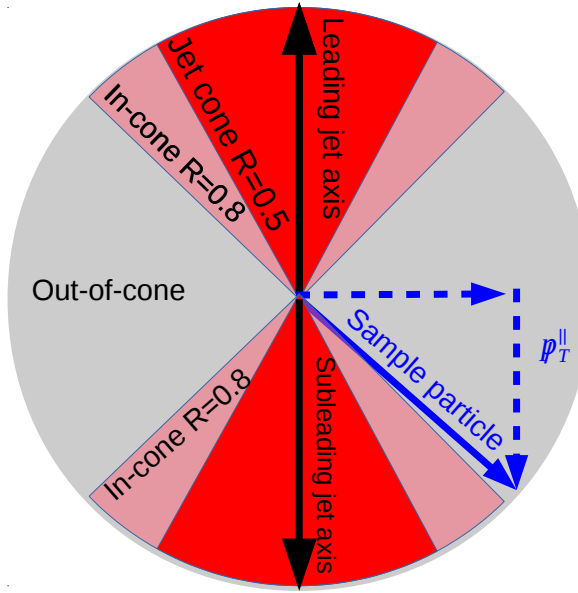


FIG. 39 Schematic diagram showing the definitions used in Figure 40.

so that it would be more collimated, for instance, but that a selection bias causes narrower jets to be selected in $\text{Pb}+\text{Pb}$ collisions for a given choice in R and jet kinematics. Additionally, as with any analysis that attempts to disentangle the effects of the medium on the jet with the jet on the medium, the ambiguity in what is considered part of the medium and what is considered part of the jet can also complicate the interpretation of this result. While the results demonstrate that there is a difference in the missing momentum in $\text{Pb}+\text{Pb}$ and $p+p$ collisions, in order to identify the mechanism responsible, the data would need to be compared to a Monte Carlo model that incorporates jet quenching, and preserves momentum and energy conservation between the jet and medium.

2. Searches for Molière scattering

The measurement of jets correlated with hard hadrons in (Adam *et al.*, 2015c) was also used to look for broadening of the correlation function between a high momentum hadron and jets. Such broadening could result from Molière scattering of hard partons off other partons in the medium, coherent effects from the scattering of a wave off of several scatterers. No such broadening is observed, although the measurement is dominated by the statistical uncertainties. Similarly, STAR observes no evidence for Molière scattering (Adamczyk *et al.*, 2017c). We note that this would mainly be sensitive to whether or not the jets are deflected rather than whether or not jets are broadened.

3. The rise and fall of the Mach cone and the ridge

Several theoretical models proposed that a hard parton traversing the medium would lose energy similar to the loss of energy by a supersonic object traveling through the atmosphere (Casalderrey-Solana *et al.*, 2005; Renk and Ruppert, 2006; Ruppert and Muller, 2005). The energy in this wave forms a conical structure about the object called a Mach cone. Early dihadron correlations studies observed a displaced peak in the away-side (Adare *et al.*, 2007b, 2008d; Adler *et al.*, 2006b; Aggarwal *et al.*, 2010). Three-particle correlation studies observed that this feature was consistent with expectations from a Mach cone (Abelev *et al.*, 2009a). Studies indicated that its spectrum was softer than that of the jet-like correlation on the near-side (Adare *et al.*, 2008d) and its composition similar to the bulk (Afanasiev *et al.*, 2008), as might be expected from a shock wave from a parton moving faster than the speed of light in the medium. Curiously, the Mach cone was present only at low momenta (Adare *et al.*, 2008a; Aggarwal *et al.*, 2010), whereas some theoretical predictions indicated that a true Mach cone would be more significant at higher momenta (Betz *et al.*, 2009).

At the same time, studies of the near-side indicated that there was a feature correlated with the trigger particle in azimuth but not in pseudorapidity (Abelev *et al.*, 2009b; Alver *et al.*, 2010), dubbed the ridge. The ridge was also observed to be softer than the jet-like correlation (Abelev *et al.*, 2009b) and to have a particle composition similar to the bulk (Bielcikova, 2008; Suarez, 2012). Several of the proposed mechanisms for the production of

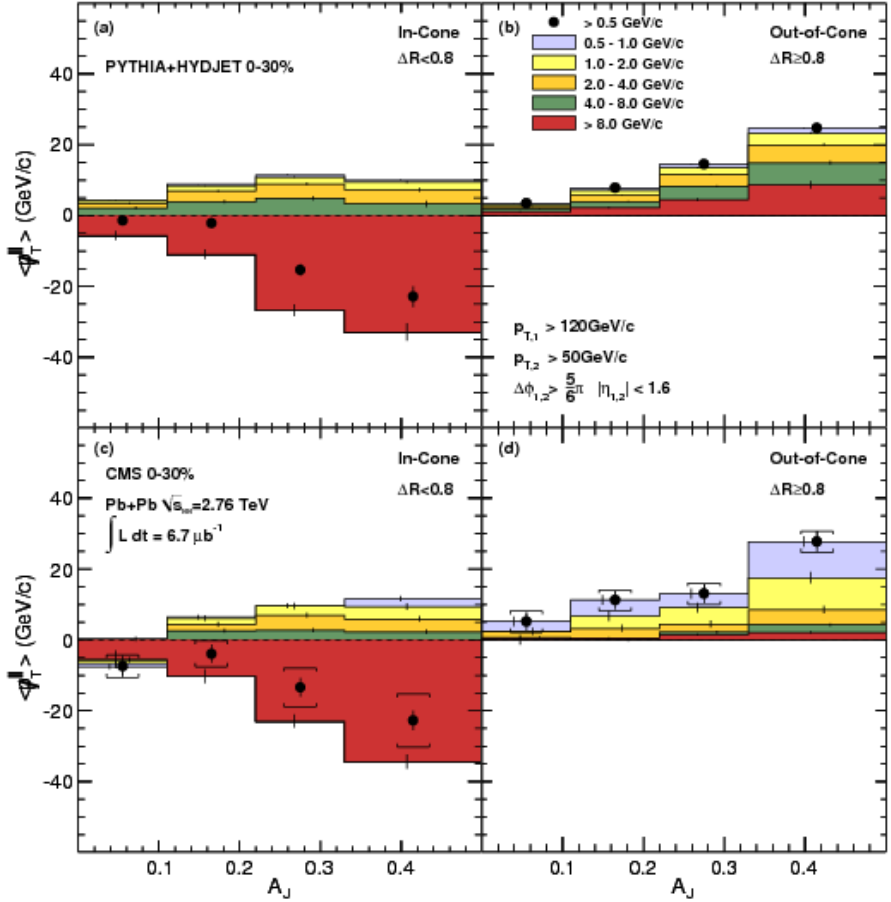


FIG. 40 Figure from CMS (Chatrchyan *et al.*, 2011b). Average missing transverse momentum for tracks with $p_T > 0.5$ GeV/c, projected onto the leading jet axis is shown in solid circles. The average missing p_T values are shown as a function of dijet asymmetry A_J for 0–30% centrality, inside a cone of $\Delta R < 0.8$ of one of the leading or subleading jet cones on the left, and outside ($\Delta R > 0.8$) the leading and subleading jet cones on the right. The solid circles, vertical bars and brackets represent the statistical and systematic uncertainties, respectively. For the individual p_T ranges, the statistical uncertainties are shown as vertical bars. This shows that missing momentum is found outside of the jet cone, indicating that the lost energy may have equilibrated with the medium.

the ridge involved interactions between the hard parton and the medium, including collisional energy loss (Wong, 2007, 2008) and recombination of the hard parton with a parton in the medium (Chiu and Hwa, 2009; Chiu *et al.*, 2008; Hwa and Yang, 2009). sists (Agakishiev *et al.*, 2014). A reanalysis of STAR dihadron correlations (Agakishiev *et al.*, 2010, 2014) using a new method for background subtraction (Sharma *et al.*, 2016) found that the Mach cone structure is not present (Nattrass *et al.*, 2016). This new analysis indicates that jets are broadened and softened (Nattrass *et al.*, 2016), as observed in studies of reconstructed jets (Aad *et al.*, 2014c; Chatrchyan *et al.*, 2014c).

However, the observation of odd v_n in heavy ion collisions (Aamodt *et al.*, 2011a; Adamczyk *et al.*, 2013; Adare *et al.*, 2011b) indicated that the Mach cone and the ridge may be an artifact of erroneous background subtraction. Since the ridge was defined as the component correlated with the trigger in azimuth but not in pseudorapidity, it is now understood to be entirely due to v_3 . Initial dihadron correlation studies after the observation of odd v_n are either inconclusive about the presence or absence of shape modifications on the away-side (Adare *et al.*, 2013b) or indicate that the shape modification per-

While the ridge is currently understood to be due to v_3 in heavy ion collisions, a similar structure has also been observed in high multiplicity $p+p$ collisions (Aaboud *et al.*, 2017; Khachatryan *et al.*, 2010). There are some hypotheses that this might indicate that a medium is formed in violent $p+p$ collisions (Khachatryan *et al.*, 2017b), although there are other hypotheses such as production due to gluon saturation (Ozonder, 2016) or string

3554 percolation (Andrs *et al.*, 2016). Whatever the produc- 3604
 3555 tion mechanism for the ridge in $p+p$ collisions, there is 3605
 3556 currently no evidence that it is related to or correlated 3606
 3557 with jet production in either $p+p$ or heavy ion collisions. 3607

3608 the medium, most observables can be incorporated into
 3609 a Bayesian analysis. We encourage exploration of com-
 3610 parisons of new observables to describe the jet structure.
 However, we caution that many observables are sensitive
 to kinematic selections and analysis techniques so that
 a replication of these techniques is required for the mea-
 3611 surements to be comparable to theory.

3558 **4. Summary of experimental evidence for modification of the
 3559 medium by jets**

3560 Measurements of the impact of jets on the medium are
 3561 difficult because of the large combinatorial background.
 3562 The background may distort reconstructed jets and re- 3611
 3563 quiring the presence of a jet may bias the event selection.
 3564 Because the energy contained within the background is 3612
 3565 large compared to the energy of the jet, even slight de- 3613
 3566 viations of the background from the assumptions of the 3614
 3567 structure of the background used to subtract its effect 3615
 3568 could skew results. A confirmation of the CMS result 3616
 3569 indicating that the lost energy is at least partially equi- 3617
 3570 librated with the medium will require more detailed the- 3618
 3571 oretical studies, preferably using Monte Carlo models so 3619
 3572 that the analysis techniques can be applied to data. The 3620
 3573 misidentification of the ridge and the Mach cone as aris- 3621
 3574 ing due to partonic interactions with the medium high- 3622
 3575 lights the perils of an incomplete understanding of the 3623
 3576 background. 3624

3577 **E. Summary of experimental results**

3578 Section III.A reviews studies of cold nuclear matter ef- 3629
 3579 fects, indicating that currently it does not appear that 3630
 3580 there are substantial cold nuclear matter effects modi- 3631
 3581 fying jets at mid-rapidity and that therefore effects ob- 3632
 3582 served thus far on jets in A+A collisions are primarily 3633
 3583 due to interactions of the hard parton with the medium. 3634
 3584 We note, however, that our understanding of cold nuclear 3635
 3585 matter effects is evolving rapidly and recommend that 3636
 3586 each observable is measured in both cold and hot nuclear 3637
 3587 matter in order to disentangle effects from hot and cold 3638
 3588 nuclear matter. Section III.B shows that there is am- 3639
 3589 ple evidence for partonic energy loss in the QGP. Nearly 3640
 3590 every measurement demonstrates that high momentum 3641
 3591 hadrons are suppressed relative to expectations from $p+p$ 3642
 3592 and $p+Pb$ collisions in the absence of quenching. Sec- 3643
 3593 tion III.C reviews the evidence that these partonic inter- 3644
 3594 actions with the medium result in more lower momentum 3645
 3595 particles and particles at larger angles relative to the par- 3646
 3596 ent parton, as expected from both gluon bremsstrahlung 3647
 3597 and collisional energy loss. Table III summarizes physics 3648
 3598 observations, selection biases and ability to constrain the 3649
 3599 initial kinematics for the measured observables. Sec- 3650
 3600 tion III.D discusses the evidence that at least some of 3651
 3601 this energy may be fully equilibrated with the medium 3652
 3602 and no longer distinguishable from the background. 3653

3603 For future studies to maximize our understanding of 3654

3611 **IV. DISCUSSION AND THE PATH FORWARD**

3612 In the last several years, we have seen a dramatic in-
 3613 crease in the number of experimentally accessible jet ob-
 3614 servables for heavy-ion collisions. During the early days
 3615 of RHIC, measurements were primarily limited to R_{AA}
 3616 and dihadron correlations, and reconstructed jets were
 3617 measured only relatively recently. Since the start of the
 3618 LHC, measurements of reconstructed jets have become
 3619 routine, fragmentation functions have been measured di-
 3620 rectly, and the field is investigating and developing more
 3621 sophisticated observables in order to quantify partonic
 3622 energy loss and its effects on the QGP. The constraint of
 3623 \hat{q} , the energy loss squared per fm of medium traversed,
 3624 using R_{AA} measurements by the JET collaboration is
 3625 remarkable. However, studies of jets in heavy ion col-
 3626 lisions largely remain phenomenological and observational.
 3627 This is probably the correct approach at this point in
 3628 the development of the field, but a quantitative under-
 3629 standing of partonic energy loss in the QGP requires a
 3630 concerted effort by both theorists and experimentalists
 3631 to both make measurements which can be compared to
 3632 models and use those measurements to constrain or ex-
 3633 clude those models.

3634 Below we lay out several of the steps we think are nec-
 3635 essary to reach this quantitative understanding of par-
 3636 tonic energy loss. We think that it is critical to quantita-
 3637 tively understand the impact of measurement techniques
 3638 on jet observables in order to make meaningful compari-
 3639 sons to theory. We encourage the developments in new
 3640 observables but urge caution – new observables may not
 3641 have as many benefits as they first appear to when their
 3642 biases and sensitivities to the medium are better under-
 3643 stood. Many experimental and theoretical developments
 3644 pave the way towards a better quantitative understand-
 3645 ing of partonic energy loss. However, we think that the
 3646 field will not fully benefit from these without discussions
 3647 targeted at a better understanding of and consistency
 3648 between theory and experiment and evaluating the full
 3649 suite of observables considering all their biases. One of
 3650 the dangers we face is that many observables are cre-
 3651 ated by experimentalists, which often yields observables
 3652 that are easy to measure such as A_J , but that are not
 3653 particularly differential with respect to constraining jet
 3654 quenching models.

3655 **A. Understand bias**

3656 As we discussed in Section II, all jet measurements in
 3657 heavy ion collisions are biased towards a particular subset
 3658 of the population of jets produced in these collisions. The
 3659 existence of such biases is transparent for many measure-
 3660 ments, such as surface bias in measurements of dihadron
 3661 correlations at RHIC. However, for other observables,
 3662 such as those relating to reconstructed jets, these biases
 3663 are not always adequately discussed in the interpreta-
 3664 tion of the results. As the comparison between ALICE,
 3665 ATLAS, and CMS jet R_{AA} at low jet momenta shows,
 3666 requiring a hard jet core in order to suppress background
 3667 and reduce combinatorial jets leads to a strong bias which
 3668 cannot be ignored. The main biases that pertain to jets
 3669 in heavy ion collisions are: fragmentation, collision ge-
 3670 ometry, kinematic and parton species bias. The frag-
 3671 mentation bias can be simply illustrated by the jet R_{AA}
 3672 measurement. Requiring a particular value of the resolu-
 3673 tion parameter, a particular constituent cut, or even the
 3674 particular trigger detector used by the experiment selects
 3675 a particular shower structure for the jet. The geometry
 3676 bias is commonly discussed as a surface bias, since the
 3677 effect of the medium increases with the path length caus-
 3678 ing more hard partons come from the surface of the QGP.
 3679 The kinematic bias is somewhat related to the fragmen-
 3680 tation bias as the fragmentation depends on the kine-
 3681 matics of the parton, but the energy loss in the medium
 3682 means that jets of given kinematics do not come from the
 3683 same selection of initial parton kinematics in vacuum and
 3684 in heavy ion collisions. The parton species bias results
 3685 as the gluons couple more strongly with the medium,
 3686 and thus are expected to be more modified. This can be
 3687 summarized by stating that nearly every technique fa-
 3688 vors measurement of more quark jets over gluon jets, is
 3689 biased towards high z fragments, and is biased towards
 3690 jets which have lost less energy in the medium.

3691 While some measurements may claim to be bias free
 3692 because they deal with the background effects in a man-
 3693 ner which makes comparisons with theoretical models
 3694 more straightforward, they still contain biases, usually
 3695 towards jets which interacted less with the medium and
 3696 therefore have lost less energy. For example, for the
 3697 hadron-jet coincidence measurements, it is correct to
 3698 state that the away side jet does not have a fragmen-
 3699 tation bias since the hadron trigger is not part of its
 3700 shower. However, this does not mean that this measure-
 3701 ment is completely unbiased since the trigger hadron may
 3702 select jets that have traveled through less medium or in-
 3703 teracted less with the medium. In addition, the very act
 3704 of using a jet finding algorithm introduces a bias (parti-
 3705 cularly toward quark jets) that is challenging to calculate.

3706 Given the large combinatorial background, such biases
 3707 are most likely unavoidable.

3708 We propose that these biases should be treated as tools
 3709 through jet geometry engineering rather than a handicap.

3710 These experimental biases should also be made transpar-
 3711 ent to the theory community. Frequently the techniques
 3712 which impose these biases are buried in the experimental
 3713 method section, with no or little mention of the impact
 3714 of these biases on the results in the discussion. Theore-
 3715 trists should not neglect the discussion of the experimental
 3716 techniques, and experimentalists should make a greater
 3717 effort to highlight potential impacts of the techniques to
 3718 suppress and subtract the background on the measure-
 3719 ment.

3720 **B. Make quantitative comparisons to theory**

With the explosion of experimentally accessible observables, much of the focus has been on making as many measurements as possible with less consideration of whether such observables are calculable, or capable of distinguishing between different energy loss models. Even without direct comparisons to theory, these studies have been fruitful because they contribute to a phenomenological understanding of the impact of the medium on jets and vice versa. While we still feel that such exploratory studies are valuable, the long term goal of the field is to measure the properties of the QGP quantitatively, making theoretical comparisons essential. Some of the dearth of comparisons between measurements and models is due to the relative simplicity of the models and their inability to include hadronization.

The field requires another systematic attempt to constrain the properties of the medium from jet measurements. The Jetscape collaboration has formed in order to incorporate theoretical calculations of partonic energy loss into Monte Carlo simulations, which can then be used to directly calculate observables using the same techniques used for the measurements. This will then be followed up by a Bayesian analysis similar to previous work (Bernhard *et al.*, 2016; Novak *et al.*, 2014) but incorporating measurements of jets. This is essential, both to improve our theoretical understanding and to provide Monte Carlo models which can be used for more reliable experimental corrections. In our opinion, it should be possible to incorporate most observables into these measurements. However, we urge careful consideration of all experimental techniques and kinematic selections in order to ensure an accurate comparison between data and theory. The experimental collaborations should cooperate with the Jetscape collaboration to ensure that response matrices detailing the performance of the detectors for different observables are available.

C. More differential measurements

The choices of what to measure, how to measure it and how to both define and treat the background are

3760 key to our quantitative understanding of the medium. 3816
 3761 There have been substantial improvements in the ability 3817
 3762 to measure jets in heavy ion collisions in recent years, 3818
 3763 such as the available kinematic reach due to accelera- 3819
 3764 tor and detector technology improvements. Addition- 3820
 3765 ally, our quantitative understanding of the effect of the 3821
 3766 background in many observables has also significantly 3822
 3767 improved. Given the continuous improvement in tech- 3823
 3768 nology and analysis techniques, it is vital that the some 3824
 3769 of the better understood observables such as R_{AA} and 3825
 3770 I_{AA} are repeated with higher precision. Theoretical mod- 3826
 3771 els should be able to simultaneously predict these pre- 3827
 3772 cisely measured jet observables with different spectral 3828
 3773 shapes and path length dependencies. While this is nec- 3829
 3774 essary it is not sufficient to validate a theoretical model. 3830
 3775 Given that these will also depend on the collision en- 3831
 3776 ergy, comparisons between RHIC and the LHC would be 3832
 3777 valuable, but again only when all biases are carefully con- 3833
 3778 sidered. Now that the era of high statistics and precision 3834
 3779 detectors is here, the field is currently exploring several 3835
 3780 new observables to attempt to identify the best observ- 3836
 3781 ables to constrain the properties of the medium. Older 3837
 3782 observables, such as R_{AA} , were built with the mindset 3838
 3783 that the final state jet reflects the kinematics of its par- 3839
 3784 ent parton, and the change in these kinematics due to 3840
 3785 interactions with the medium would be reflected in the 3841
 3786 change in the jet distributions. One of the lessons learned 3842
 3787 is that the majority of the modification of the fragmen- 3843
 3788 tation occurs at a relatively low p_T compared to the mo- 3844
 3789 mentum of the jet. However, jet finding algorithms were 3845
 3790 specifically designed in order to not be sensitive to the de- 3846
 3791 tails of the soft physics, which means that the very thing 3847
 3792 we are trying to measure and quantify is obscured by jet 3848
 3793 finder. The new observables are based on the structure of 3849
 3794 the jet, rather than on its kinematics alone. Specifically, 3850
 3795 they recognize that a hard parton could split into two 3851
 3796 hard daughters. If this splitting occurs in the medium, 3852
 3797 not only can the splitting itself be modified by the pres- 3853
 3798 ence of the medium, but each of the daughters could 3854
 3799 lose energy to the medium independently. This would be 3855
 3800 actually be rather difficult to see in an ensemble struc- 3856
 3801 ture measurement such as the jet fragmentation function, 3857
 3802 which yields a very symmetric picture of a jet about its 3858
 3803 axis, and so requires the specific structures within the jet 3859
 3804 to be quantified. While these new observables hold a lot 3860
 3805 of promise in terms of our understanding, caution must 3861
 3806 also be used in interpreting them until precisely how the 3862
 3807 background removal process or the detector effects will 3863
 3808 play a role in these measurements is carefully studied. 3864

3809 The investigations into these different observables are 3865
 3810 very important, since we have likely not identified the ob- 3866
 3811 servables most sensitive to the properties of the medium. 3867
 3812 We cannot forget that we want to quantify the tempera- 3868
 3813 ture dependence of the jet transport coefficients, as well 3869
 3814 as determine the size of the medium objects the jets are 3870
 3815 scattering off of. While these are global and fundamen- 3871

tal descriptors of a medium, the fact that the process by which we make these measures is statistical means that the development of quantitative Monte Carlo simulations is key. Not only will they allow calculations of jet quenching models to be compared with the same initial states, hadronization schemes, etc, but they also could make the calculations of even more complicated observables feasible.

However, the sensitivity of simple observables should not be underestimated as with every set of new observables there are new mistakes to be made, and we can be reasonably sure that we understand the biases inherent in these simple observables. While it is not likely that comparison between R_{AA} and theories will constrain the properties of the medium substantially better than the JET collaboration's calculation of \hat{q} , calculations of γ -hadron, dihadron, and jet hadron correlations are feasible with the development of realistic Monte Carlo models. The relative simplicity of these observables makes them promising for subsequent attempts to constrain \hat{q} and other transport coefficients, especially since we now have a fairly precise quantitative experimental understanding of the background. This may be a good initial focus for systematic comparisons between theory and experiment. Interpreting a complicated result with a simple model that misses a lot of physics is a misuse of that model, and can lead to incorrect assumptions.

We caution against overconfidence, and encourage scrutiny and skepticism of measurement techniques and all observables. For each observable, an attempt needs to be made to quantify its biases, and determine which dominate. Observables should be measured in the same kinematic region and, if possible, with the same resolution parameters in order to ensure consistency between experiments. If initial studies of a particular observable reveal that it is either not particularly sensitive to the properties of the medium, or that it is too sensitive to experimental technique, we should stop measuring that observable. We urge caution when using complicated background subtraction and suppression techniques, which may be difficult to reproduce in models and requires Monte Carlo simulations that accurately model both the hard process that has produced the jet and the soft background. Given that the response of the detector to the background is different from experiment to experiment, complicated subtraction processes may make direct comparisons across experiments and energies difficult.

We also caution against the overuse and blind use of unfolding. Unfolding is a powerful technique which is undoubtedly necessary for many measurements. It also has the potential to impose biases by shifting measurements towards the Monte Carlo used to calculate the response matrix, and obfuscating the impact of detector effects and analysis techniques. When unfolding is necessary, it should be done carefully in order to make sure all effects are understood and that the result is robust. Since most

3872 effects are included in the response matrix rather than 3925 corrected for separately, it can be difficult to understand 3926 the impact of different effects, such as track reconstruc- 3927 tion efficiency and energy resolution. Unfolding is not 3928 necessarily superior to careful studies of detector effects 3929 and corrections, and attempts to minimize their impact 3930 on the observables chosen. Given the relative simplicity 3931 of folding a result, for all observables we should perform 3932 a theory-experiment closure test where the theoretical re- 3933 sults are folded and compared to the raw data. Since the 3934 robustness of a particular measurement depends on the 3935 unfolding corrections, the details of the unfolding method 3936 should be also transparent to both experimental and the- 3937 oretical communities. 3938

3886 Of course making more differential measurements is 3939 aided by better detectors. The LHC detectors use ad- 3940 vanced detector technology, and are designed for jet mea- 3941 surements. However, the current RHIC detectors were 3942 not optimized for jet measurements, which has limited 3943 the types of jet observables at these lower energies. Pre- 3944 cise measurements of jets over a wide range of energies 3945 is necessary to truly understand partonic energy loss. 3946 The proposed sPHENIX detector will greatly aid these 3894 measurements by utilizing some of the advanced detec- 3895 tor technology that has been developed since the design 3947 of the original RHIC experiments (Adare *et al.*, 2015). 3898 The high rate and hermetic detector will improve the re- 3948 sults by reducing detector uncertainties and increasing 3949 the kinematic reach so that a true comparison between 3950 RHIC and LHC can be made. In particular, upgrades 3951 at both RHIC and LHC will make precise measurements 3952 of heavy-flavor tagged jets and boson-tagged jets, which 3953 constrain the initial kinematics of the hard scattering, 3954 possible. 3955

3906 **D. An agreement on the treatment of background in heavy 3907 ion collisions**

3908 The issues we listed above are complicated and require 3961 substantive, ongoing discussions between theorists and 3909 experimentalists. A start in this direction can be found 3962 in the Lisbon Accord where the community agreed to use 3963 Rivet (Buckley *et al.*, 2013), a C++ library which 3964 provides a framework and tools for calculating observables 3965 at particle level developed for particle physics. Rivet al- 3966 lowed event generator models and experimental observ- 3967 ables to be validated. Agreeing on a framework that 3968 all physicists can use is an important first step, however 3969 it is not sufficient. It would not prevent a comparison 3970 of two observables with different jet selection criteria, 3971 or a comparison of a theoretical model with a different 3972 treatment or definition of the background than a simi- 3973 lar experimental observable. The problems we face are 3974 similar to those faced by the particle physics community 3975 as they learned how to study and utilize jets, to make 3976

them one of the best tools we have for understanding the Standard Model. An agreement on the treatment of the background in heavy ion collisions experimentally and theoretically is required as it is part of the definition of the observable. Theorists and experimentalists need to understand each other's techniques and find common ground, to define observables that experimentalists can measure and theorists can calculate. We need to recognize that observables based on pQCD calculations are needed if we are to work towards a text-book formulation of jet quenching, and what we learn about QCD from studying the strongly coupled QGP. However, observables that are impossible to measure are not useful, nor is it useful to measure observables that are impossible to calculate or are insensitive to the properties of the medium. We propose a targeted workshop to address these issues in heavy ion collisions with the goal of an agreement similar to the Snowmass Accord. Ideally we would agree on a series of jet algorithms, including selection criteria, that all experiments can measure, and a background strategy that can be employed both in experiment and theory.

V. ACKNOWLEDGEMENTS

We thank Will Witt for productive discussions about unfolding. We thank Redmer Bertens, Jana Bielčíkova, Leticia Cunqueiro Mendez, Kate Jones, Kolja Kauder, Abhijit Majumder, Jaki Noronha-Hostler, Thomas Pennington, Dennis Perepelitsa, Jörn Putschke, Soren Sorensen, Peter Steinberg, and Giorgio Torrieri for useful advice on the manuscript and useful discussions. We thank Raghav Elayavalli Kunnavalkam, Boris Hippolyte, Kurt Jung, Igor Lokhtin, Thomas Ullrich, and the experimental collaborations for permission to reproduce their figures for this work. This material is based upon work supported by the Division of Nuclear Physics of the U.S. Department of Energy under Grant No. DE-FG02-96ER40982 and by the National Science Foundation under Grant Nos. 1352081 and 1614474.

REFERENCES

- (2009), “Particle-Flow Event Reconstruction in CMS and Performance for Jets, Taus, and MET,” .
- (2013), .
- (2015a), *Jet energy scale and its uncertainty for jets reconstructed using the ATLAS heavy ion jet algorithm*, Tech. Rep. ATLAS-CONF-2015-016 (CERN, Geneva).
- (2015b), “Measurement of dijet p_T correlations in $\text{Pb}+\text{Pb}$ and pp collisions at $\sqrt{s_{NN}} = 2.76$ TeV with the ATLAS detector,” ATLAS-CONF-2015-052.
- (2016), “Measurement of charged particle spectra in pp collisions and nuclear modification factor R_{pPb} at $\sqrt{s_{NN}} = 5.02$ TeV with the ATLAS detector at the LHC,” ATLAS-CONF-2016-108.

3977 (2016a), "Measurement of the charged particle nuclear modi- 4041 Acharya, S., *et al.* (ALICE) (2017), arXiv:1702.00804 [nucl-
3978 fication factor in PbPb collisions at $\sqrt{s_{NN}} = 5.02$ TeV," 4042 ex].
3979 CMS-PAS-HIN-15-015.
3980 (2016b), "Study of B^+ meson production in pp and PbPb 4044 Ackermann, K. H., *et al.* (STAR) (2003), Nucl. Instrum.
3981 collisions at $\sqrt{s_{NN}} = 5.02$ TeV using exclusive hadronic 4045 Meth. **A499**, 624.
3982 decays," CMS-PAS-HIN-16-011.
3983 Aaboud, M., *et al.* (ATLAS) (2017), Phys. Rev. **C96** (2), 4046 Ackerstaff, K., *et al.* (OPAL) (1999), Eur. Phys. J. **C8**, 241.
3984 024908, arXiv:1609.06213 [nucl-ex].
3985 Aad, G., *et al.* (ATLAS) (2008), JINST **3**, S08003.
3986 Aad, G., *et al.* (ATLAS) (2010), Phys. Rev. Lett. **105**, 252303.
3987 Aad, G., *et al.* (ATLAS) (2012), Phys. Lett. **B710**, 363.
3988 Aad, G., *et al.* (ATLAS) (2013a), Phys. Rev. Lett. **111** (15), 4052 Adam, J., *et al.* (ALICE) (2015a), JHEP **11**, 205.
3989 152301.
3990 Aad, G., *et al.* (ATLAS) (2013b), Phys. Lett. **B719**, 220.
3991 Aad, G., *et al.* (ATLAS) (2014a), Phys. Rev. **C90** (2), 024905.
3992 Aad, G., *et al.* (ATLAS) (2014b), Eur. Phys. J. **C74** (11), 4056 Adam, J., *et al.* (ALICE) (2015b), Phys. Lett. **B746**, 385.
3993 3157.
3994 Aad, G., *et al.* (ATLAS) (2014c), Phys. Lett. **B739**, 320.
3995 Aad, G., *et al.* (ATLAS) (2014d), Phys. Rev. **C90** (4), 044906.
3996 Aad, G., *et al.* (ATLAS) (2015a), Phys. Lett. **B748**, 392.
3997 Aad, G., *et al.* (ATLAS) (2015b), Phys. Rev. Lett. **114** (7), 4061 Adam, J., *et al.* (ALICE) (2016b), Phys. Lett. **B753**, 511.
3998 072302.
3999 Aad, G., *et al.* (ATLAS) (2016a), Phys. Lett. **B756**, 10.
4000 Aad, G., *et al.* (ATLAS) (2016b), Phys. Rev. Lett. **116** (17), 4064 Adam, J., *et al.* (ALICE) (2016c), Eur. Phys. J. **C76** (5), 271.
4001 172301.
4002 Aad, G., *et al.* (ATLAS) (2016c), .
4003 Aamodt, K., *et al.* (ALICE) (2008), JINST **3**, S08002.
4004 Aamodt, K., *et al.* (ALICE) (2010), Phys. Rev. Lett. **105**, 4068 Adamczyk, L., *et al.* (STAR) (2013), Phys. Rev. **C88** (1),
4005 252301.
4006 Aamodt, K., *et al.* (ALICE) (2011a), Phys. Rev. Lett. **107**, 4070 Adamczyk, L., *et al.* (STAR) (2014a), Phys. Rev. Lett. **112** (12), 122301.
4007 032301.
4008 Aamodt, K., *et al.* (ALICE) (2011b), Phys. Lett. **B696**, 30.
4009 Aamodt, K., *et al.* (ALICE) (2012), Phys. Rev. Lett. **108**, 4073 Adamczyk, L., *et al.* (STAR) (2014b), Phys. Rev. Lett. **113** (14), 142301.
4010 092301.
4011 Abe, F., *et al.* (CDF) (1992), Phys. Rev. **D45**, 1448.
4012 Abelev, B., *et al.* (STAR) (2009a), Phys. Rev. Lett. **102**, 4076 Adamczyk, L., *et al.* (STAR) (2017a), arXiv:1707.01988
4013 052302.
4014 Abelev, B., *et al.* (STAR) (2009b), Phys. Rev. **C80**, 064912.
4015 Abelev, B., *et al.* (STAR) (2010a), Phys. Lett. **B683**, 123.
4016 Abelev, B., *et al.* (ALICE) (2012a), JHEP **1203**, 053.
4017 Abelev, B., *et al.* (ALICE) (2012b), JHEP **09**, 112.
4018 Abelev, B., *et al.* (ALICE) (2013a), Phys. Lett. **B719**, 18.
4019 Abelev, B., *et al.* (ALICE) (2013b), Phys. Rev. **C88**, 044910.
4020 Abelev, B., *et al.* (ALICE) (2013c), Phys. Rev. **C88** (4), 4083 Adamczyk, L., *et al.* (STAR) (2015), Phys. Lett. **B751**, 233.
4021 044909, arXiv:1301.4361 [nucl-ex].
4022 Abelev, B., *et al.* (ALICE) (2013d), Phys. Lett. **B722**, 262.
4023 Abelev, B., *et al.* (ALICE) (2013e), Phys. Rev. Lett. **110** (8), 4087 Adamczyk, L., *et al.* (STAR) (2016), Phys. Lett. **B760**, 689.
4024 082302.
4025 Abelev, B., *et al.* (ALICE Collaboration) (2014a), JHEP **1403**, 013.
4026 Adamczyk, L., *et al.* (STAR) (2007a), arXiv:1707.01988
4027 Abelev, B., *et al.* (ALICE) (2016), Phys. Rev. **C94** (1), 014910.
4028 Abelev, B. B., *et al.* (ALICE) (2013f), Phys. Rev. Lett. **111**, 4092 Adamczyk, L., *et al.* (STAR) (2003b), Phys. Rev. Lett. **91**,
4029 222301.
4030 Abelev, B. B., *et al.* (ALICE) (2013g), Phys. Lett. **B727**, 371.
4031 Abelev, B. B., *et al.* (ALICE) (2014b), Phys. Lett. **B728**, 216,
4032 [Erratum: Phys. Lett. B734, 409 (2014)].
4033 Abelev, B. I., *et al.* (STAR) (2006), Phys. Rev. Lett. **97**, 4097 Adare, A., *et al.* (PHENIX) (2007a), Phys. Rev. Lett. **98**,
4034 152301.
4035 Abelev, B. I., *et al.* (STAR) (2008), Phys. Rev. **C77**, 044908.
4036 Abelev, B. I., *et al.* (STAR) (2009c), Phys. Rev. Lett. **103**, 4100 Adare, A., *et al.* (STAR) (2004a), Phys. Rev. Lett. **93**, 252301.
4037 251601.
4038 Abelev, B. I., *et al.* (STAR) (2010b), Phys. Rev. **C81**, 064904.
4039 Abelev, B. I., *et al.* (STAR) (2010c), Phys. Rev. **C82**, 034909.
4040 Abreu, P., *et al.* (DELPHI) (1996), Z. Phys. **C70**, 179.
4041 Acharya, S., *et al.* (ALICE) (2017), arXiv:1702.00804 [nucl-
4042 ex].
4043 Ackermann, K. H., *et al.* (STAR) (2003), Nucl. Instrum. Meth. **A499**, 624.
4044 Ackerstaff, K., *et al.* (OPAL) (1999), Eur. Phys. J. **C8**, 241.
4045 Acton, P. D., *et al.* (OPAL) (1993), Z. Phys. **C58**, 387.
4046 Adam, J., *et al.* (ALICE) (2015a), JHEP **11**, 205.
4047 Adam, J., *et al.* (ALICE) (2015b), Phys. Lett. **B746**, 385.
4048 Adam, J., *et al.* (ALICE) (2015c), JHEP **09**, 170.
4049 Adam, J., *et al.* (ALICE) (2015d), Phys. Lett. **B746**, 1.
4050 Adam, J., *et al.* (ALICE) (2016a), Phys. Rev. Lett. **116** (13),
4051 132302.
4052 Adam, J., *et al.* (ALICE) (2016b), Phys. Lett. **B753**, 511.
4053 Adam, J., *et al.* (ALICE) (2016c), Eur. Phys. J. **C76** (5), 271.
4054 Adam, J., *et al.* (ALICE) (2016d), Phys. Rev. Lett. **116** (22),
4055 222302.
4056 Adam, J., *et al.* (ALICE) (2016e), Phys. Rev. **C93** (3),
4057 034913.
4058 Adam, J., *et al.* (ALICE) (2016f), Phys. Rev. **C93** (4),
4059 044903.
4060 Adam, J., *et al.* (ALICE) (2016g), Phys. Lett. **B754**, 235.
4061 Adam, J., *et al.* (ALICE) (2016h), Phys. Lett. **B753**, 126.
4062 Adam, J., *et al.* (ALICE) (2016i), Phys. Rev. **C94** (3),
4063 034903.
4064 Adam, J., *et al.* (ALICE) (2016j), Phys. Rev. **C93** (2),
4065 024917.
4066 Adam, J., *et al.* (ALICE) (2016k), JHEP **03**, 081.
4067 Adamczyk, L., *et al.* (STAR) (2013), Phys. Rev. **C88** (1),
4068 014904.
4069 Adamczyk, L., *et al.* (STAR) (2014a), Phys. Rev. Lett. **112** (12), 122301.
4070 Adamczyk, L., *et al.* (STAR) (2014b), Phys. Rev. Lett. **113** (14), 142301.
4071 Adamczyk, L., *et al.* (STAR) (2015), Phys. Lett. **B751**, 233.
4072 Adamczyk, L., *et al.* (STAR) (2016), Phys. Lett. **B760**, 689.
4073 Adamczyk, L., *et al.* (STAR) (2017a), arXiv:1707.01988
4074 [nucl-ex].
4075 Adamczyk, L., *et al.* (STAR) (2017b), Phys. Rev. Lett. **119** (6), 062301, 1609.03878.
4076 Adamczyk, L., *et al.* (STAR) (2017c), arXiv:1702.01108
4077 [nucl-ex].
4078 Adamczyk, L., *et al.* (STAR) (2003), Nucl. Instrum. Meth. **A499**, 437.
4079 Adams, J., *et al.* (STAR) (2003a), Phys. Rev. Lett. **91**,
4080 072304.
4081 Adams, J., *et al.* (STAR) (2003b), Phys. Rev. Lett. **91**, 172302.
4082 Adams, J., *et al.* (STAR) (2004a), Phys. Rev. Lett. **93**, 252301.
4083 Adams, J., *et al.* (STAR) (2004b), Phys. Rev. **C70**, 054907.
4084 Adams, J., *et al.* (STAR) (2005a), Phys. Rev. Lett. **95**, 152301.
4085 Adams, J., *et al.* (STAR) (2005b), Nucl. Phys. **A757**, 102.
4086 Adams, J., *et al.* (STAR) (2006), Phys. Rev. Lett. **97**, 162301.
4087 Adare, A., *et al.* (PHENIX) (2007a), Phys. Rev. Lett. **98**,
4088 232301.
4089 Adare, A., *et al.* (PHENIX) (2007b), Phys. Rev. Lett. **98**,
4090 232302.
4091 Adare, A., *et al.* (PHENIX) (2008a), Phys. Rev. **C78**, 014901.
4092 Adare, A., *et al.* (PHENIX) (2008b), Phys. Rev. **C77**, 064907.
4093 Adare, A., *et al.* (PHENIX) (2008c), Phys. Rev. Lett. **101**,
4094 232301.
4095 Adare, A., *et al.* (PHENIX) (2010a), Phys. Rev. Lett. **104**,
4096 132301.
4097 Adare, A., *et al.* (PHENIX) (2010b), Phys. Rev. **D82**, 072001.

4105 Adare, A., *et al.* (PHENIX) (2010c), Phys. Rev. **C82**, 011902. 4169
 4106 Adare, A., *et al.* (PHENIX Collaboration) (2011a), Phys. Rev. 4170
C84, 044905. 4171
 4108 Adare, A., *et al.* (PHENIX) (2011b), Phys. Rev. Lett. **107**, 4172
 4109 252301. 4173
 4110 Adare, A., *et al.* (PHENIX) (2011c), Phys. Rev. **C84**, 044902. 4174
 4111 Adare, A., *et al.* (PHENIX) (2011d), Phys. Rev. Lett. **107**, 4175
 4112 172301. 4176
 4113 Adare, A., *et al.* (PHENIX) (2012a), Phys. Rev. Lett. **109**, 4177
 4114 109 (24), 242301. 4178
 4115 Adare, A., *et al.* (PHENIX) (2012b), Phys. Rev. Lett. **109**, 4179
 4116 152301. 4180
 4117 Adare, A., *et al.* (PHENIX) (2012c), Phys. Rev. Lett. **109**, 4181
 4118 122302. 4182
 4119 Adare, A., *et al.* (PHENIX) (2013a), Phys. Rev. **C88** (6), 4183
 4120 064910. 4184
 4121 Adare, A., *et al.* (PHENIX) (2013b), Phys. Rev. Lett. **111** (3), 4185
 4122 032301. 4186
 4123 Adare, A., *et al.* (PHENIX) (2013c), Phys. Rev. **C87** (3), 4187
 4124 034911. 4188
 4125 Adare, A., *et al.* (PHENIX) (2013d), Phys. Rev. Lett. **111** (20), 4189
 4126 202301. 4190
 4127 Adare, A., *et al.* (PHENIX) (2013e), Phys. Rev. **C88** (2), 4191
 4128 024906. 4192
 4129 Adare, A., *et al.* (PHENIX) (2014a), Phys. Rev. **C90** (3), 4193
 4130 034902. 4194
 4131 Adare, A., *et al.* (PHENIX) (2014b), Phys. Rev. **C89** (3), 4195
 4132 034915. 4196
 4133 Adare, A., *et al.* (2015), arXiv:1501.06197 [nucl-ex]. 4197
 4134 Adare, A., *et al.* (PHENIX) (2016a), Phys. Rev. **C94** (6), 4198
 4135 064901. 4199
 4136 Adare, A., *et al.* (PHENIX) (2016b), Phys. Rev. Lett. **116** (12), 4200
 4137 122301. 4201
 4138 Adare, A., *et al.* (PHENIX) (2016c), Phys. Rev. **C93** (2), 4202
 4139 024904. 4203
 4140 Adare, A., *et al.* (PHENIX) (2016d), Phys. Rev. **C93** (2), 4204
 4141 024911. 4205
 4142 Adare, A., *et al.* (PHENIX) (2016e), Phys. Rev. **C93** (2), 4206
 4143 024901. 4207
 4144 Adcox, K., *et al.* (PHENIX) (2003), Nucl. Instrum. Meth. **A499**, 4208
 4145 469. 4209
 4146 Adcox, K., *et al.* (PHENIX) (2004), Phys. Rev. **C69**, 024904. 4210
 4147 Adcox, K., *et al.* (PHENIX) (2005), Nucl. Phys. **A757**, 184. 4211
 4148 Adler, C., *et al.* (STAR) (2001), Phys. Rev. Lett. **87**, 182301. 4212
 4149 Adler, C., *et al.* (STAR) (2003a), Phys. Rev. Lett. **90**, 082302. 4213
 4150 Adler, S., *et al.* (PHENIX) (2003b), Phys. Rev. Lett. **91**, 4214
 4151 072301. 4215
 4152 Adler, S., *et al.* (PHENIX) (2006a), Phys. Rev. Lett. **96**, 4216
 4153 222301. 4217
 4154 Adler, S., *et al.* (PHENIX) (2006b), Phys. Rev. Lett. **97**, 4218
 4155 052301. 4219
 4156 Adler, S., *et al.* (PHENIX) (2006c), Phys. Rev. **D74**, 072002. 4220
 4157 Adler, S., *et al.* (PHENIX) (2006d), Phys. Rev. **C73**, 054903. 4221
 4158 Adler, S., *et al.* (PHENIX) (2007a), Phys. Rev. **C76**, 034904. 4222
 4159 Adler, S. S., *et al.* (PHENIX) (2003c), Phys. Rev. Lett. **91**, 4223
 4160 182301. 4224
 4161 Adler, S. S., *et al.* (PHENIX) (2004), Phys. Rev. **C69**, 034909. 4225
 4162 Adler, S. S., *et al.* (PHENIX) (2005), Phys. Rev. **C71**, 034908. 4226
 4163 [Erratum: Phys. Rev. C71, 049901 (2005)]. 4227
 4164 Adler, S. S., *et al.* (PHENIX) (2007b), Phys. Rev. Lett. **98**, 4228
 4165 172302. 4229
 4166 Adye, T. (2011), in *Proceedings, PHYSTAT 2011 Workshop* 4230
 4167 *on Statistical Issues Related to Discovery Claims in Search* 4231
 4168 *Experiments and Unfolding*, CERN, Geneva, Switzerland 4232
 17-20 January 2011, CERN (CERN, Geneva) pp. 313–318.
 4169 Afanasiev, S., *et al.* (PHENIX) (2008), Phys. Rev. Lett. **101**, 4170
 082301.
 4171 Afanasiev, S., *et al.* (PHENIX) (2012), Phys. Rev. Lett. **109**, 4172
 152302.
 4173 Agakishiev, G., *et al.* (STAR) (2012a), Phys. Rev. Lett. **108**, 4174
 072302.
 4175 Agakishiev, G., *et al.* (STAR) (2012b), Phys. Rev. Lett. **108**, 4176
 072301, arXiv:1107.2955 [nucl-ex].
 4177 Agakishiev, G., *et al.* (STAR) (2012c), Phys. Rev. **C85**, 4178
 014903.
 4179 Agakishiev, H., *et al.* (STAR) (2010), arXiv:1010.0690 [nucl-4180
 ex].
 4181 Agakishiev, H., *et al.* (STAR) (2011), Phys. Rev. **C83**, 061901.
 4182 Agakishiev, H., *et al.* (STAR) (2014), Phys. Rev. **C89** (4), 4183
 041901.
 4184 Aggarwal, M., *et al.* (STAR) (2010), Phys. Rev. **C82**, 024912.
 4185 Akers, R., *et al.* (OPAL) (1995), Z. Phys. **C68**, 179.
 4186 Akiba, Y., *et al.* (2015), arXiv:1502.02730 [nucl-ex].
 4187 Albacete, J. L., N. Armesto, J. G. Milhano, C. A. Salgado, 4188
 and U. A. Wiedemann (2005), Phys. Rev. **D71**, 014003.
 4189 Alver, B., *et al.* (PHOBOS) (2007), Phys. Rev. Lett. **98**, 4190
 242302.
 4191 Alver, B., *et al.* (PHOBOS) (2010), Phys. Rev. Lett. **104**, 4192
 062301.
 4193 Alves, Jr., A. A., *et al.* (LHCb) (2008), JINST **3**, S08005.
 4194 Alvioli, M., B. A. Cole, L. Frankfurt, D. V. Perepelitsa, and 4195
 M. Strikman (2016), Phys. Rev. **C93** (1), 011902.
 4196 Alvioli, M., L. Frankfurt, V. Guzey, and M. Strikman (2014), 4197
 Phys. Rev. **C90**, 034914.
 4198 Alvioli, M., and M. Strikman (2013), Phys. Lett. **B722**, 347.
 4199 Andrs, C., A. Moscoso, and C. Pajares (2016), *Proceedings, 37th International Conference on High Energy Physics (ICHEP 2014)*, Nucl. Part. Phys. Proc. **273-275**, 1513.
 4200 Aprahamian, A., *et al.* (2015), “Reaching for the horizon: The 2015 long range plan for nuclear science.”.
 4201 Armesto, N., L. Cunqueiro, and C. A. Salgado (2009), Eur. Phys. J. **C63**, 679.
 4202 Armesto, N., D. C. Glhan, and J. G. Milhano (2015), Phys. Lett. **B747**, 441.
 4203 Arnald, P. B., G. D. Moore, and L. G. Yaffe (2002), JHEP **06**, 030.
 4204 Arsene, I., *et al.* (BRAHMS) (2005a), Phys. Rev. **C72**, 4205
 014908.
 4206 Arsene, I., *et al.* (BRAHMS) (2005b), Nucl. Phys. **A757**, 1.
 4207 Arsene, I. G., *et al.* (BRAHMS) (2010), Phys. Lett. **B684**, 22.
 4208 Aureneche, P., and B. G. Zakharov (2009), JETP Lett. **90**, 4209
 237.
 4210 Back, B., *et al.* (PHOBOS) (2004), Phys. Rev. **C70**, 061901.
 4211 Back, B. B., *et al.* (PHOBOS) (2003), Nucl. Instrum. Meth. **A499**, 603.
 4212 Back, B. B., *et al.* (2005), Nucl. Phys. **A757**, 28.
 4213 Back, B. B., *et al.* (PHOBOS) (2007), Phys. Rev. **C75**, 4214
 024910.
 4215 Baier, R., Y. L. Dokshitzer, A. H. Mueller, S. Peigne, and 4216
 D. Schiff (1997), Nucl. Phys. **B483**, 291.
 4217 Baier, R., Y. L. Dokshitzer, A. H. Mueller, and D. Schiff (1998), Phys. Rev. **C58**, 1706.
 4218 Baier, R., Y. L. Dokshitzer, S. Peigne, and D. Schiff (1995), 4219
 Phys. Lett. **B345**, 277.
 4220 Baier, R., D. Schiff, and B. G. Zakharov (2000), Ann. Rev. Nucl. Part. Sci. **50**, 37.

4233 Barate, R., *et al.* (ALEPH) (1998), Phys. Rept. **294**, 1. 4297 Chatrchyan, S., *et al.* (CMS) (2012f), Phys. Lett. **B715**, 66.
 4234 Bazavov, A., *et al.* (HotQCD) (2014), Phys. Rev. **D90** (9), 4298 Chatrchyan, S., *et al.* (CMS) (2012g), JHEP **05**, 063.
 4235 094503. 4299 Chatrchyan, S., *et al.* (CMS Collaboration) (2013a), Phys.
 4236 Bernhard, J. E., J. S. Moreland, S. A. Bass, J. Liu, and 4300 Lett. B **730** (arXiv:1310.0878. CMS-HIN-12-002. CERN-
 4237 U. Heinz (2016), Phys. Rev. **C94** (2), 024907. 4301 PH-EP-2013-189), 243. 31 p.
 4238 Berta, P., M. Spousta, D. W. Miller, and R. Leitner (2014), 4302 Chatrchyan, S., *et al.* (CMS) (2013b), Phys. Lett. **B718**, 773.
 4239 JHEP **06**, 092. 4303 Chatrchyan, S., *et al.* (CMS) (2014a), Phys. Rev.
 4240 Bertocchi, L., and D. Treleani (1977), J. Phys. **G3**, 147. 4304 Lett. **113** (13), 132301, [Erratum: Phys. Rev. Lett. 115,no.2,029903(2015)].
 4241 Betz, B., M. Gyulassy, M. Luzum, J. Noronha, J. Noronha- 4305 Chatrchyan, S., *et al.* (CMS) (2014b), Phys. Rev. **C89** (4),
 4242 Hostler, I. Portillo, and C. Ratti (2017), Phys. Rev. 4306 044906.
 4243 **C95** (4), 044901. 4307 Chatrchyan, S., *et al.* (CMS) (2014c), Phys. Rev. **C90** (2),
 4244 Betz, B., M. Gyulassy, J. Noronha, and G. Torrieri (2009), 4308 024908.
 4245 Phys. Lett. **B675**, 340. 4309 Chen, X.-F., C. Greiner, E. Wang, X.-N. Wang, and Z. Xu
 4246 Bielcikova, J. (STAR) (2008), in *Proceedings, 43rd Rencontres* 4310 (2010), Phys. Rev. **C81**, 064908.
 4247 *de Moriond on QCD and high energy interactions.* 4311 Chiu, C. B., and R. C. Hwa (2009), Phys. Rev. C **79**, 034901.
 4248 Bielcikova, J., S. Esumi, K. Filimonov, S. Voloshin, and 4312 Chiu, C. B., R. C. Hwa, and C. B. Yang (2008), Phys. Rev.
 4249 J. Wurm (2004), Phys. Rev. **C69**, 021901. 4313 C **78** (4), 044903.
 4250 Bjorken, J. D. (1982), “Energy Loss of Energetic Partons in 4314 CMS, C. (2010), “CMS collision events: from lead ion col-
 4251 Quark - Gluon Plasma: Possible Extinction of High p(t) 4315 lisions,” CMS-PHO-EVENTS-2010-003.
 4252 Jets in Hadron - Hadron Collisions,” FERMILAB-PUB- 4316 Coleman-Smith, C. E., and B. Muller (2014), Phys. Rev.
 4253 82-059-THY, FERMILAB-PUB-82-059-T. 4317 **D89**, 025019.
 4254 Borghini, N., P. M. Dinh, and J.-Y. Ollitrault (2000), Phys. 4318 Collaboration, C. (CMS) (2013a), “Performance of
 4255 Rev. **C62**, 034902. 4319 quark/gluon discrimination in 8 TeV pp data,” CMS-PAS-
 4256 Buckley, A., J. Butterworth, L. Lonnblad, D. Grellscheid, 4320 JME-13-002.
 4257 H. Hoeth, J. Monk, H. Schulz, and F. Siegert (2013), Com- 4321 Collaboration, C. (CMS) (2013b), “Study of isolated pho-
 4258 put. Phys. Commun. **184**, 2803, arXiv:1003.0694 [hep-ph]. 4322 ton+jet correlation in PbPb and pp collisions at $\sqrt{s_{NN}} =$
 4259 Burke, K. M., *et al.* (JET) (2014), Phys. Rev. **C90** (1), 014909. 4323 2.76 TeV and pPb collisions at $\sqrt{s_{NN}} = 5.02$ TeV,” CMS-
 4260 Buskulic, D., *et al.* (ALEPH) (1996), Phys. Lett. **B384**, 353. 4324 PAS-HIN-13-006.
 4261 Butterworth, J. M., A. R. Davison, M. Rubin, and G. P. 4325 Collaboration”, J. (2017), “<http://jetscape.wayne.edu/>” .
 4262 Salam (2008), Phys. Rev. Lett. **100**, 242001. 4326 Collins, J. C., D. E. Soper, and G. F. Sterman (1985), Nucl.
 4263 Buzzatti, A., and M. Gyulassy (2012), Phys. Rev. Lett. **108**, 4327 C **B261**, 104.
 4264 022301. 4328 Cowan, G. (2002), *Advanced Statistical Techniques in Particle
 4265 Bzdak, A., V. Skokov, and S. Bathe (2016), Phys. Rev. 4329 Physics. Proceedings, Conference, Durham, UK, March 18-
 4266 **C93** (4), 044901. 4330 22, 2002, Conf. Proc. **C0203181**, 248, [248(2002)].
 4267 Cacciari, M., J. Rojo, G. P. Salam, and G. Soyez (2011), 4331 Cunqueiro, L. (ALICE) (2016), *Proceedings, 25th Interna-
 4268 Eur.Phys.J. **C71**, 1539. 4332 tional Conference on Ultra-Relativistic Nucleus-Nucleus
 4269 Cacciari, M., G. P. Salam, and G. Soyez (2008a), JHEP **04**, 4333 Collisions (Quark Matter 2015): Kobe, Japan, September
 063. 4334 27-October 3, 2015, Nucl. Phys. **A956**, 593.
 4271 Cacciari, M., G. P. Salam, and G. Soyez (2008b), JHEP 4335 D’Agostini, G. (1995), Nucl. Instrum. Meth. **A362**, 487.
 4272 **0804**, 005. 4336 Das, S. J., G. Giacalone, P.-A. Monard, and J.-Y. Ollitrault
 4273 Cacciari, M., G. P. Salam, and G. Soyez (2012), Eur.Phys.J. 4337 (2017), arXiv:1708.00081 [nucl-th].
 4274 **C72**, 1896. 4338 Dasgupta, M., A. Fregoso, S. Marzani, and G. P. Salam
 4275 Casalderrey-Solana, J., D. Gulhan, G. Milhano, D. Pablos, 4339 (2013), Journal of High Energy Physics **2013** (9), 1.
 4276 and K. Rajagopal (2017), JHEP **03**, 135. 4340 Djordjevic, M., and M. Gyulassy (2004), Nucl. Phys. **A733**,
 4277 Casalderrey-Solana, J., Y. Mehtar-Tani, C. A. Salgado, and 4341 265.
 4278 K. Tywoniuk (2013), Phys. Lett. **B725**, 357. 4342 Djordjevic, M., M. Gyulassy, and S. Wicks (2005), Phys. Rev.
 4279 Casalderrey-Solana, J., E. V. Shuryak, and D. Teaney 4343 Lett. **94**, 112301.
 4280 (2005), *Proceedings, 18th International Conference on* 4344 Djordjevic, M., and U. W. Heinz (2008), Phys. Rev. Lett.
 4281 *Ultra-Relativistic Nucleus-Nucleus Collisions (Quark* 4345 **101**, 022302.
 4282 *Matter 2005)*, J. Phys. Conf. Ser. **27**, 22, [Nucl. 4346 Dokshitzer, Y. L., and D. E. Kharzeev (2001), Phys. Lett. B
 4283 Phys. A774,577(2006)]. 4347 **519**, 199.
 4284 Chatrchyan, S., *et al.* (CMS) (2008), JINST **3**, S08004. 4348 Dover, C. B., U. W. Heinz, E. Schnedermann, and J. Zimanyi
 4285 Chatrchyan, S., *et al.* (CMS) (2011a), JHEP **08**, 141. 4349 (1991), Phys. Rev. **C44**, 1636.
 4286 Chatrchyan, S., *et al.* (CMS) (2011b), Phys. Rev. **C84**, 4350 Ellis, S. D., C. K. Vermilion, and J. R. Walsh (2010), Phys.
 4287 024906. 4351 Rev. D **81**, 094023.
 4288 Chatrchyan, S., *et al.* (CMS) (2011c), Phys. Rev. Lett. **106**, 4352 Eskola, K. J., H. Honkanen, C. A. Salgado, and U. A. Wiede-
 4289 212301. 4353 mann (2005), Nucl. Phys. **A747**, 511.
 4290 Chatrchyan, S., *et al.* (CMS) (2012a), Phys. Rev. Lett. **109**, 4354 Field, R., and R. C. Group (CDF) (2005), arXiv:hep-
 4291 022301. 4355 ph/0510198 [hep-ph].
 4292 Chatrchyan, S., *et al.* (CMS) (2012b), Phys. Lett. **B710**, 256. 4356 Floris, M. (2014), *Proceedings, 24th International Conference*
 4293 Chatrchyan, S., *et al.* (CMS) (2012c), JHEP **1210**, 087. 4357 *on Ultra-Relativistic Nucleus-Nucleus Collisions (Quark*
 4294 Chatrchyan, S., *et al.* (CMS) (2012d), Phys. Rev. Lett. **109**, 4358 *Matter 2014)*: Darmstadt, Germany, May 19-24, 2014,
 4295 152303. 4359 Nucl. Phys. **A931**, 103.
 4296 Chatrchyan, S., *et al.* (CMS) (2012e), Eur.Phys.J. **C72**, 1945. 4360**

4361 Fodor, Z., and S. D. Katz (2004), JHEP **04**, 050. 4425 *Energy Nuclear Collisions (Hard Probes 2015)*.
 4362 Fries, R. J., B. Muller, C. Nonaka, and S. A. Bass (2003), 4426 Larkoski, A. J., S. Marzani, G. Soyez, and J. Thaler (2014),
 4363 Phys. Rev. Lett. **90**, 202303. 4427 JHEP **05**, 146, arXiv:1402.2657 [hep-ph].
 4364 Gelis, F., E. Iancu, J. Jalilian-Marian, and R. Venugopalan 4428 Levai, P., G. Papp, G. I. Fai, M. Gyulassy, G. G. Barnafoldi,
 4365 (2010), Ann. Rev. Nucl. Part. Sci. **60**, 463, arXiv:1002.0333 4429 I. Vitev, and Y. Zhang (2002), *Quark matter 2001. Pro-
 4366 [hep-ph]. 4430 ceedings, 15th International Conference on Ultrarelativistic
 4367 Greco, V., C. M. Ko, and P. Levai (2003), Phys. Rev. Lett. 4431 nucleus nucleus collisions, QM 2001, Stony Brook, USA,
 4368 **90**, 202302. 4432 January 15-20, 2001, Nucl. Phys. **A698**, 631.
 4369 Gubser, S. S. (2007), Phys. Rev. **D76**, 126003. 4433 Lisa, M. A., and S. Pratt (2008).
 4370 Gyulassy, M., and M. Plumer (1990), Phys. Lett. **B243**, 432. 4434 Lisa, M. A., S. Pratt, R. Soltz, and U. Wiedemann (2005),
 4371 Harris, J. W., and B. Muller (1996), Ann. Rev. Nucl. Part. 4435 Ann. Rev. Nucl. Part. Sci. **55**, 357.
 4372 Sci. **46**, 71. 4436 Lokhtin, I. P., L. V. Malinina, S. V. Petrushanko, A. M. Snigirev, I. Arsene, and K. Tywoniuk (2009a), Comput. Phys.
 4373 Heinz, U., and R. Snellings (2013), Ann. Rev. Nucl. Part. 4437 Commun. **180**, 779.
 4374 Sci. **63**, 123. 4438 Lokhtin, I. P., L. V. Malinina, S. V. Petrushanko, A. M. Snigirev, I. Arsene, and K. Tywoniuk (2009b), *Proceedings,
 4375 Hocker, A., and V. Kartvelishvili (1996), Nucl. Instrum. 4439 4th International Workshop on High $p(T)$ physics at LHC*,
 4376 Meth. **A372**, 469. 4440 Pos **High-pT physics09**, 023.
 4377 Horowitz, W. A., and M. Gyulassy (2008), Phys. Lett. B 4441 Majumder, A. (2007a), *Proceedings, 19th International
 4378 **666**, 320. 4442 Conference on Ultra-Relativistic nucleus-nucleus collisions
 4379 Huang, J., Z.-B. Kang, and I. Vitev (2013), Phys. Lett. **B726**, 4443 (Quark Matter 2006): Shanghai, P.R. China, November
 4380 251. 4444 14-20, 2006, J. Phys. **G34**, S377.
 4381 Huang, J., Z.-B. Kang, I. Vitev, and H. Xing (2015), Phys. 4445 Majumder, A. (2007b), J. Phys. G **G34**, S377.
 4382 Lett. **B750**, 287. 4446 Majumder, A. (2012), Phys. Rev. **D85**, 014023.
 4383 Huth, J. E., et al. (1990), in *1990 DPF Summer Study on 4447 Majumder, A. (2013), *Proceedings, 5th International Conference
 4384 High-energy Physics: Research Directions for the Decade 4448 on Hard and Electromagnetic Probes of High-Energy
 4385 (Snowmass 90) Snowmass, Colorado, June 25-July 13, 4449 Nuclear Collisions (Hard Probes 2012): Cagliari, Italy,
 4386 1990*, pp. 0134-136. 4450 May 27-June 1, 2012, Nucl. Phys. **A910-911**, 367.
 4387 Hwa, R. C., and C. B. Yang (2003), Phys. Rev. **C67**, 034902. 4451 Majumder, A., and J. Putschke (2016), Phys. Rev. **C93** (5),
 4388 Hwa, R. C., and C. B. Yang (2009), Phys. Rev. C **79**, 044908. 4452 054909.
 4389 Iancu, E., A. Leonidov, and L. D. McLerran (2001), Nucl. 4453 Majumder, A., and M. Van Leeuwen (2011), Prog. Part.
 4390 Phys. **A692**, 583. 4454 Nucl. Phys. **66**, 41.
 4391 Jeon, S., and G. D. Moore (2005), Phys. Rev. **C71**, 034901. 4455 Mehtar-Tani, Y., and K. Tywoniuk (2015), Phys. Lett. **B744**,
 4392 Jia, J. (2013), Phys. Rev. **C87** (6), 061901. 4456 284.
 4393 Jia, J., W. A. Horowitz, and J. Liao (2011), Phys. Rev. **C84**, 4457 Milhano, G. T. D. A. (2017), "the origin of the modification
 4394 034904. 4458 of the zg distribution in aa collisions", "Quark Matter".
 4395 Karsch, F. (2002), in *Lectures on Quark Matter*, Lecture 4459 Milhano, J. G., U. A. Wiedemann, and K. C. Zapp (2017),
 4396 Notes in Physics, Vol. 583, edited by W. Plessas and 4460 arXiv:1707.04142 [hep-ph].
 4397 L. Mathelitsch (Springer Berlin Heidelberg) pp. 209-249. 4461 Miller, M. L., K. Reygers, S. J. Sanders, and P. Steinberg
 4398 Kauder, K. (2017), "star measurements of the shared mo- 4462 (2007), Ann. Rev. Nucl. Part. Sci. **57**, 205.
 4399 mentum fraction zg using jet reconstruction in p+p and 4463 Moreland, J. S., J. E. Bernhard, and S. A. Bass (2015), Phys.
 4400 au+au", "Quark Matter". 4464 Rev. **C92** (1), 011901.
 4401 Khachatryan, V., et al. (CMS) (2010), JHEP **1009**, 091. 4465 Muller, B. (2013), *Proceedings, 5th International Conference
 4402 Khachatryan, V., et al. (CMS) (2015a), Phys. Rev. Lett. 4466 on Hard and Electromagnetic Probes of High-Energy Nu-
 4403 **115** (1), 012301. 4467 clear Collisions (Hard Probes 2012): Cagliari, Italy, May
 4404 Khachatryan, V., et al. (CMS) (2015b), Eur. Phys. J. 4468 27-June 1, 2012, Nucl. Phys. **A910-911**, 5.
 4405 **C75** (5), 237. 4469 Nattrass, C., N. Sharma, J. Mazer, M. Stuart, and A. Be-
 4406 Khachatryan, V., et al. (CMS) (2016a), JHEP **02**, 156. 4470 jnood (2016), Phys. Rev. **C94** (1), 011901.
 4407 Khachatryan, V., et al. (CMS) (2016b), Eur. Phys. J. 4471 Neufeld, R. B., I. Vitev, and B. W. Zhang (2011), Phys. Rev.
 4408 **C83**, 034902.
 4409 Khachatryan, V., et al. (CMS) (2016c), JHEP **01**, 006. 4472 Nonaka, C., and S. A. Bass (2007), Phys. Rev. **C75**, 014902.
 4410 Khachatryan, V., et al. (CMS) (2016d), Phys. Lett. **B754**, 4473 Noronha-Hostler, J., B. Betz, J. Noronha, and M. Gyulassy
 4411 59. 4474 (2016), Phys. Rev. Lett. **116** (25), 252301.
 4412 Khachatryan, V., et al. (CMS) (2017a), JHEP **04**, 039. 4475 Novak, J., K. Novak, S. Pratt, J. Vredevoogd, C. Coleman-
 4413 Khachatryan, V., et al. (CMS) (2017b), Phys. Lett. **B765**, 4476 Smith, and R. Wolpert (2014), Phys. Rev. **C89** (3),
 4414 193. 4477 034917.
 4415 Khachatryan, V., et al. (CMS) (2017c), Phys. Rev. **C96** (1), 4478 Ozonder, S. (2016), Phys. Rev. **D93** (5), 054036.
 4416 015202, arXiv:1609.05383 [nucl-ex]. 4479 Poskanzer, A. M., and S. A. Voloshin (1998), Phys. Rev.
 4417 Khachatryan, V., et al. (CMS) (2017d), Phys. Lett. **B768**, 4480 **C58**, 1671.
 4418 103. 4481 Pumplin, J., D. R. Stump, J. Huston, H. L. Lai, P. M. Nadol-
 4419 Kodolova, O., I. Vardanian, A. Nikitenko, and A. Oulianov 4482 sky, and W. K. Tung (2002), JHEP **07**, 012.
 4420 (2007), Eur. Phys. J. **C50**, 117. 4483 Qin, G.-Y., J. Ruppert, C. Gale, S. Jeon, and G. D. Moore
 4421 Krohn, D., J. Thaler, and L.-T. Wang (2010), Journal of 4484 (2009), Phys. Rev. **C80**, 054909.
 4422 High Energy Physics **2010** (2), 1. 4485****

4423 Kucera, V. (ALICE) (2016), in *Proceedings, 7th International 4486 Conference on Hard and Electromagnetic Probes of High- 4487*

4488 Qin, G.-Y., J. Ruppert, C. Gale, S. Jeon, G. D. Moore, and 4530 Suarez, C. (2012), *Baryon to Meson Ratio in Relativistic
4489 M. G. Mustafa (2008)*, Phys. Rev. Lett. **100**, 072301. 4531 Heavy Ion Collisions

4490 Qin, G.-Y., and X.-N. Wang (2015), Int. J. Mod. Phys. 4532 thesis (University of Illinois
4491 **E24** (11), 1530014, [,309(2016)]. 4533 at Chicago).

4492 Qiu, J.-w., and I. Vitev (2006), Phys. Lett. **B632**, 507, 4534 Tachibana, Y., N.-B. Chang, and G.-Y. Qin (2017), Phys.
4493 arXiv:hep-ph/0405068 [hep-ph]. 4535 Rev. **C95** (4), 044909, arXiv:1701.07951 [nucl-th].

4494 Qiu, Z., and U. Heinz (2012), Phys. Lett. **B717**, 261. 4536 Tannenbaum, M. J. (2017), arXiv:1702.00840 [nucl-ex].

4495 Qiu, Z., C. Shen, and U. Heinz (2012), Phys. Lett. **B707**, 4537 Van Hove, L., and A. Giovannini (1988), Acta Phys. Polon.
4496 151. 4538 **B19**, 917.

4497 Ranft, J. (1999), arXiv:hep-ph/9911232 [hep-ph]. 4539 Veldhoen, M. (ALICE) (2013), *Proceedings, 5th International
4498 Renk, T. (2008), Phys. Rev. **C78**, 034908. 4540 Conference on Hard and Electromagnetic Probes of High-
4499 Renk, T. (2009), Phys. Rev. **C80**, 014901, arXiv:0904.3806 4541 Energy Nuclear Collisions (Hard Probes 2012)*, Nucl. Phys.
4500 [hep-ph]. 4542 **A910-911**, 306.

4501 Renk, T. (2013a), Phys. Rev. **C88** (1), 014905. 4543 Vitev, I. (2007), Phys. Rev. **C75**, 064906, arXiv:hep-
4502 Renk, T. (2013b), Phys. Rev. **C87** (2), 024905. 4544 ph/0703002 [hep-ph].

4503 Renk, T., and J. Ruppert (2006), Phys. Rev. **C73**, 011901. 4545 Vitev, I., S. Wicks, and B.-W. Zhang (2008), JHEP **11**, 093.

4504 Ruppert, J., and B. Muller (2005), Phys. Lett. **B618**, 123. 4546 Voloshin, S. A., A. M. Poskanzer, and R. Snellings (2008),
4505 Salam, G. P. (2010), Eur. Phys. J. **C67**, 637. 4547 in *Relativistic Heavy Ion Physics*, edited by R. Stock,
4506 Sapeta, S., and U. A. Wiedemann (2008), Eur. Phys. J. **C55**, 4548 Chap. 23 (Springer Berlin Heidelberg) pp. 293–333.

4507 293. 4549 Wang, X.-N., and X.-f. Guo (2001), Nucl. Phys. **A696**, 788,
4508 Schenke, B., S. Jeon, and C. Gale (2010), Phys. Rev. **C82**, 4550 arXiv:hep-ph/0102230 [hep-ph].

4509 014903. 4551 Wang, X.-N., and Z. Huang (1997), Phys. Rev. **C55**, 3047.

4510 Schenke, B., S. Jeon, and C. Gale (2011), Phys. Rev. Lett. 4552 Wicks, S., W. Horowitz, M. Djordjevic, and M. Gyulassy
4511 **106**, 042301. 4553 (2007), Nucl. Phys. **A784**, 426.

4512 Sharma, N., J. Mazer, M. Stuart, and C. Nattrass (2016), 4554 Wiedemann, U. A. (2000a), Nucl. Phys. **B588**, 303.

4513 Phys. Rev. **C93** (4), 044915. 4555 Wiedemann, U. A. (2000b), Nucl. Phys. **B582**, 409.

4514 Shuryak, E. V. (1980), Phys. Rept. **61**, 71. 4556 Wiedemann, U. A. (2001), Nucl. Phys. **A690**, 731.

4515 Sickles, A., M. P. McCumber, and A. Adare (2010), 4557 Wong, C.-Y. (2007), Phys. Rev. C **76**, 054908.

4516 Phys. Rev. **C81**, 014908. 4558 Wong, C.-Y. (2008), Phys. Rev. C **78**, 064905.

4517 Sirunyan, A. M., *et al.* (CMS) (2017a), arXiv:1708.09429 4559 X.-N. Wang, and M. Gyulassy, (1991), Phys. Rev. D **44**, 3501.

4518 [nucl-ex]. 4560 Zakharov, B. G. (1996), JETP Lett. **63**, 952.

4519 Sirunyan, A. M., *et al.* (CMS) (2017b), Phys. Lett. **B772**, 4561 Zapp, K. C. (2014a), Phys. Lett. **B735**, 157.

4520 306. 4562 Zapp, K. C. (2014b), Eur. Phys. J. **C74** (2), 2762.

4521 Sirunyan, A. M., *et al.* (CMS) (2017c), Phys. Rev. Lett. 4563 Zardoshti, N. (ALICE) (2017), in *26th International Conference
4522 **119** (8), 082301, arXiv:1702.01060 [nucl-ex]. 4564 on Ultrarelativistic Nucleus-Nucleus Collisions (Quark
4523 Sjostrand, T., S. Mrenna, and P. Z. Skands (2006), JHEP 4565 Matter 2017) Chicago, Illinois, USA, February 6-11, 2017,
4524 **0605**, 026. 4566 arXiv:1705.03383 [nucl-ex].*

4525 Skands, P. Z. (2010), Phys. Rev. **D82**, 074018. 4567 Zhang, H., J. F. Owens, E. Wang, and X.-N. Wang (2007),
4526 Song, H., and U. W. Heinz (2008a), Phys. Rev. **C77**, 064901. 4568 Phys. Rev. Lett. **98**, 212301.

4527 Song, H., and U. W. Heinz (2008b), Phys. Lett. **B658**, 279. 4569 Zhang, H., J. F. Owens, E. Wang, and X.-N. Wang (2009),
4528 Srivastava, D. K., R. Chatterjee, and M. G. Mustafa (2016), 4570 Phys. Rev. Lett. **103**, 032302, arXiv:0902.4000 [nucl-th].

4529 arXiv:1609.06496 [nucl-th]. 4571 Zimmermann, A. (ALICE) (2015), in *10th International
4530 4572 Workshop on High- p_T Physics in the RHIC/LHC Era
4531 (HPT 2014) Nantes, France, September 9-12, 2014.*

4532 4573 4574